Spectral classification

Jesús Maíz Apellániz[a], Ignacio Negueruela[b] and José A. Caballero[a]
[a]Centro de Astrobiología, Campus ESAC, Camino bajo del castillo s/n, 28 692 Villanueva de la Cañada, Madrid, Spain
[b]Universidad de Alicante, Departamento de Física Aplicada, Carretera de San Vicente s/n, 03 690 San Vicente del Raspeig, Alicante, Spain

Glossary

Dwarf or class V is a spectroscopic luminosity class in the MK system for stars with low luminosity for their spectral type.
Giant or class III is a spectroscopic luminosity class in the MK system for stars with intermediate luminosity for their spectral type.
Harvard system is the spectral classification system designed by the Harvard group between the 1890s and the 1910s.
MK system is the spectral classification system designed by William W. Morgan and Philip C. Keenan in the 1940s.
Secchi system is the first spectral classification system, designed by Angelo Secchi in the 1860s.
Spectral classification is the division of stars into classes based on their spectra, with the most common system being the MK one.
Supergiant or class I is a spectroscopic luminosity class in the MK system for stars with high luminosity for their spectral type.

Nomenclature

AGB, pAGB	(Post-) Asymptotic Giant Branch, evolutionary phase for a low- or intermediate-mass star burning He in a shell
CMD, CAMD	Color-(Absolute)-Magnitude Diagram
CTTS/WTTS	Classical/Weak-lined T-Tauri Star, low-mass PMS star with strong/weak emission lines
CV	Cataclysmic Variable, binary system composed of a white dwarf and a mass-donor star
DIB	Diffuse Interstellar Band
EW	Equivalent Width
FWHM	Full Width at Half Maximum
GOSSS	Galactic O-Star Spectroscopic Survey, Maíz Apellániz et al. (2011)
HB	Horizontal Branch, evolutionary phase for a low-metallicity low-mass star burning He in its core
HRD	Hertzsprung-Russell Diagram
LBV	Luminous Blue Variable, evolutionary phase for massive stars with high spectroscopic and photometric variability
LPV	Long Period Variable, red luminous star characterized by its large variability in long time scales
LiLiMaRlin	**Li**brary of **Li**braries of **Ma**ssive-Star High-**R**eso**l**uti**o**n Spectra, Maíz Apellániz et al. (2019a)
LMC	Large Magellanic Cloud
log g	Logarithmic surface gravity
MS	Main Sequence, evolutionary phase during which a star burns ^{1}H in its core
PMS	Pre-Main Sequence, evolutionary phase prior to ^{1}H ignition in its core
PNN	Planetary Nebula Nucleus, evolutionary phase for a low- or intermediate-mass star after ejecting its outer layers
RC	Red Clump, evolutionary phase for a high-metallicity low-mass star burning He in its core
SB2, SB3	Double- or triple-lined spectroscopic binary (multiple) star
sd	Subdwarf star, spectroscopic luminosity class located below the dwarf sequence
SMC	Small Magellanic Cloud
$T_{\rm eff}$	Effective temperature
WD	White Dwarf, evolutionary end phase of most low- and intermediate-mass stars
WR	Wolf-Rayet star. spectroscopic class with broad emission lines of H, He, C, N, and/or O
ZAMS	Zero-Age Main Sequence, evolutionary phase at which a star ignites ^{1}H in its core

Abstract

Spectral classification is the division of stars into classes based on their spectral characteristics. Different classification systems have existed since the 19th century but the term is used nowadays mostly to refer to the Morgan-Keenan (MK) system, which was established in the 1940s and has been developed since then. The MK classification has three components: a spectral type, a luminosity class, and (possibly) suffixes or qualifiers. The first two components represent temperature and luminosity sequences (a 2-D grid), respectively, and the third one includes additional information. The MK system is an Aristotelian morphological classification system that uses the MK process, an inductive approach based on specimens (standard stars) that define the system. In that respect, it is different from and a required preliminary step for quantitative spectroscopy, whose goal is to extract the physical properties and chemical composition of the stars. In this entry we provide a brief history of spectral classification, describe the general properties of the classification criteria of the MK system, analyze the specific spectral type and luminosity class criteria used for each spectral class, and introduce the different peculiar types that can be found within the 2-D classification grid and at its edges.

Keywords: Spectral classification, Morgan-Keenan classification, Luminosity classification, Harvard classification, O stars, B stars, A stars, F stars, G stars, K stars, M stars, ultracool dwarfs

1 Introduction

Spectral classification (sometimes referred to as stellar classification) is a generic term for the division of stars into classes based on their spectral characteristics. In principle, one can do spectral classification based on any of the stellar properties reflected on the spectrum but, in most circumstances, the term is currently used to refer to the Morgan-Keenan (MK) system. The MK classification system is described in more detail below, but it basically consists of three components:

1. The spectral type using the seven letters OBAFGKM as a temperature sequence from hot to cool, with each letter possibly followed by a number, called the spectral subtype. Those seven letters form the original standard sequence, but others are also used nowadays.
2. The luminosity class, added after the spectral type and separated by a space, as a luminosity sequence designated by a Roman numeral. Originally, the sequence ran from I (supergiants, more luminous) to V (dwarfs, less luminous), but it was eventually expanded at both ends and class subdivisions also appeared.
3. Possibly suffixes (or qualifiers) to represent other characteristics, such as line width, composition anomalies, the presence of emission lines, uncertainty in the classification, and other peculiarities.

In addition, two or more stars can be identified in a single spectrum if they belong to very different classes or if they can be separated in velocity, as in the case of double-lined spectroscopic binaries (SB2), for which the spectral classification of each component is separated by a plus sign i.e. +. As an example, the SB2 system BD +60 497 was classified as O6.5 V(n)((f))z + B0: V(n) by Maíz Apellániz et al. (2019b). The primary is a star with a spectral type of O6.5 and a luminosity class of V, with the qualifiers (n), ((f)), and z respectively indicating [a] slightly broadened lines, [b] strong He II λ4686 absorption[1] accompanied by weak N III $\lambda\lambda\lambda$4634-40-42 emission, and [c] the He II λ4686 absorption being more intense than both He I λ4471 and He II λ4542. The secondary has an uncertain (indicated by the : qualifier) B0 spectral type and a luminosity class of V, with (n) indicating again slightly broadened lines. This example shows the possible complexity of spectral classification.

Spectral classification should be differentiated from quantitative spectroscopy, whose aims are to measure physical properties such as effective temperature ($T_{\rm eff}$) and logarithmic surface gravity ($\log g$) and to determine the chemical composition of stars. Spectral classification is a morphological process whose aim is to provide an image of nature as an intermediate step prior to its understanding by a subsequent analysis via quantitative spectroscopy (Walborn, 2011). Such a process is necessary when the objects of scientific analysis constitute a complex and diverse sample. If it is not properly followed, our image of nature will be inadequate and physics will not be able to provide a correct understanding. In that way, spectral classification yields a category for a star that does not require a computation and is (unless the classification system changes) permanent, while the physical properties obtained from quantitative spectroscopy change according to the input physics of the model used to derive them (see page 31 in Morgan and Keenan 1973, written by Dimitri Mihalas). The MK system is defined by a series of standard stars that define the spectral classes, of which the most robust ones are called anchor points (Garrison, 1994). For example, α Psc has had an A3 V spectral classification and ρ Boo a K3 III one since the MK system was established in the 1940s, but their values of $T_{\rm eff}$ and $\log g$ determined from quantitative spectroscopy have changed since then (see Holgado et al. 2018 for some examples with O stars). Spectral classification has given us the same image of nature during that period and quantitative spectroscopy has shown how our understanding has improved.

A common confusion regarding spectral classification arises from most stellar classes having two definitions: a spectroscopic (or morphological) one and an evolutionary (or astrophysical) one. For example, the answer to "what is a red supergiant?" can be "a star with spectral type K or M and luminosity class Ib to Ia" or "a massive star (of a certain mass range) in its final stages before core collapse during which it greatly expands until reaching low surface temperatures". There are several problems with such a double definition:

- A one-to-one correspondence between observational and evolutionary definitions is prone to have exceptions. Using the example above, some intermediate-mass stars may have phases during which their spectra mimic that of a red supergiant and a massive star during their final stages may at some point have a different spectral classification.
- Taking the previous point to an extreme, some objects with spectroscopic characteristics similar enough to be grouped in the same morphological category (e.g. Wolf-Rayet stars) correspond to objects of quite different nature.
- Most stars have a fixed spectral type during a human lifetime. However, the spectral types of some stars vary, either (quasi)-periodically, such as spectroscopic binaries, cepheids, and Of?p stars, or otherwise, such as Luminous Blue Variables and OBe stars. In those cases, one should indicate that the spectral classification corresponds to a given phase or epoch of the star, e.g. "the cepheid was observed in an F8 Ib phase" or "the cepheid had an F8 Ib spectrum on Julian date X", but not "the cepheid is an F8 Ib star". Excluding such variable cases, one can say e.g. "the Sun is a G2 V star".
- Some commonly used broad generalizations are wrong or misleading. For example, the vast majority of dwarf stars (MK luminosity class V) are in the main sequence phase (burning hydrogen in their cores) and viceversa, but some exceptions exist in both directions. The term "red giant" is especially misleading, as in some contexts it refers to "cool stars of luminosity class III" (spectroscopic definition) and in others to "stars in the red giant branch" (evolutionary definition that is a subset of the spectroscopic one).

For those reasons, in this entry we will attempt to describe each stellar class in both spectroscopic and evolutionary terms and make explicit those cases where both definitions may be in conflict.

[1] Throughout this entry, spectral lines are identified by their ion followed by the wavelength in Å rounded to the nearest integer value.

2 Early history of spectral classification

In 1811-1814, the Bavarian physicist Joseph von Fraunhofer used a prism to decompose the solar spectrum and discovered the existence of hundreds of absorption lines, labelling the strongest using letters of the alphabet (Fig. 1, see Curtiss 1932 and Hearnshaw 1990 for a more detailed account of this and other aspects of this section). He did not try to explain the origin of the lines in the spectrum, most of which were discovered in the following decades to originate in the solar photosphere and the rest in our own atmosphere (the so-called telluric lines). The following decades saw further progress in the extension of the spectrum to the infrared, the introduction of photography to record the solar spectrum, and, most importantly, the work by Robert Bunsen and Gustav Kirchoff that allowed the identification of lines in the solar spectrum by comparing it with the emission lines seen in the spectra of flames, arcs, and sparks. In that way, it was shown that it was possible to identify the elements the Sun[2] was made of, a question that had been deemed impossible by the French philosopher Auguste Compte in 1835. Astronomy started its evolution into astrophysics.

Several astronomers observed stellar spectra in the decades after Fraunhofer, but the establishment of spectral classification did not take place until the 1860s, when the Italian Jesuit astronomer Angelo Secchi observed and classified at least 4000 stars at the Collegio Romano at the Vatican. His key idea, later exploited at great lengths by subsequent observers, was to study a large sample of spectra in order to be able to group them into classes with a significant number of objects in each group. In this way, Secchi first introduced three classes, I, II, and III, with blue/white, yellow, and red respective (intrinsic) colors that we know today correspond to a decreasing temperature scale (Fig. 1). In addition, he noted the existence of an Orion subtype for class I, where the lines were narrower and that today are known to be the hotter ones of the group, and later included a class IV that corresponds to carbon stars. Secchi also produced insights into the nature of the Balmer lines, correctly identifying hydrogen as the element responsible for them, suggesting that exceptional pressure caused their broadening in Sirius, and detecting them in emission in some active stars. For the latter type of stars with Balmer lines in emission he defined a class V. His class I stars have a spectrum dominated by those Balmer lines in a relatively clean continuum; his class II stars by a solar-like collection of many narrow metallic lines; his class III and IV stars by wide molecular bands of metallic oxides and carbon compounds, respectively; and his class V stars are similar to his class I stars but with the Balmer (and possibly others) lines in emission. The distinct morphology of the five Secchi classes is on display in Fig. 1 using modern data from the LiLiMaRlin project (Maíz Apellániz et al., 2019a).

Between the 1860s and the end of the century, other types of astronomical objects had their spectra identified: Wolf-Rayet (WR) stars by Charles Wolf and Georges Rayet, emission nebulae and novae by William Huggins, and the first supernova by Nicholas von Konkoly. William Huggins also established two pillars for future developments in stellar spectroscopy by ascribing lines to several elements and starting the field of spectrophotography (spectral classification was done visually until about 1890). Another major development was the discovery of terrestrial helium in 1895 by William Ramsay. This led to the identification of Fraunhofer's D_3 line as He I λ5876 and to an evolution of Secchi's original classification by Hermann Carl Vogel to include the presence or not of helium lines in class I stars, which we now know is a temperature effect.

The period between 1885 and 1924 saw the development of the Harvard system of spectral classification, led by Edward C. Pickering and carried out for the most part by Williamina Fleming, Antonia Maury, and Annie J. Cannon. Using objective-prism spectroscopy, they eventually published spectral classifications for 225 300 stars using a new classification system that led to the now famous OBAFGKM sequence, which is remembered by many using the English mnemonic "Oh, Be A Fine Girl/Guy, Kiss Me"[3]. To get there:

- A first catalog with 10 351 stars, the Draper Memorial Catalogue (Pickering, 1890), was first published with most of the classifications done by Williamina Fleming. This first classification system divided the Secchi types as follows: I into A+B+C+D, II into E+F+G+H+I+K+L, III as M, and IV as N. In addition, O was used for Wolf-Rayet stars (not the current notation), P for planetary nebulae, and Q for objects that did not fall into any of the previous categories. Given the limitations in apparent magnitude and declination (all data were obtained from the Harvard College Observatory in Cambridge, Massachusetts, USA), no N-type stars and only one O-type star were included.
- In 1889 Harvard started operating a telescope in Arequipa, Perú, that allowed access to the southern hemisphere, where a number of star-forming regions, the Large Magellanic Cloud (LMC), and the Small Magellanic Cloud (SMC) led to a broader sample of the hotter stars. That availability allowed Fleming to drop some letters and reorder the sequence into ABFEHGKMNO in her study of stellar clusters (Pickering and Fleming, 1897).
- In 1897 Antonia Maury was the first to introduce a second dimension in spectral classification when she found out stars whose lines were narrow and others that were wide and hazy (Maury and Pickering, 1897). The latter category was a mixed bag of objects with rapid rotators and unresolved SB2 systems, but the former category (her class c) was more interesting, as it included objects of high luminosity, as proposed later in 1905 by Ejnar Hertzsprung.
- Edward C. Pickering observed that some of the unknown lines in the spectrum of ζ Pup (the earliest O-type star he had available, even though that was unknown to him) could be reproduced by the same pattern derived by Balmer for the hydrogen but allowing for half-integer values (Pickering, 1897): such lines are now known as the Pickering series. In 1913 Niels Bohr showed that those lines were produced by ionized helium, yielding the path to the understanding of O stars as the hotter end of the spectral sequence.
- Annie J. Cannon (Cannon and Pickering, 1901) exploited the southern spectra from Perú to make two contributions that have survived to the present: the final reordering of the sequence into OBAFGKM (Fig. 2, plus P and Q as above and N and R that she added later on),

[2] And later on, the stars.

[3] There are many alternatives, such as the English "Our Bright Astronomers Frequently Generate Killer Mnemonics", the Spanish "Obesos, Bebed Aceite Filtrado, Ganaréis Kilos Masivamente", the French "Observez Bien Au Firmament: Grandiose Kalèidoscope Multicolore", and the German "Offenbar Benutzen Astronomen Furchtbar Gerne Komische Merksätze".

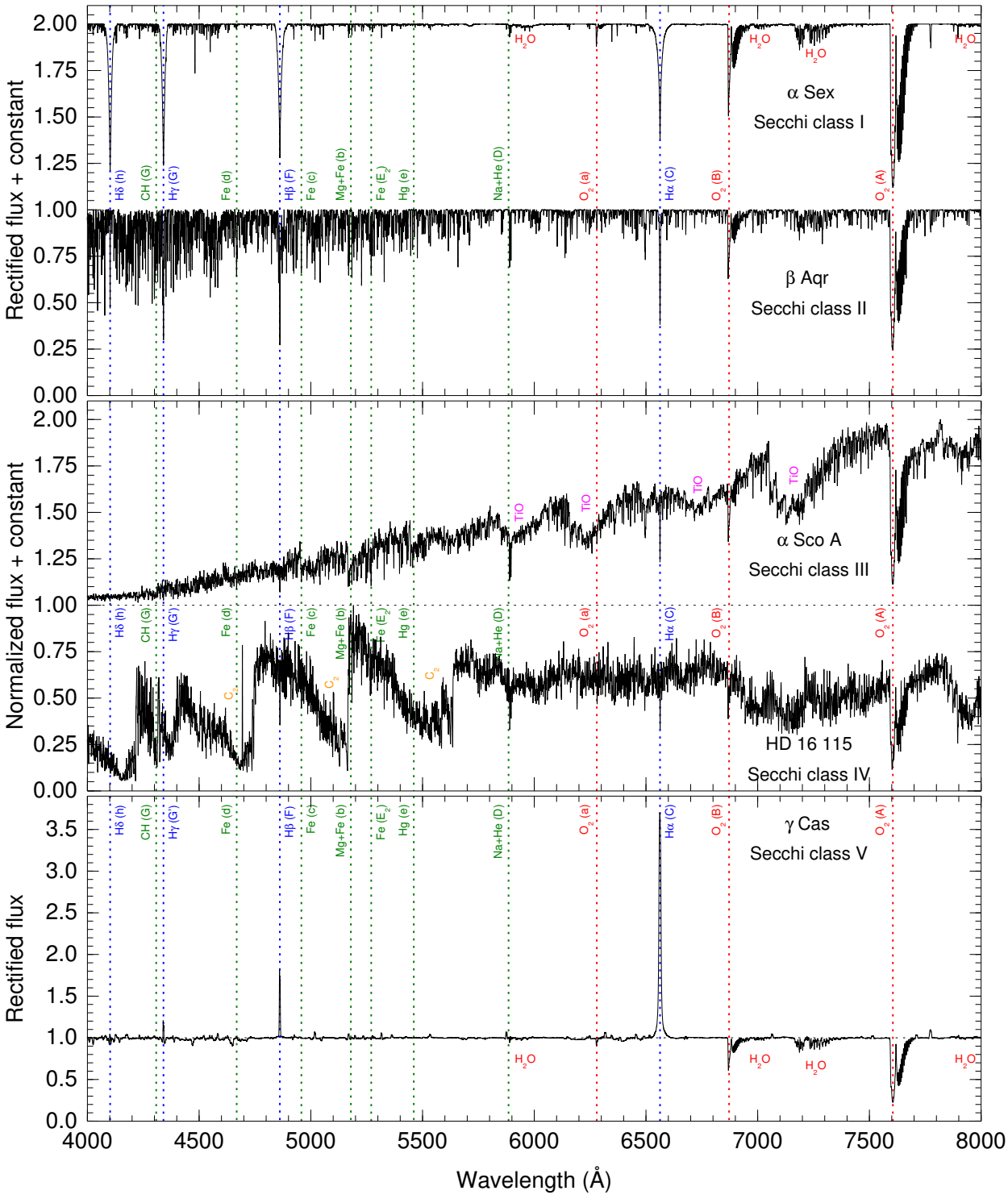

Fig. 1 Spectrograms at a spectral resolution of 4000 of examples of the five Secchi classes. The spectra in the top and bottom panels are rectified and those in the middle panel are normalized to their maxima, in all cases separated by a continuum unit. The bottom panel has a different vertical scale to accommodate the Hα emission. Blue lines show the Fraunhofer lines from hydrogen and green lines the rest of the Fraunhofer lines. Red, magenta, and orange text is used for telluric, TiO, and C_2 bands, respectively.

thanks to the availability of a large sample of O stars in the southern hemisphere; and the introduction of spectral subtypes, which were originally written as e.g. B3A instead of B3, something that she changed afterwards. Note that in spectral classification it is customary to define hotter spectral types or subtypes as "earlier" and cooler ones as "later".

- During the first two decades of the 20th century, W. Fleming first and A. J. Cannon later extended the sample and studied objects that

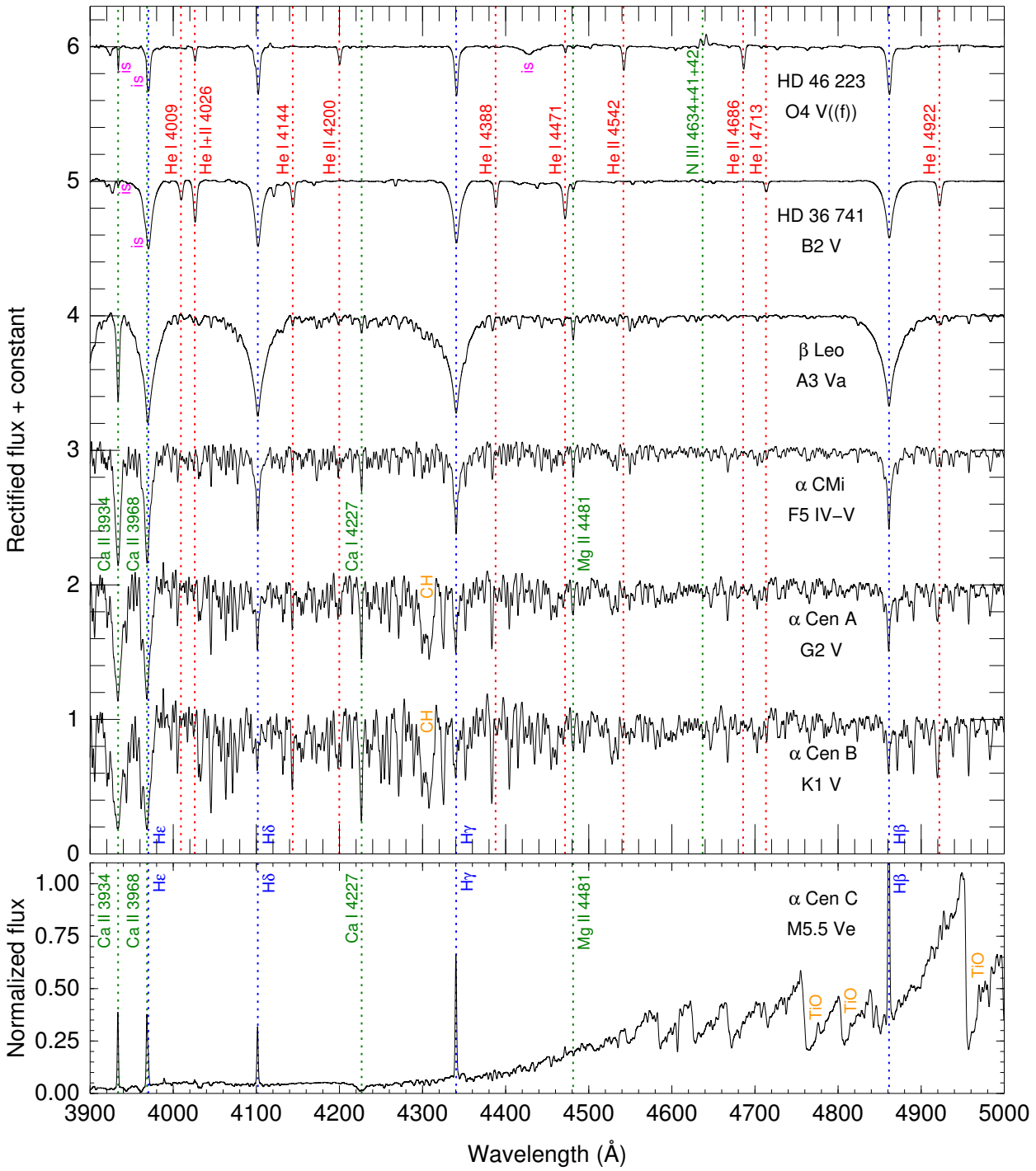

Fig. 2 Blue-violet spectrograms at a spectral resolution of 2500 for seven dwarfs representing the OBAFGKM sequence from the LiLiMaRlin project (Maíz Apellániz et al., 2019a). The spectra in the top panel are rectified and separated by a continuum unit, while the one in the bottom panel is normalized. Blue, red, and green lines show the most relevant stellar hydrogen, helium, and metallic lines, respectively. Orange text is used for molecular bands and magenta text for interstellar lines.

were rare or anomalous: O, N, and R stars; variables; spectroscopic binaries; emission-line stars; novae; gaseous nebulae; and other peculiar objects.

Finally, the Henry Draper (HD) Catalogue was published in the period 1918–1924, covering with relative uniformity the whole sky. A. J. Cannon continued classifying stars until her death, and the Henry Draper Extension (HDE) was published a quarter of a century later (Cannon and Mayall, 1949).

The spectral classifications of the Harvard group allowed for the modern science of stellar astrophysics to appear in the first three

decades of the 20th century. Ejnar Hertzsprung and Henry Norris Russell independently derived the existence of luminosity effects for a given spectral type, producing the first diagrams that carry their names (HRDs). The first stellar temperatures were determined through spectrophotometry, which is affected by interstellar and atmospheric extinction. In 1921 the Indian astronomer Megh Nad Saha proposed the idea that the stellar spectral sequence was the consequence of the progressive ionization of the different species as $T_{\rm eff}$ increases and was able to derive a reasonably accurate temperature scale based on it (Saha, 1921). The application of Saha's work led to the discovery that the ionization state also depends on pressure, making giants of a given spectral type cooler than the equivalent dwarfs due to their lower atmospheric pressures (and $\log g$), and supergiants even cooler. Even more interesting, Saha's work led to Cecilia Payne's PhD thesis conclusion that most stars are primarily made of hydrogen and helium and have relatively similar compositions despite their widely different spectra (Payne, 1925).

3 The MK system

3.1 Historical development and summary

As early as 1922, Adams and Joy (1922b) had established that Balmer lines become narrower as luminosity increases, which Struve (1929) correctly identified as a consequence of the Stark effect, where pressure broadening makes Balmer lines in high-gravity stars "nebulous" (using the terminology applied back then, meaning broad; note that giants and supergiants have lower gravities due to their large sizes). William. W. Morgan (1937) was the first to determine surface gravities for a large sample of stars and to plot a $\log g$ vs. $\log T_{\rm eff}$ diagram. Such a diagram is an equivalent form of an HRD and its use opened the possibility towards 2-D classification by defining Morgan's luminosity classes as a second dimension to be added to the spectral type sequence from the Harvard system. The next year he used those results to define the classes as supergiants (I), bright giants (II, originally "intermediate between giants and supergiants"), giants (III), subgiants (IV), and dwarfs (V, originally "main-sequence stars"[4]) for the first time (Morgan, 1938a). The original division extended only from F4 to K5, with class IV only for G5–K2, but also included the subdivision of F4–F8 supergiants into Ia (higher luminosity) and Ib (lower luminosity). The work of Morgan and others culminated in the seminal atlas of Morgan, Keenan, and Kellman, widely known as the MKK atlas (Morgan et al., 1943), which included 55 prints with photographic spectrograms for the "practical astronomer" that became the basis for spectral classification in the following decades using the MK system defined from them. The MKK atlas could be easily used today with only minor modifications (e.g. it included no M dwarfs, carbon or S stars, and luminosity classes for types earlier than O9 were not defined).

The MK system was described by Morgan and Keenan (1973) and Garrison (1994). In this section we provide a description of its characteristics and in subsequent ones we briefly detail it for different types of stars. For a more thorough analysis, the reader is referred to Gray and Corbally (2009). The MK system is an Aristotelian classification system that uses the MK process, an inductive approach based on specimens that define the system. The specimens are the spectra of standard stars arranged in a 2-D grid, with one axis being the spectral type and the other one the luminosity class. The grid is finite, i.e. one or several stars define a given box and the classification process puts a given spectrum in one box or another. The 2-D grid is complemented by the third component of MK spectral classification: suffixes or qualifiers that provide additional information detected in the spectrum.

The MK system evolves in time, as better data become available, in at least two ways: by expanding the 2-D grid outside its boundaries in spectral type and luminosity class and by making a finer grid dividing former large boxes into smaller ones. The latter is needed because the original grid had many boxes without a standard, so stars that would be assigned to them had to be compared with "interpolated" spectra, making the need to enlarge the sample of standards clear from the beginning. However, when enough stars are obtained that could fill those boxes, the classifier may experience the temptation to define a new intermediate box and, indeed, this has happened in the past (e.g. by introducing a full O9.7 spectral subtype between O9.5 and B0, see Sota et al. 2011). Four warnings about updating the MK grid are in order: (a) new standards should be chosen with care and old ones may be dropped but only with good reason (e.g. when shown to be composite spectra by being double- or tripled-lined spectroscopic binaries), (b) new boxes should be sufficiently differentiated from the old ones, (c) one should try to avoid the "one known star per box" syndrome when covering parts of the grid with few stars, and (d) more importantly, anchor points should not be moved, as there is a hierarchy of standards that fixes the MK system in place (Garrison, 1994).

The system was developed using photographic spectra in the blue-violet region (approximately, 3900–5000 Å, Fig. 3). In the last part of the 20th century, the MK system was transformed into one based on digital spectra (see e.g. Walborn and Fitzpatrick 1990) to ensure its continuity and extended to other wavelength ranges (see below). Morgan and Keenan specified that "These standard reference points do not depend on values of any specific line intensities or ratios of intensities; they have come to be defined by the appearance of the totality of lines, blends, and bands in the ordinary photographic region" (Morgan and Keenan, 1973). This text refers to two important points. First, the whole spectrum has to be used to define spectral classifications and specific line strengths or ratios can be a primary or secondary criterion, but should be always analyzed in the context of a full comparison with the standard star. Morgan and Keenan wrote that text in a moment when intermediate and narrow-band photometry was producing alternate quantitative classifications that some thought would render the MK system obsolete, something they specifically said was a false conclusion. The current danger Morgan and Keenan would see would be different: digital spectra are sometimes used to automatically determine line strengths or ratios and assign a numerical MK classification

[4]For the sake of consistency, throughout this entry we will consider luminosity classes as spectroscopic or morphological categories. Therefore, we will avoid equating dwarfs or luminosity class V with the main sequence (as originally done), for which we will reserve its evolutionary or astrophysical meaning of being composed of stars burning ^{1}H in their cores.

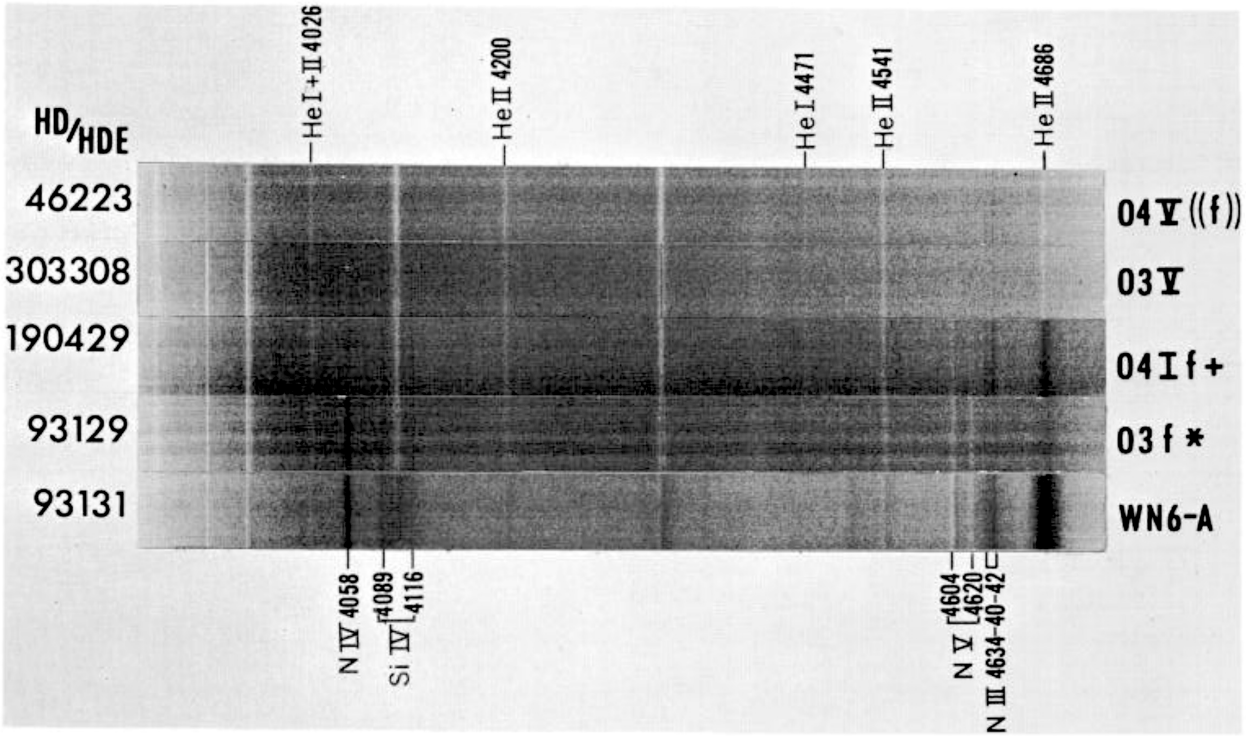

Fig. 3 Photographic spectra of very early type stars from Walborn (1971b). The first star from the top (HD 46 223) is the same as the first one in Fig 2. The photographic and digital spectra yield the same spectral type but the digital one is more sensitive to faint and/or diffuse structures. As this is a negative, absorption bands are light and emission lines are dark.

(sometimes ignoring the division in boxes and inventing spectral subclasses with two digits after the decimal point, which should be avoided in the MK system) without considering whether the spectrum fits that of the standard: that is not a proper MK process. Second, the criteria used to determine membership to a class can be "lines, blends, or bands", meaning that some will correspond to individual transitions and some to a combination of them. The more relevant issue is that the classification criteria are based on line strengths ("intensities" in the Morgan and Keenan text, or equivalent widths or EWs in numerical terms) and strength ratios, not in depths, and should be kept that way (see below for more on this).

3.2 Luminosity classes

The spectral type sequence of the MK system is essentially the same as for the Harvard system, with the Saha ionization equation determining which ionization state is dominant for a given element at a given $T_{\rm eff}$ (and, to a second order, pressure). Luminosity classification, on the other hand, depends on specific criteria for the spectral type of the star. For example, the width of the Balmer lines is a primary criterion for B and A stars but is irrelevant for M stars. For that reason, the criteria are prtesented in the specific sections for each spectral type. If a spectral feature strengthens with increasing luminosity (or decreasing luminosity class), it has a positive luminosity effect. If it weakens with increasing luminosity, it has a negative luminosity effect (as it is the case with the width of Balmer lines in B and A stars, see below).

The original five or six classes (depending on the division of I into Ia and Ib or not) retain their basic structure with some minor modifications. Supergiants are nowadays divided into three subclasses (Ia, Iab, and Ib in order of decreasing luminosity) but the subdivision is patchy in coverage (for example, it does not include the earliest O supergiants). There is also a luminosity class above Ia, the hypergiants, designated as Ia+ or 0 (numeral zero, not letter capital O). For O stars there are two classes of very luminous stars (Sota et al., 2014) that have characteristics that are intermediate between O supergiants and Wolf-Rayet types called early Of/WN stars (or "hot slash") and O Iafpe stars (formerly known as "cool slash"), but they do not form a proper luminosity class, at least at this stage. For late-B and early-A dwarfs, where the Balmer lines are stronger, it is possible to subdivide the V class into Vb (Zero Age Main Sequence, ZAMS) and Va (normal dwarfs). In a similar manner, the ZAMS can be distinguished for O2-O8 stars, but in that case a z suffix is used instead of a luminosity subclass. Finally, two luminosity classes can also be defined below the dwarf one: subdwarfs and white dwarfs, which in the past were assigned classes VI and VII, respectively. However, that is mostly deprecated and subdwarfs are currently designed with the prefix sd attached to the spectral type (e.g. sdB0, see also below for M and ultracool dwarfs) and white dwarfs by the prefix D attached to a composition symbol (A, B, C, O, Z, or Q).

We make one final note regarding nomenclature for luminosity classes. Intermediate classes are sometimes used, with e.g. III-IV meaning intermediate between III and IV. However, the nomenclature IV-III means something different: the luminosity range between classes IV and III, for example, due to an uncertainty in the classification. However, this rule is not always used in the literature.

Table 1 Suffixes/qualifiers frequently used for spectral classification.

Qual.	Range	Description
:	All	Uncertain classification, may be applied to either the spectral type or the luminosity class, sometimes ? also used (see below for f?p)
comp	All	Composite spectrum
k	All	Interstellar absorption present, commonly ignored for O+B+WR stars due to ubiquity
p	All	Peculiar spectrum (general, see below for B+A stars), sometimes … and ! also used
var	All	Variation in line spectrum intensities or content, v sometimes also used
w	All	Weak lines (metal poor), wl and wk sometimes also used
(n)	O-F	Slightly broadened ("nebulous") absorption lines (O stars: $v \sin i \sim 200$ km/s), Fig. 4
n	O-F	Broadened absorption lines (O stars: $v \sin i \sim 300$ km/s), Fig. .4
nn	O-F	More broadened absorption lines (O stars: $v \sin i \sim 400$ km/s), Fig. 4
nnn	O-F	Even more broadened absorption lines (O stars: $v \sin i \sim 500$ km/s)
[n]	O+B	H absorption lines more broadened than He lines
s	All	Very narrow ("sharp") lines
sh	O-F	Shell star, very broad profiles in some lines, narrow in others, possible Balmer (and others) lines in emission
e	All	Emission components in H lines and possibly in He I and even some metallic lines, Fig. 5
(e)	All	Weak version of above e.g. probable Hα emission but no red spectrogram available, Fig .5
[e]	All	Emission spectrum including Fe forbidden lines
eq	All	One or several emission line(s) with P Cyg profile in the blue-violet region, Fig .5 and Feast et al. (1960)
neb	All	Nebular emission spectrum present
b	WN	Broad lines, FWHM (He II λ4686) > 30 Å or FWHM (He II λ5412) > 40 Å
d	WC	Star with dust-production episodes
o	WN	No hydrogen component in non-pure-Pickering He II wind emission lines (usually left off)
(h)	WN	Weak hydrogen component in non-pure-Pickering He II wind emission lines
h	WN	Strong hydrogen component in non-pure-Pickering He II wind emission lines
ha	WN	Hydrogen lines from wind with a combination of emission (blue-shifted) and absorption
((f))	O3.5-O8.5	Weak N III $\lambda\lambda\lambda$4634-40-42 emission, strong He II λ4686 absorption
(f)	O4-O8.5	Medium N III $\lambda\lambda\lambda$4634-40-42 emission, neutral or weak He II λ4686 absorption
f	O4-O8.5	Strong N III $\lambda\lambda\lambda$4634-40-42 emission, He II λ4686 emission above continuum
((f*))	O2-O3	N IV λ4058 emission ≥ N III $\lambda\lambda\lambda$4634-40-42 emission, strong He II λ4686 absorption
(f*)	O2-O3.5	N IV λ4058 emission ≥ N III $\lambda\lambda\lambda$4634-40-42 emission, weaker He II λ4686 absorption
f*	O2-O3.5	N IV λ4058 emission ≥ N III $\lambda\lambda\lambda$4634-40-42 emission, He II λ4686 emission
c	O2-O8.5	Added to one of the six previous cases as e.g. ((fc)) or fc* when C III $\lambda\lambda\lambda$4647-50-51 emission ≥ N III $\lambda\lambda\lambda$4634-40-42 emission
f?p	O6-O8.5	Variable C III $\lambda\lambda\lambda$4647-50-51 emission ≥ N III $\lambda\lambda\lambda$4634-40-42 emission at maximum; variable sharp absorption, emission, and/or P Cygni features at H and He I lines
(n)fp	O	He II λ4686 centrally reversed emission, slightly broadened absorption lines
nfp	O	He II λ4686 centrally reversed emission, broadened absorption lines
z	O2-O8	He II λ4686 in absorption and > than both He I λ4471 and He II λ4542
N	O+B	N absorption enhanced, C and O deficient
N str	O+B	Moderate case of above. Nstr sometimes also used
C	O+B	C absorption enhanced, N deficient
N wk	O+B	Moderate case of above, Nwk sometimes also used
He str	B0-B3	Exceptionally strong He lines
He wk	B3-B9	Exceptionally weak He lines
p	B+A	Abnormally strong selected metal lines, additional notation for different elements
m	A	Abnormally strong metal lines, additional notation for Ca, H, and metallic spectral types
λ Boo	A+F	λ Boo population I stars, additional notation for Ca, H, and metallic spectral types
shell	B-F	Shell star
CN	G+K	Abnormal CN bands, followed by a numerical qualifier
CH	G+K	Abnormal CH bands, followed by a numerical qualifier
Ba	G-M	Abnormally strong Ba lines (and other s-process element lines), followed by a numerical qualifier
Fe	G-M	Abnormal Fe lines, followed by a numerical qualifier

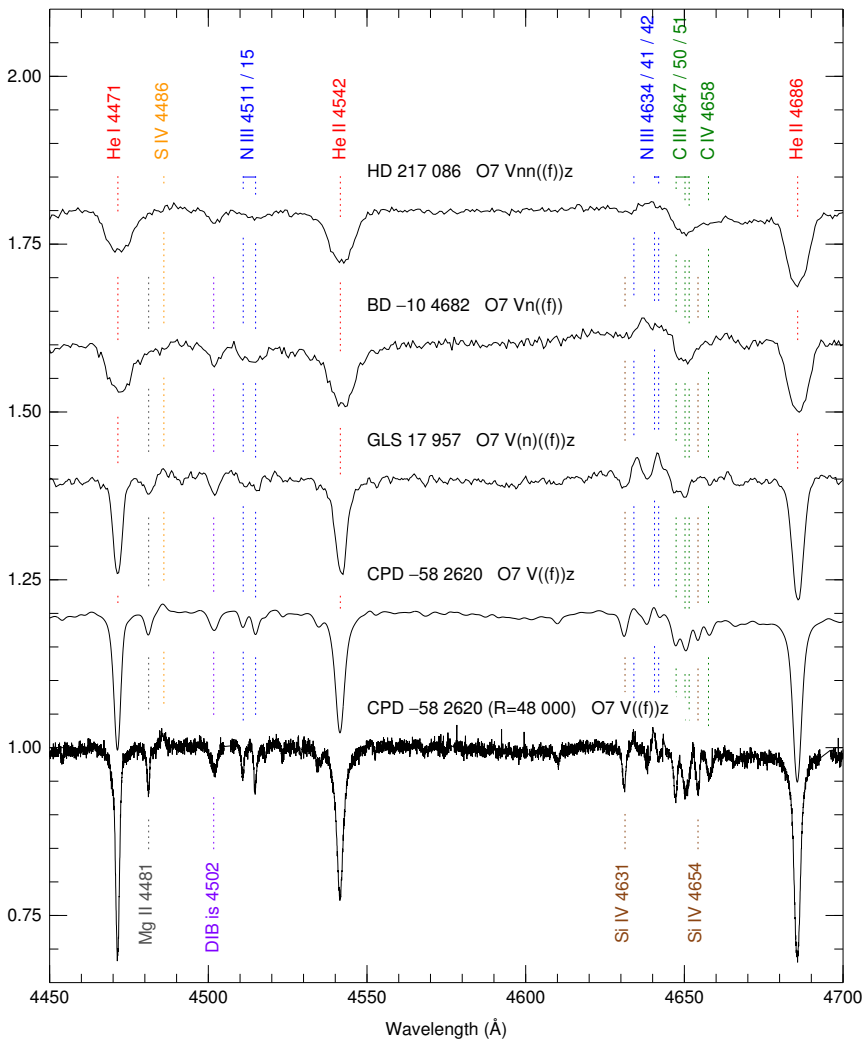

Fig. 4 Examples of line broadening or n index. We show four stars with very similar spectral classifications except for their n indices. The bottom star is shown at high spectral resolution and at the standard $\mathcal{R} \approx 2500$ resolution for spectral classification, which is the one used for the other three stars. All spectra are from GOSSS or LiLiMaRlin and are rectified and separated by 0.2 continuum units. Rotation broadening dilutes lines while approximately maintaining their EWs, something that can be appreciated in the constancy of the ratio of He II λ4542/He I λ4471 ($\sim$1, as required for the O7 subtype) despite the different ratio of the depths (a consequence of how Stark broadening acts for neutral and ionized He). Weak lines are hard to detect for high $v \sin i$ values (increase in n index). The diffuse interstellar band (DIB) maintains its shape but has a different EW for each star.

3.3 Suffixes/qualifiers: line broadening, emission lines, and others

The possible third component of the MK system is a suffix or qualifier. A list of the most common ones is given in Table 1, note that the Aristotelian morphological nature of the MK process leads to an organic growth in their number with time, as more stars are observed and in more detail. Most suffixes qualify the whole classification except for the : qualifier used to express uncertainty in either the spectral type or the luminosity class. For that reason, suffixes are written at the end of the spectral classification but : may be written after the spectral type: As a result, G2: V means that the spectral type is uncertain and G2 V: that the luminosity class is uncertain. The rest of the qualifiers indicate additional characteristics that cannot be described by the spectral type and luminosity class. In Table 1 the suffixes are grouped by theme, first the general ones that apply to all or most spectral types divided in miscellaneous, line width, and emission line presence; and then the ones that apply to certain spectral ranges. Here we discuss some aspects of the general suffixes and leave the specific ones for later.

In general, cool-star spectra (Secchi class II, see Fig. 1) are dominated by numerous narrow absorption metallic lines while hot stars (Secchi class I, see Fig. 1) have fewer lines of different intrinsic widths: narrow metallic lines followed by lines of He I, He II, and H of increasing intrinsic width due to the Stark (pressure) broadening effect. In addition to intrinsic effects, lines may be broadened by extrinsic effects, of which the three most common ones are double (or triple) spectroscopic binarity, stellar rotation, and the Zeeman effect. For SB2/SB3 systems whose observed radial orbital velocity difference is large enough, one can provide two or three spectral classifications, one for each stellar component. However, when the observed velocity values are small (because the system was observed in an unfavorable orbital phase or the radial velocity amplitude is small), only a broadened profile is observed for all or some of the absorption lines. In those cases, a broadening index is used for O-F stars (see Table 1) in the temporary spectral classification until one with multiple components can be provided (sometimes through techniques such as spectral disentangling, e.g. Simon and Sturm 1994).

The second major effect that can cause line broadening is stellar rotation, which is usually a small effect for late-type unevolved stars but can be very significant in other cases such as early-type stars of different evolutionary stages. For those, the rotation speeds can be measured in hundreds of km/s. When the broadening becomes significant, we start with an (n) index (some authors even include an ((n))

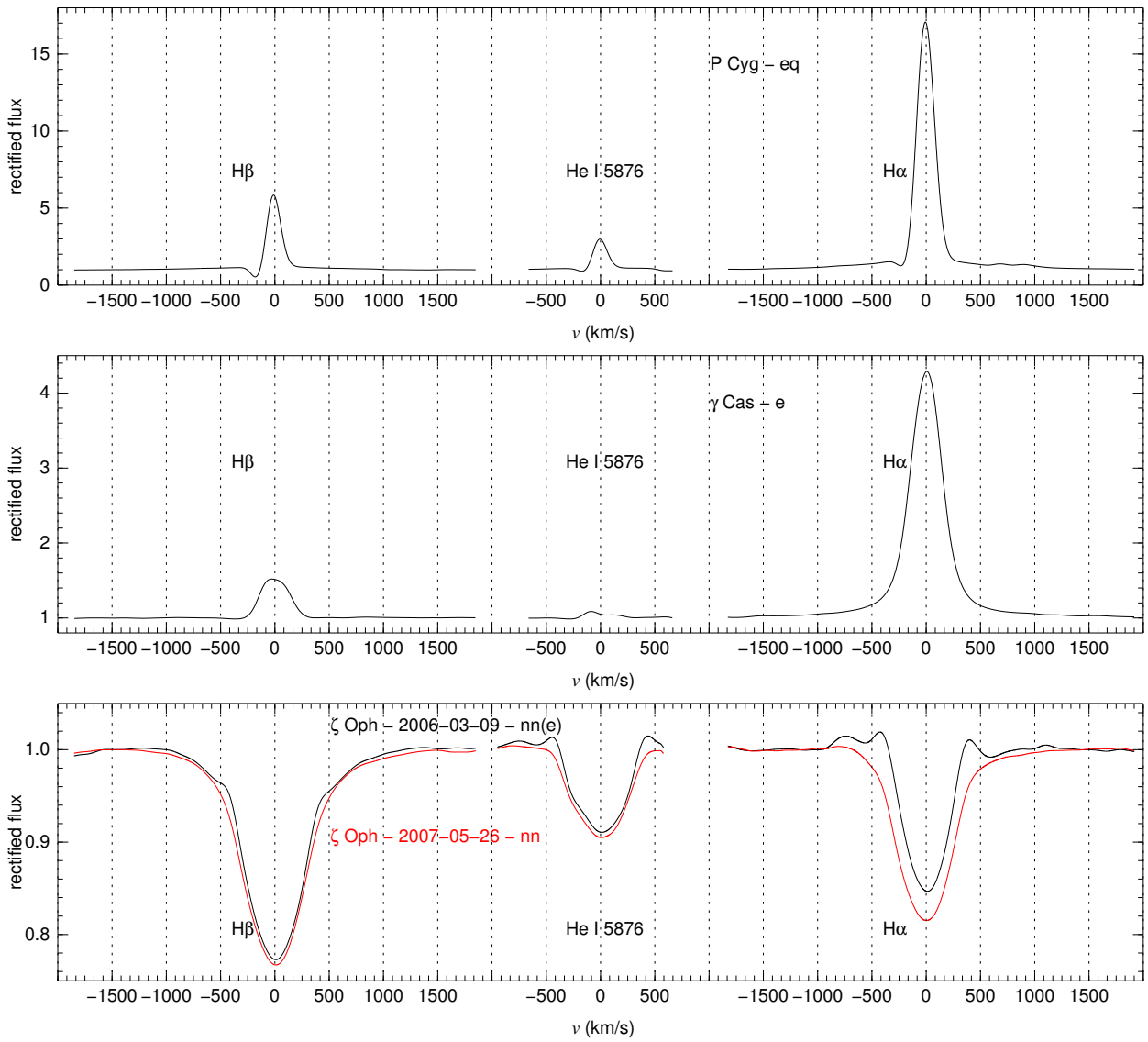

Fig. 5 Examples of e emission suffix and its variants (P Cygni, strong, and weak) for three stars for which we show relevant lines at $\mathcal{R} \approx 2500$ resolution using the same velocity scale. All spectra are from LiLiMaRlin and are rectified. Note the very different vertical scales for each star. ζ Oph goes through nn(e) and nn states, one example is given of each (dates indicated). The use of the suffix and its variants is not uniform among authors, with some reserving e for when the line rises above the continuum.

index for a broadening detectable only at high spectral resolution) and we progress to n, nn, and nnn as the projected rotational velocity ($v \sin i$) becomes larger (Fig. 4). An approximate correspondence between n-type indices and $v \sin i$ for O stars is given in Table 1 (Sota et al., 2011; Holgado et al., 2022). The effect of rotation broadening has to be considered because it affects lines of different intrinsic width differently: it is more easily noticeable in intrinsically narrow lines (e.g. metallic) than in intrinsically broad ones (e.g. hydrogen). Rotation broadening should not significantly affect line ratios measured from line strengths (determined as area eye estimates or equivalent widths) but can affect those measured from line depths (a notorious example is He I λ4471/He II λ4542, the primary spectral subtype criterion for O stars, see Fig. 4), which is the reason why the latter should be avoided. Modern software used to classify spectra by comparing with standards (e.g. MGB, Maíz Apellániz et al. 2012) includes this effect by selecting only standards with low $v \sin i$, which can be artificially broadened for comparison purposes.

A caveat that affects the determination of line broadening is the dependence on the spectral resolution of the spectrograph (Fig. 4). Unless mentioned otherwise, we assume a spectral resolution $\mathcal{R} \equiv \Delta\lambda/\lambda \approx 2500$, which is the closest one to the original one in the MK atlas[5], though

[5]The standard $\mathcal{R}$ is defined as approximately 2500 (meaning in the 2200-2800 range) because, in practical terms, it is not feasible to have spectra with exactly $\mathcal{R} = 2500$ for a large ground-based sample, either because of calibration issues or because one or several of the spectrographs provide a constant $\Delta\lambda$ instead of a constant $\mathcal{R}$.

other works have experimented with a higher $\mathcal{R}$ of 4000 (Walborn, 1971c; Negueruela et al., 2024). It is possible to compare standards at that resolution with stellar spectra at higher resolution if the latter are degraded to $\mathcal{R}$ = 2500 (easy to do with digital data, Fig. 4) and one gets the added benefit of an improved S/N (Signal-to-Noise ratio) in the process. If the stellar spectra are of lower resolution, limitations arise due to the difficulty in detecting weak lines, separating them, and correctly assigning an n-type index, so the spectral classifications will be of lower quality.

The most common emission lines present in stellar spectra are the Balmer lines, either of wind, chromospheric, circumstellar (e.g. disk accretion), or nebular origin, but others may be present. The first three origins are considered intrinsic to the stellar spectrum and the fourth one is regarded as a contaminant and neb is used in that case (Table 1). The e emission suffix and its variants are used to indicate the presence of emission lines (mostly Balmer lines but possibly others, see Table 1 and Fig. 5) and the f and related indices are reserved for O stars, where weak emission features from strong winds are common. In later-type stars, emission is sometimes related to youth (pre-main-sequence stars, most commonly Herbig Ae/Be and T Tauri stars), chromospheric activity, or both. Chromospheric activity manifests itself preferentially in the Ca H & K lines in the blue-violet range but in the reddest cooler stars and with the newest instrumentation, this chromospheric emission is better investigated in Hα and Ca II $\lambda\lambda\lambda$8498,542,662. In the system devised by Gray et al. (2003), a weak emission reversal in these lines is indicated by the qualifier (k), while a stronger emission core is marked by k. When the emission goes above the continuum, the standard qualifier e is added, but in cases with strong emission and accompanying Balmer emission, kee is used. A different issue is that of stars dominated by emission lines, such as Wolf-Rayet stars, for which the classification criteria are determined by the emission lines themselves and the few absorption lines (usually from hydrogen) that may be present are included in the qualifier.

3.4 Beyond OBAFGKM and 2-D classification

The classical textbook definition of the MK system as a 2-D classification system with seven spectral types is challenged from three different points of view:

- **More than seven spectral types.** A century after the beginning of the development of the Harvard system, three new spectral types (L, T, and Y) were added to the sequence at the low-temperature end thanks to the discovery of brown dwarfs. Therefore, the current sequence is OBAFGKMLTY, which has made the famous English mnemonic evolve into "Oh, Be A Fine Girl/Guy, Kiss My Lips Tonight, Yo" or "... Kiss Me, Less Talk, Yo" (and the Spanish one to "Obesos, Bebed Aceite Filtrado, Ganaréis Kilos Mirando La Televisión Ya(ciendo)"). The new types are described in the ultracool spectral types subsection below.
- **Evolved stars with anomalous compositions.** From the pioneering times of the 1860s, two types of stars were discovered that could never be fit into the normal spectral-type sequence: Carbon (C) stars and Wolf-Rayet stars. Both cases turned out to be objects with large anomalous surface compositions (and conditions, especially so for WRs) that resulted from being evolved objects (especially so for carbon stars) at the cool and hot edges of the $T_{\rm eff}$ scale. Later on, other types of stars with different large anomalous compositions caused by stellar evolution such as S stars and some white dwarfs (WDs) were added to the list. In contrast, some other objects have relatively minor composition anomalies that allow them to be included in the standard 2-D grid with the help of qualifiers (see examples in Table 1 and below), but the first four classes (C and S stars, WRs, and WDs) deserve their own independent categories.
- **A third dimension?** The obvious candidate for a third dimension in spectral classification is metallicity. Starting with Roman (1950), spectral differences that depend on the initial composition of the star were determined and a rich field that eventually measured metallicities in Galactic metal-poor stars was established. For spectral classification purposes, anomalous compositions or metallicity differences are determined by comparing ratios of lines from the same species (composition or metallicity independent) with ratios of lines from different species (dependent) and establishing classification criteria from them. Such systems that add a third dimension through suffixes exist but with limitations (Gray and Corbally, 2009): they are mostly confined to the regions of the HRD that can be sampled on nearby Galactic populations and the criteria may rely on weak lines only easily observable at resolutions higher than 2500 or be confined to a spectral-type range. The efforts to study low-metallicity stars have recently gained strength with the advent of large telescopes equipped with multi-fiber spectrographs, which allow for the execution of massive spectroscopic surveys of Galactic metal poor populations (e.g. Gaia-ESO, Gilmore et al. 2012; Randich et al. 2022) and reach nearby galaxies containing large numbers of metal-poor stellar types that cannot be easily found in the Milky Way. Most of the LMC stars are likely not metal poor enough to detect a large effect (Walborn et al., 2014) but we may have better luck with the SMC (Lennon, 1997, 1999; Evans and Howarth, 2003; Vink et al., 2023). Such efforts are mostly directed towards quantitative spectroscopy, but they can in principle be used for spectral classification as well.

3.5 Other wavelength ranges

It is possible to transport the MK system to other wavelengths outside the 3900–5000 Å reference range by observing the standards in both ranges and establishing the corresponding classification criteria. However, it is beyond the scope of this entry to review the large field of spectral classification outside the blue-violet range for lack of space, so the reader is referred to Gray and Corbally (2009) for details on how this is done. Here we just briefly mention some of the advantages and disadvantages of this field.

The advantages of using other wavelength ranges can be divided in intrinsic and extrinsic ones. Intrinsic advantages are those associated with the stars themselves. For example, OB stars are bright and rich in lines (some without correspondence in the optical) in the ultraviolet, so their UV spectral classification allows us access to new characteristics such as wind effects (Walborn et al., 1985, 1995; Rountree and Sonneborn, 1991; Smith Neubig and Bruhweiler, 1997, 1999). For M and cooler objects, there is very little flux shortward of 5000 Å, making the red and infrared ranges preferred. Extrinsic advantages are those not associated with the targets, of which the most obvious example is the use of the infrared to observe targets with high extinction. The disadvantages of using other wavelength ranges are the possible difficulty or impossibility in accessing them (e.g. the UV or regions of the mid-infrared from the ground) and the lack of lines

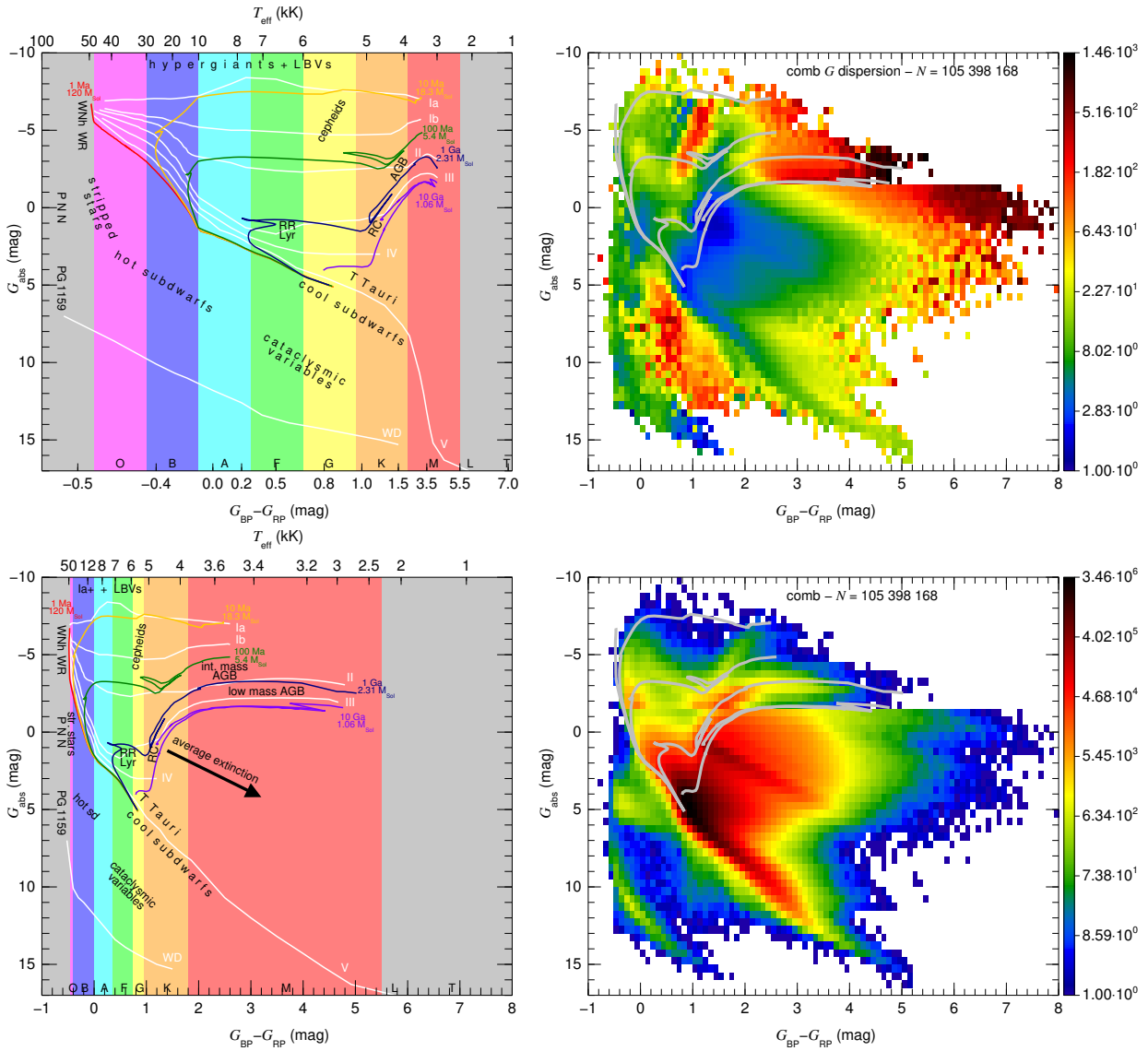

Fig. 6 Exploring the spectral classes. (Left column) HRD (top) and CAMD (bottom) with the sequences for different luminosity classes and white dwarfs (white), solar-metallicity isochrones of different ages (in color and labelled with their ages and maximum initial masses, all minimum initial masses are set to 1 $M_\odot$), and different types of stars labelled (black). The two frames use common spectral type - $T_{\rm eff}$ - color scales that are only approximate, as they depend also on luminosity and metallicity. (Right column) *Gaia* data from Maíz Apellániz et al. (2023) to use as comparison, with objects brighter that $G_{\rm abs} = -1.5$ mag selected from the LMC sample (weak extinction) and objects fainter than that from the Milky Way sample (highly variable extinction, approximate direction marked with an arrow but see Maíz Apellániz 2024). The top panel shows the average amplitude of the variability in the G band in mmag and the bottom panel the source density, see Maíz Apellániz et al. (2023) for details.

required to accurately classify some spectral types. One should keep in mind that the blue-violet region is rich in spectral lines (especially for some spectral types) and without telluric lines (Fig. 1), which are some of the reasons for the success of the original MK system.

One particular mission that is likely to revolutionize spectral classification in the next decade is *Gaia* (Prusti et al., 2016), as it has already obtained more optical spectra that the rest of the astronomical spectrographs in history combined. One instrument, the Radial Velocity Spectrometer (Cropper et al., 2018; Recio-Blanco et al., 2023), is obtaining $\mathcal{R}$ = 11 500 spectroscopy in the 8470-8740 Å range for unobscured stars as faint as V = 16.5 for spectral type G2 V (the V limiting magnitude depends on spectral type and extinction) and can be used for standard spectral classification in the Ca triplet window. Alternatively, the data from the two low-resolution spectrographs can be combined to obtain $\mathcal{R}$ =30-100 spectra in the 3400-10 200 Å reaching even fainter stars (De Angeli et al., 2023). The low resolution implies that only strong lines are easily detected and the variable $\mathcal{R}$ across the range requires some special techniques to analyze the spectra (Weiler et al., 2023) but the exceptional *Gaia* flux calibration may compensate for it by e.g. measuring several Wolf-Rayet lines or the amplitude of the Balmer jump.

3.6 A brief excursion through the spectral classes

Before embarking on the spectral classification of different types of stars, we present Fig 6 as a tool to explore their different locations in an HRD or CAMD. The top left panel is a standard HRD with a linear scale in the seven spectral types OBAFGKM. As a means of comparing scales, we also show in the horizontal axes the $T_{\rm eff}$ (top) and *Gaia* $G_{\rm BP} - G_{\rm RP}$ color (bottom, see Maíz Apellániz and Weiler 2018 for band definitions), but note that those are approximate correspondences, as the $T_{\rm eff}$ and color of a given star also depend on luminosity class (or gravity) and metallicity. We plot the location in the HRD of different types of stars mentioned later in the text, as well as different luminosity classes (morphologically defined) and solar-metallicity isochrones (astrophysically calculated).

The bottom left panel of Fig. 6 is the *Gaia* CAMD equivalent to the HRD in the top left panel. It is presented as a way to directly compare observational CAMD diagrams (see description of right column panels) with the expected location for the different classes and types of stars presented below in the text. Two immediate observations can be made: [1] Late-type stars (and especially those of M type) cover a much larger dynamical range in $G_{\rm BP} - G_{\rm RP}$ (and in most optical colors) than in spectral type. Note in particular how hot stars are hard to differentiate based on $G_{\rm BP} - G_{\rm RP}$ alone. [2] The direction of an average extinction is marked by an arrow, but the direction of a given extinction can be somewhat different, as it also depends on the spectral type of the star and the amount and type of dust (Maíz Apellániz, 2024).

The bottom right panel of Fig. 6 is the density of *Gaia* sources, with objects brighter than $G_{\rm abs} = -1.5$ mag selected from the LMC sample and objects fainter than that from the Milky Way sample. The reason for the division is that most of the LMC has a low extinction and a large population of luminous stars that is easy to associate with the different stellar types described in the text. *Gaia* includes a much larger sample of Galactic stars but the highly variable degree of extinction blurs their location in the CAMD, something that is especially important for the most luminous stars due to their high average extinction in the Galactic sample. The most graphic tracer of the effect of extinction in this panel is how the Red Clump (RC) locus is transformed from a point into a (nearly straight but not perfectly so) line.

Finally, the top right panel of Fig. 6 is the average G band photometric dispersion of the stars in the lower right panel (see Maíz Apellániz et al. 2023 for details). This panel is included to be used with the discussions below on the photometric variability of different types of stars.

4 Spectral classification of hot stars

We define hot (or early-type) stars as those originally in Secchi's classes I and V, which in the standard spectral type sequence corresponds to O, B, A, and some F stars. The rest of the Secchi's classes correspond to cool (or late-type) stars and are analyzed in the next section, where we include all F stars (the transition spectral type) except RR Lyrae for simplicity. For an extensive description of the spectral classification of hot stars, the reader is referred to Gray and Corbally (2009), including its chapter 3 on OB stars by Nolan R. Walborn. Most of Gray and Corbally (2009) remains up to date save for some significant modifications for O stars from the GOSSS project (Maíz Apellániz et al., 2011) and some minor ones for B stars (Negueruela et al., 2024) and WR stars (Crowther and Walborn, 2011), as described below. One important nomenclature issue (often missed in the literature) is that an OB star is not simply a star of either O or B spectral type, as one additional condition is required: that it is a massive star ($M \gtrsim 8$ M$_\odot$). In spectral types terms, a working approximate definition is that it is of spectral subtype B2 or earlier if a dwarf, of B5 or earlier if a giant, and of any O or B type if a supergiant (Morgan 1951 and chapter by Walborn cited above). The distinction is important because most B stars are mid-to-late dwarfs, hence, of intermediate mass.

This section is divided into four parts: one each for "normal" stars of spectral types O, B, and A, and a last one for other hot stars, most of them highly evolved objects.

4.1 O stars

O stars are the hot end of the spectral type sequence and, as such, were one of the last spectral types to have a fully developed classification grid. The original MKK atlas had O4 as the earliest spectral subtype and luminosity classes were only defined for O9 and O9.5 stars. Most of the subsequent work was done by Nolan R. Walborn or under his auspices from the 1970s to the 2010s[6]. He proposed luminosity classification criteria for the whole spectral type range (Walborn, 1971c), extended the spectral subtype range first to O3 (Walborn, 1971b) and then to O2 (Walborn et al., 2002), discovered the existence of carbon and nitrogen anomalies (Walborn, 1971a, 1976) and of the Onfp and Of?p phenomena described below (Walborn, 1972), and compiled an atlas of extreme stars of different OB types (Walborn and Fitzpatrick, 2000). He also helped to found the GOSSS project that has introduced further refinements to the spectral classification of O stars: the discovery of the Ofc phenomenon (Walborn et al., 2010), the extension of the O9.7 subtype to all luminosity classes (Sota et al., 2011), the definition of the O9.2 subtype (Sota et al., 2014), the extension of luminosity class IV to subtype O4 (Maíz Apellániz et al., 2016), and the first large study of the OVz phenomenon (Arias et al., 2016). In a future paper with GOSSS data (Maíz Apellániz et al. in preparation) the luminosity class II will be extended to the full O spectral type range.

4.1.1 Classification criteria for O stars

Spectral type. The primary classification criterion for spectral subtype is the He II λ4542/He I λ4471 ratio, which is unity at O7 (Figs. 4, 7), higher for earlier subtypes, and lower for later ones. Near both extremes of the sequence, additional criteria are used. For the earliest subtypes, the N IV λ4058/N III $\lambda\lambda\lambda$4634-40-42 ratio is used instead due to the common contamination of He I λ4471 by hidden OB

[6] See also the series of papers by Peter Conti and collaborators starting with Conti and Alschuler (1971).

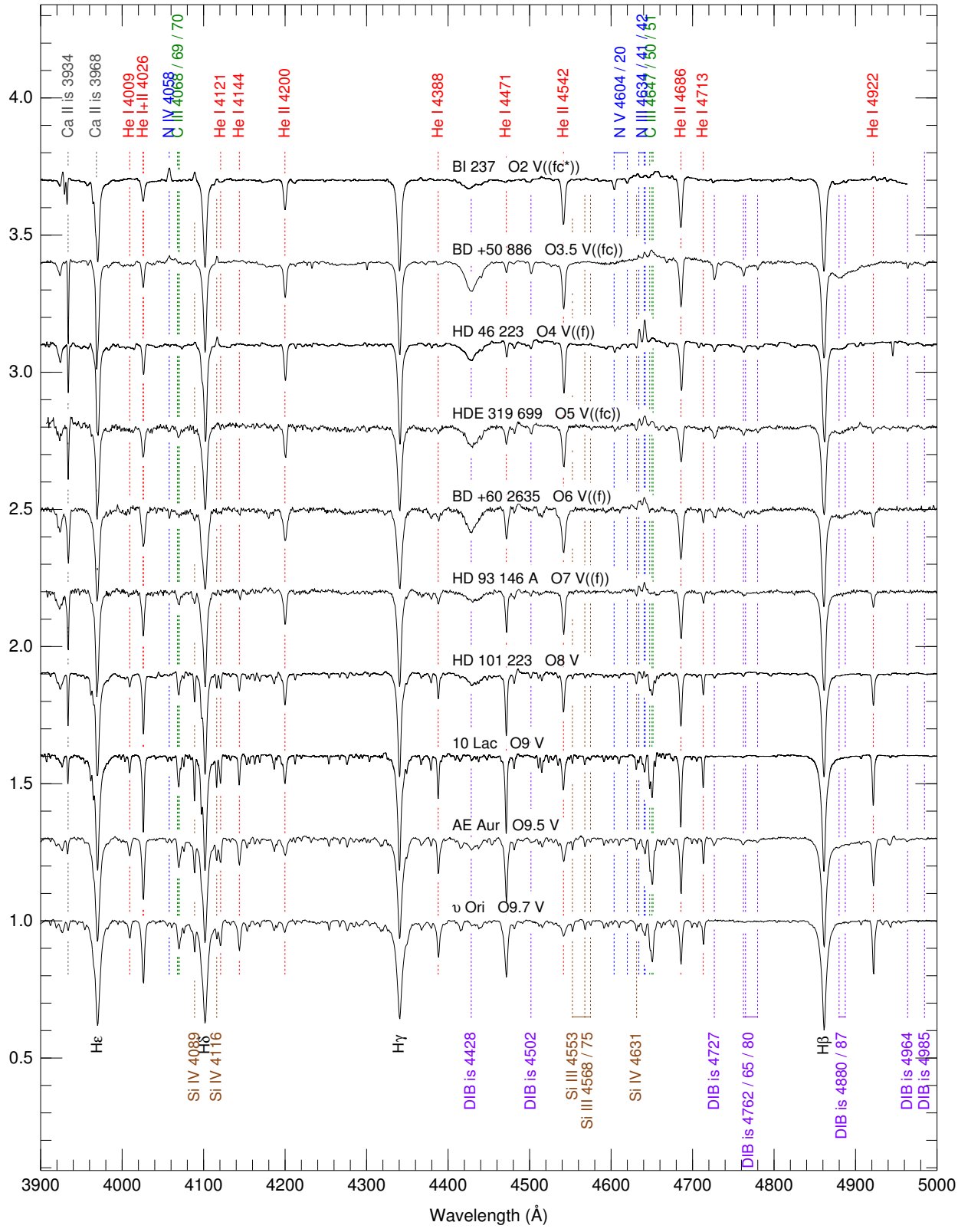

Fig. 7 Spectral type sequence for O dwarfs at $\mathcal{R} \sim 2500$. Spectra are rectified, separated by 0.3 units, and from GOSSS or LiLiMaRlin.

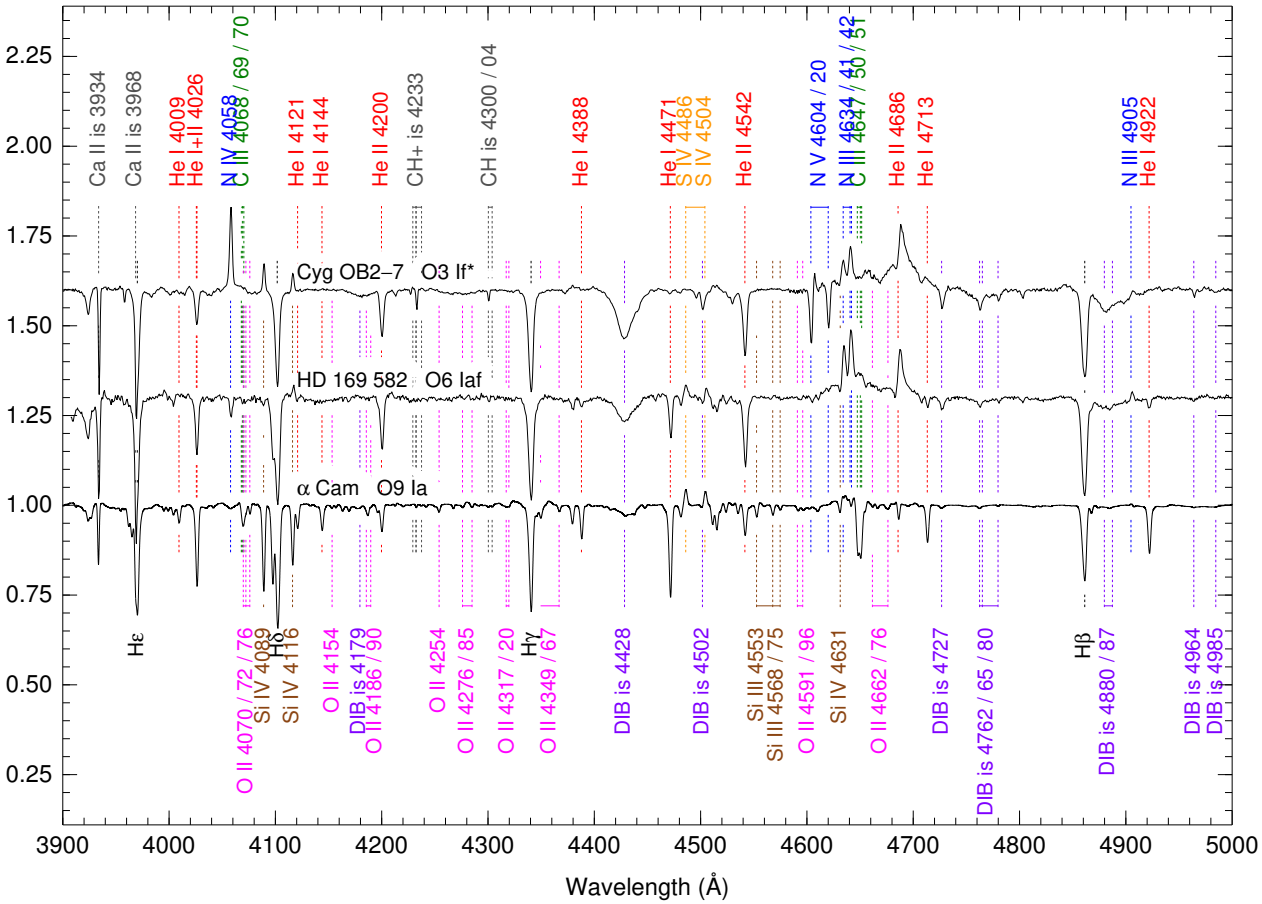

Fig. 8 Examples of an early-, a mid-, and a late-type supergiants at $\mathcal{R} \sim 2500$. Spectra are rectified, separated by 0.3 units, and from GOSSS or LiLiMaRlin.

companions (Table 3 in Walborn et al. 2002). For late-O stars, the additional criteria are He II λ4542/He I λ4438 and He II λ4200/He I λ4144 (both unity at O9) on the one hand and Si III λ4552/He II λ4542 (unity at O9.7) on the other (Table 3 in Sota et al. 2014). Originally, O stars were defined as those having He II lines but, with modern digital spectra at good S/N and $R \approx 2500$, He II λ4542 is now detected until ~B0.5 and He II λ4686 until ~B1.

Luminosity class. The primary luminosity criterion for O stars is the Of phenomenon (Walborn, 1971c), by which (a) He II λ4686 goes from strong absorption in dwarfs to emission in supergiants (a negative luminosity effect from the point of view of absorption) and (b) N III $\lambda\lambda\lambda$4634-40-42 in emission increases in intensity along the same sequence. The Of phenomenon is expressed using the qualifiers in Table 1. He II λ4686 and N III $\lambda\lambda\lambda$4634-40-42 are selective emission lines, that is, they can be in emission while other lines of the same ion remain in absorption. The OVz phenomenon (Arias et al. 2016, see criterion in Table 1) is the opposite of the Of effect: OVz stars correspond to objects near the ZAMS and have He II λ4686 in absorption stronger than normal class V stars. The location of the normal V sequence above the ZAMS can be seen in the top left panel of Fig. 6 by comparing it with the 1 Ma isochrone, which is a reasonable approximation to the latter.

The Of and OVz phenomena are not caused directly by luminosity but indirectly: they represent the infilling of absorption lines by the increase in the strength of the wind that accompanies an increase in luminosity for a constant $T_{\rm eff}$. The Of phenomenon appears in early- and mid-O supergiants and is stronger for the earliest subtypes (Fig. 8). The standard Of phenomenon is shown in the left panel of Fig. 9 but for early types the phenomenon is even stronger and involves other selective emission lines such as N IV λ4068, Si IV λ4089 and Si IV λ4116 (top panel of Fig. 9). For late-O stars (right panel of Fig. 9) the OVz phenomenon disappears and only a weak version of the Of phenomenon is present, not affecting N III $\lambda\lambda\lambda$4634-40-42 and only showing up with a progressive infilling of He II λ4686.

The decay of the Of effect with increasing spectral subtype leads to the development of other luminosity criteria for late-O stars (which extend into the B stars, as we will see below). The most commonly used one is the ratio of either Si IV λ4089 or Si IV λ4116 to He I λ4026 or He I λ4144 (right panel of Fig. 9), with the Si absorption lines showing a positive luminosity effect. Note that the use of a Si/He line ratio may be sensitive to metallicity effects while some He lines experience complex behaviors when originating from unresolved binary systems composed of a late-O and an early-B star (which are quite common, see Simón-Díaz et al. 2015), and so luminosity discrepancies between

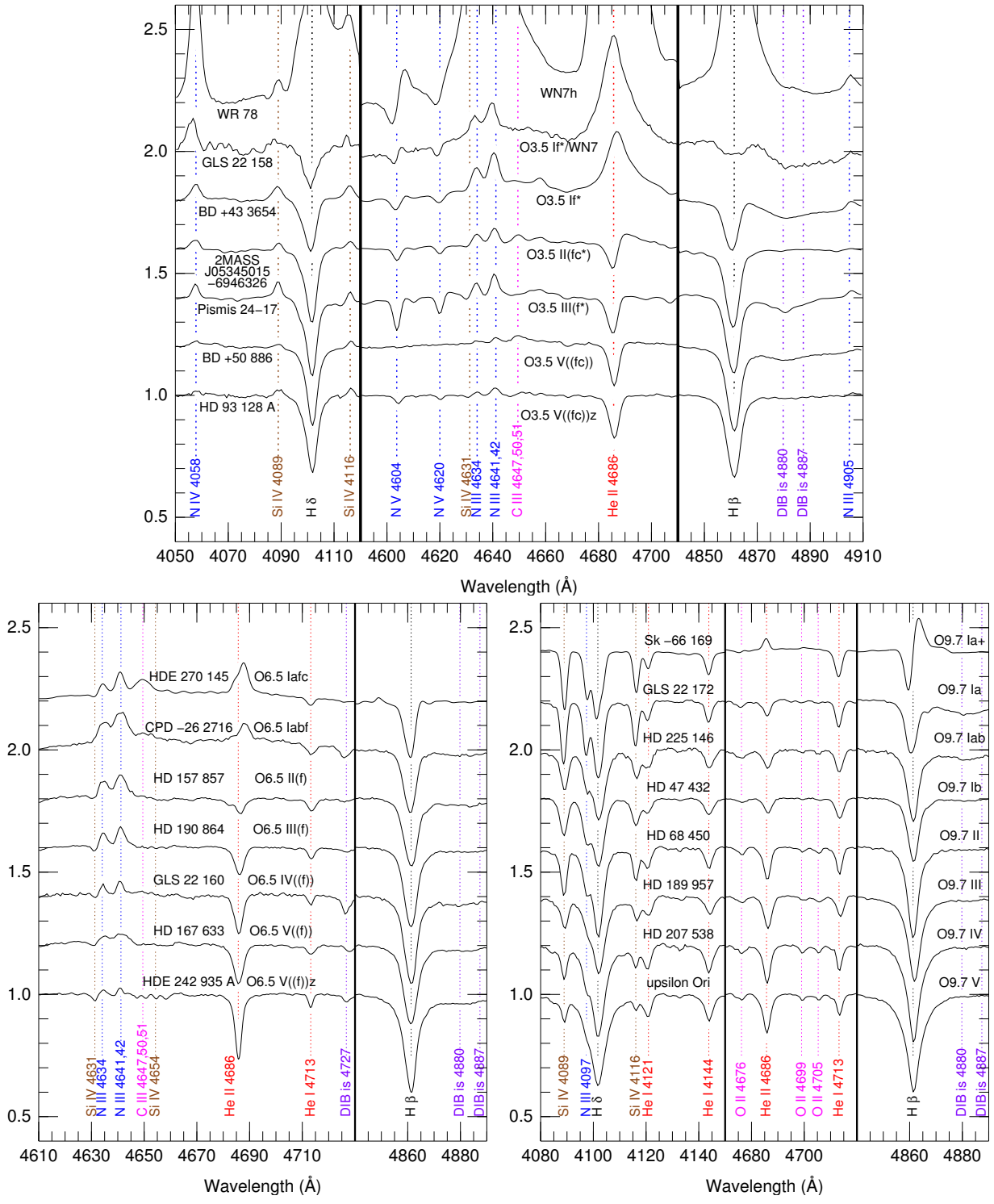

Fig. 9 Luminosity class sequences for O3.5 (top), O6.5 (left), and O9.7 (right) at $\mathcal{R} \sim 2500$. Spectra are rectified, separated by 0.2 continuum units, and from GOSSS or LiLiMaRlin. The O3.5 sequence includes an Of/WN star (GLS 22 158) and a WN star (WR 78), with part of the intense emission lines of the second object outside the frame.

different criteria in the spectral subtype range are common (Walborn et al., 2014).

We also point out that one of the luminosity criteria for B and A stars, the width of the Balmer lines, may also be used to some degree for O stars. The negative luminosity effect due to the Stark effect is clear for late-O types (right panel of Fig. 9) and is combined with a wind

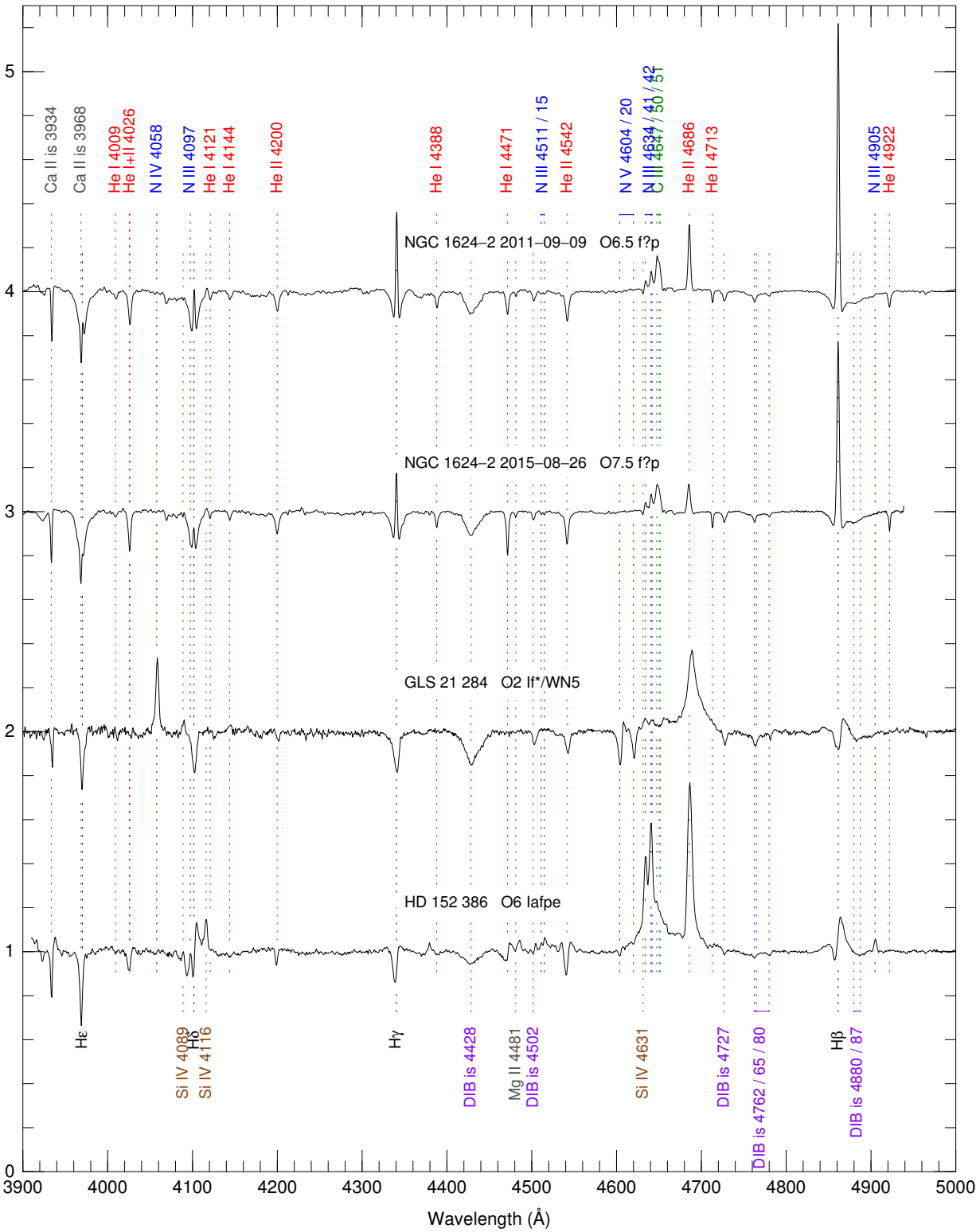

Fig. 10 Examples of an Of?p, an Of/WN, and an O Iafpe stars at $\mathcal{R} \sim 2500$. For the Of?p star, two epochs with different spectral types due to the infilling of He I λ4471 are shown. Spectra are rectified, separated by one continuum unit, and from GOSSS or LiLiMaRlin.

infilling analogous to the Of phenomenon that is strong enough to create P-Cygni profiles in Hβ for O9.7 hypergiants and Of/WN stars (top panel of Fig. 9, be careful with the broad double DIB to the right of Hβ, Maíz Apellániz et al. 2014). The wind infilling effect is even more noticeable for Hα, outside the blue-violet range, but is weak or disappears for Hγ and higher-order Balmer lines.

For O stars, one should not equate the main sequence (MS) phase of stellar evolution with luminosity class V. O-type giants and even supergiants are still burning hydrogen in their cores (Martins and Palacios, 2017). For most B and A stars, the transition between core and shell hydrogen burning happens during or near the end of their giant phase. Some early-B supergiants may also be burning hydrogen in their cores, but this issue is still controversial (de Burgos et al., 2024). Therefore, in general the main sequence extends beyond luminosity class V for early-type stars.

4.1.2 Peculiar O stars

Here we briefly describe the peculiar categories for O stars.

- **Early Of/WN.** The Of phenomenon reaches its extreme with WNh stars (see below): high-luminosity, narrow-line, late-type WN stars (Walborn, 1974), which are early O supergiants on steroids in terms of wind strength. An intermediate class between those WN stars and early-O supergiants is the early Of/WN (or "hot slash") category (Walborn, 1982a; Sota et al., 2014). The dividing criterion is set by Hβ: It is in absorption for supergiants, has a P-Cyg profile for "hot slash" stars, and is in emission for WN stars (Crowther and Walborn 2011, top panel of Fig. 9 and Fig. 10).
- **O Iafpe.** Another class of extreme Of stars are the O Iafpe objects, which have a complex identification history. They were originally known as Ofpe/WN9, late Of/WN, or "cool slash" (Walborn, 1982b) but were subsequently reclassified as a cool extension to the late WN sequence (WN9-11, Crowther and Smith 1997). Some authors prefer their division into either O or WR stars (Crowther and Bohannan, 1997) while others group them in a single one as O Iafpe (Sota et al., 2014) because the category now includes stars as early as O4.5 and because they are not an intermediate stage between O supergiants and WN stars. Instead, they are objects that can be characterized as either. They are defined by having He I λ4471 P-Cyg profiles and a complex morphology in the Hδ region (Fig. 10).
- **Of?p.** Of?p stars (Walborn, 1972) are magnetic oblique rotators (Muñoz et al., 2020) that are characterized by strong and variable C III $\lambda\lambda\lambda$4647-50-52 emission accompanied by variable H and He lines that can appear in absorption, emission, or as P-Cyg profiles (Walborn et al., 2010). The variability is produced by the change in the direction from which the magnetosphere is observed and the variations in the infilling of He I λ4471 cause changes in the observed spectral type as a function of the rotational phase (Fig. 10). There are currently six known examples in the Milky Way (Maíz Apellániz et al., 2019b) and six in the Magellanic Clouds (Walborn et al., 2015a; Hubrig et al., 2024). Of?p stars are of mid-O spectral type and are isolated or in non-interacting binaries, but magnetism can occur in O stars under different circumstances and exhibiting different spectral phenomena (Nazé et al., 2016, 2017; Wade et al., 2020).
- **Ofc.** The Ofc phenomenon was discovered by Walborn et al. (2010) by analyzing the large sample of GOSSS stars with good-quality digital data. It takes place at early- and mid-O types and is characterized by C III $\lambda\lambda\lambda$4647-50-52 stable emission comparable to that of N III $\lambda\lambda\lambda$4634-40-42, sometimes with the addition of C IV λ4658 for the earliest types. Hence, it is integrated in the same nomenclature as the Of phenomenon adding a c (Table 1).
- **Onfp.** Onfp stars were defined by Walborn (1972) as Of spectra with He II λ4686 emission with a central reversal. Most of them are rapid rotators, hence the Onfp denomination.
- **ON/OC.** Walborn (1971a, 1976) discovered the existence of anomalous C and N line strengths with respect to the He+Si reference frame and devised a nomenclature for this class in the form of suffixes: N→N str→normal→N wk→C in order of decreasing N and increasing C strengths (Table 1). The surface composition of O stars may show signs of CNO processing in their interiors, having N enrichment and C depletion. Normal evolved O stars are N enriched with respect to their initial composition but some are more so (ON stars) and some less so (OC stars). The ON/OC phenomenon appears at late O and early B stars (though some very early O stars also show significant differences in the strength of N lines) and some ON giants are rapid rotators (ONn or "double n" stars, Walborn et al. 2011), pointing towards rotational mixing as a source of the additional enrichment.
- **Oe.** Oe stars are the hotter equivalent of Be stars (Negueruela et al., 2004), see below and Fig. 5.

4.2 B stars

Starting with the B spectral class we find significant differences between the natures of dwarfs and supergiants, with the latter being massive stars (8 $M_\odot$ or more, so they are able to fuse elements beyond helium in their advanced stages) and most of the former being of intermediate mass (which only reach helium burning and do so without a flash). For the earliest B types (B0-2), the difference is not yet large, as their luminosity class V are still massive and have MS lifetimes of 8-30 Ma. However, by the time we reach B9 V we find stars with masses around 3 $M_\odot$ and MS lifetimes around 300 Ma. Hence, early-B and late-B dwarfs are very different types of stars.

The whole range of the B spectral type was already covered in the MKK atlas, even though only the B0, B0.5, B1, B2, B3, B5, and B8 subtypes were included at first. By the time of Johnson and Morgan (1953) the B1.5, B6, B7, and B9 subtypes had already been added. The list was completed with B2.5 and B4 by Lesh (1968) and with B0.2 and B0.7 by Walborn (1971c). Morgan et al. (1978) also introduced the B9.5 subtype but the recent analysis by Negueruela et al. (2024) recommends not using it because it is difficult to differentiate from either B9 or A0. The reader is referred to Negueruela et al. (2024) for details, noting that reference also suggests the possibility of dropping the B4 subtype and merging B6 and B7 into one.

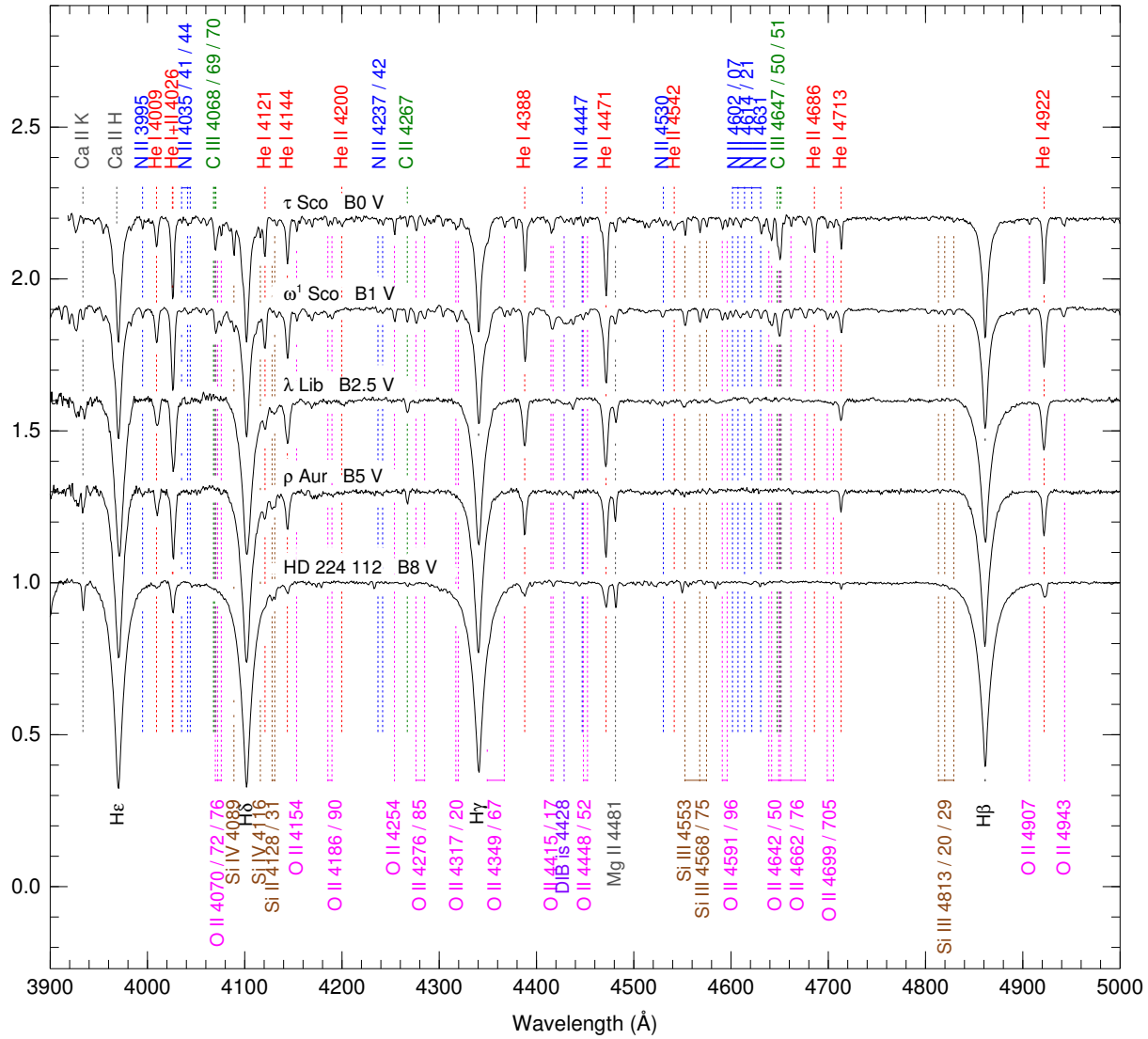

Fig. 11 Spectral type sequence for B dwarfs at $\mathcal{R} \sim 2500$. Spectra are rectified, separated by 0.3 continuum units, and from GOSSS or LiLiMaRlin. The Ca II H+K lines are of interstellar origin for the early-to-mid subtypes.

4.2.1 Classification criteria for B stars

Spectral type. There are three criteria that can be used to obtain the spectral subtype for B stars. Each one has its pros and cons, so they should be used in combination if possible. The spectral sequences for dwarfs and supergiants are shown in Figs. 11 and 12, respectively. See Gray and Corbally (2009) and Negueruela et al. (2024) for more details:

- *H and He.* Originally, B stars were defined as those with He I and without He II lines, but that is no longer valid with modern digital data. On the one hand, He II λ4542 can be detected until B0.5 and He II λ4686 until B1. On the other, He I λ4471 can be detected in early A stars, especially in supergiants. Besides the He II lines, the strength of the He I lines changes along the B spectral range and Balmer lines become increasingly stronger for later types. The combination of H and He lines can be used to determine or constrain the horizontal classification, especially for early subtypes, with two caveats: [a] the additional dependence of both of luminosity (Fig. 13) and [b] the possibility of He abundance anomalies, see subsection below on peculiar B stars.
- *Si.* The preferred criterion for obtaining the spectral subtype are the line ratios of Si lines: Si IV λ4089/Si III λ4552 for early subtypes and Si III λ4552/Si II $\lambda\lambda$4128,32 for mid and late subtypes. The main advantage is its independence of composition anomalies or metallicities. The main disadvantage is that the strength of the metal lines is luminosity dependent, making this criterion difficult to apply in mid and late dwarfs and late giants. This is worsened by the significant fraction of fast rotators among B stars, which can make weak Si lines more difficult to detect.
- *Mg/He and others.* The difficulty detecting weak Si lines may force the use of other criteria. Mg I λ4481/He I λ4471 is the most

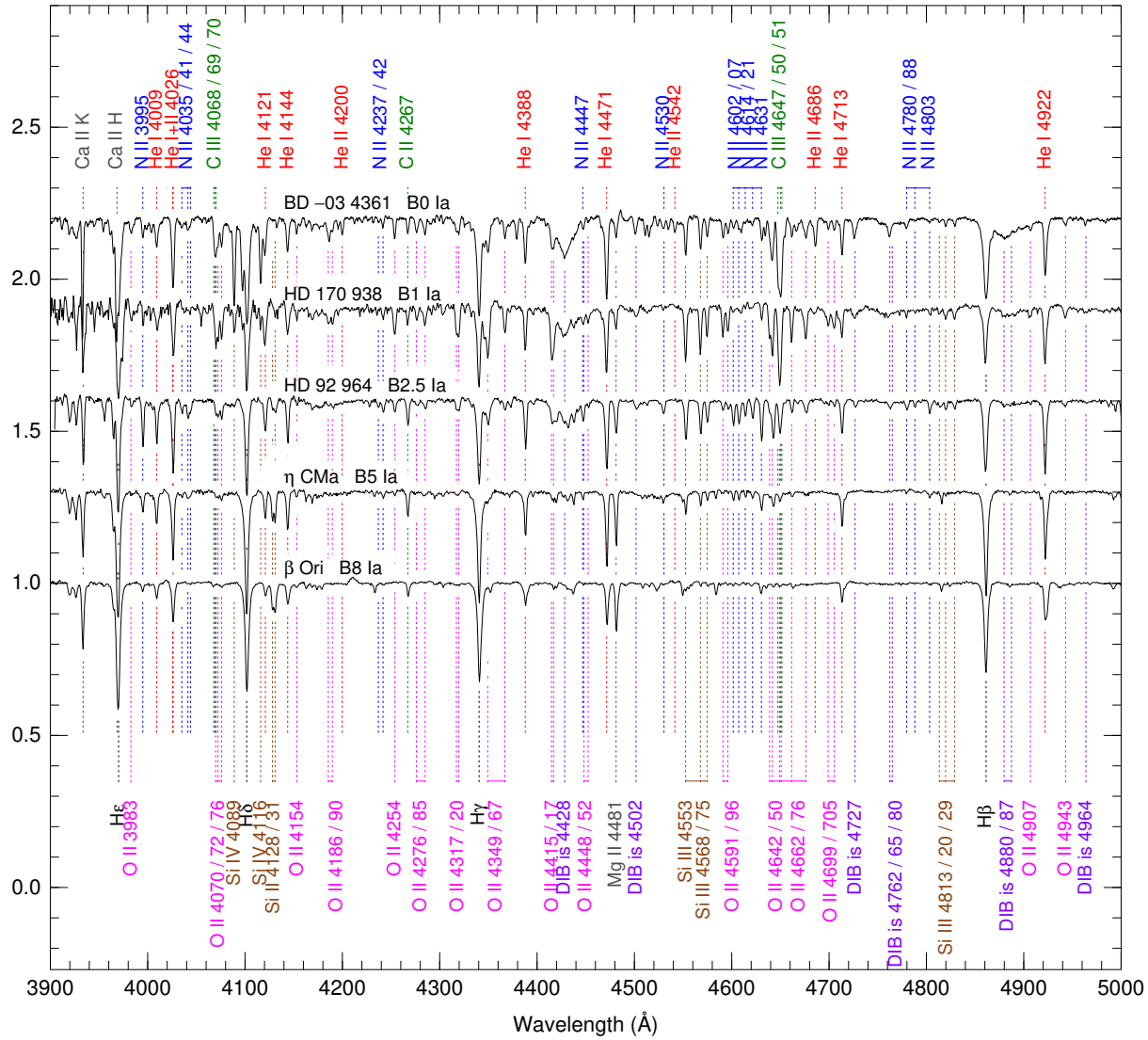

Fig. 12 Spectral type sequence for B supergiants at $\mathcal{R} \sim 2500$. Spectra are rectified, separated by 0.3 continuum units, and from GOSSS or LiLiMaRlin. The Ca II H+K lines are of interstellar origin for the early-to-mid subtypes.

important one, increasing with subtype until it becomes unity at B8. Two caveats are in order for this criterion: [a] He I λ4471 is intrinsically broader due to the Stark effect, so line strengths should be used, not depth (see line broadening above) and [b] the ratio is metallicity dependent, leading to different spectral subtypes than those from Si ratios at low metallicities (Lennon, 1997). In addition to Mg, other metallic lines can be used to constrain the spectral subtype. For example, C II λ4267 reaches its maximum strength at B2 for class V.

Luminosity class. As with the spectral type, there are also three luminosity classification criteria for B stars. Also, due to the effect of composition anomalies and metallicity effects, if possible they should be used simultaneously.

- *Si/He.* In general, metal lines show a positive luminosity effect and, of those, the most used ratios are Si IV λ4116/He I λ4121 for early-B subtypes and Si III λ4552/He I λ4387 or Si III λ4552/He I λ4471 for early- and mid-B subtypes. As those same Si lines are used to obtain the spectral subtype, both classifications have to be done simultaneously. The two objections to this criterion are its metallicity and He anomalies dependences and the weakness of the lines for late types.
- *H.* The width and EW of the Balmer lines depend on both the spectral subtype and the luminosity class (Balona and Crampton, 1974), leading to the diagonal effect where stars in a grid diagonal have a similar profile (Fig. 13): both the width and the EW increase with spectral subtype and with luminosity. Therefore, using a combination of the spectral type criteria and the diagonal effect, a full classification can be obtained. Traditionally, this method was used mostly for mid- and late-subtypes but Negueruela et al. (2024) have shown it can be used for all the B subtypes. For hypergiants (class Ia+) Hβ shows a P Cyg or emission profile, sometimes with a broad

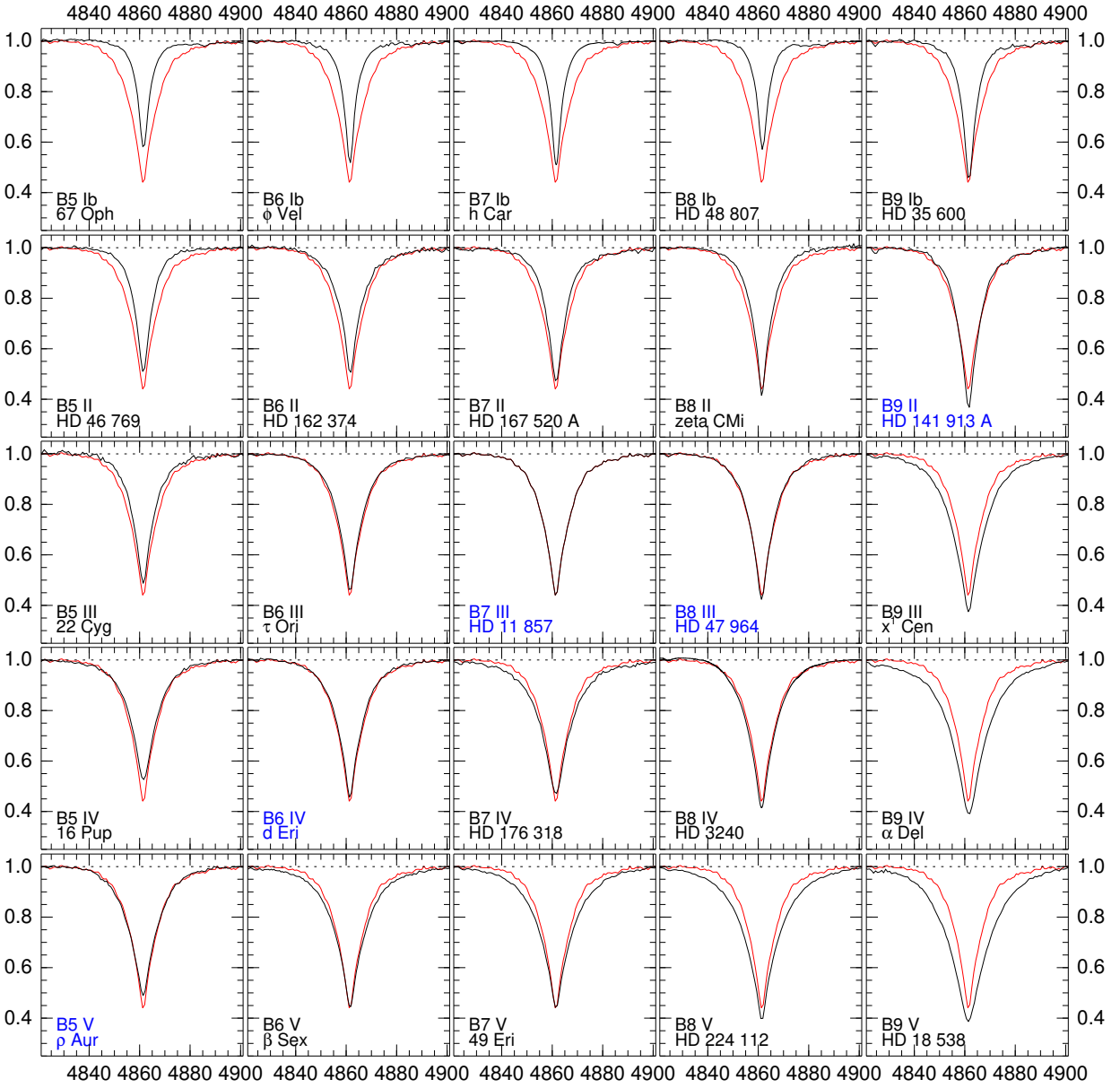

Fig. 13 The diagonal effect as observed in Hβ at $\mathcal{R} \sim 2500$, compare with Garrison and Gray (1994) The grid of plots shows the rectified line for the spectral subtype range B5-B9 and the luminosity class range V-Ib. Stars with names in blue mark the diagonal where the Hβ profile is very similar. The profile of the B7 III star (HD 11 857) is shown in all plots in red for comparison. Profiles above the diagonal are narrower and of lower EW while those below it are broader and of higher EW.

pedestal (Walborn et al., 2015b).

- *Other metallic lines.* Lines such as O II λ4070, O II λ4416, O II λ4348, and N II λ3995 also show a positive luminosity effect and can be used for classification. However, some B stars are affected by anomalous C and N strengths in a similar way to some late O stars, so the luminosity classification should be confirmed by another criterion or, otherwise, the anomaly should be noted.

4.2.2 Peculiar B stars

Here we briefly describe the peculiar categories for B stars.

- **He strong and He weak.** Some B stars have large He abundance anomalies. The cases among the earlier subtypes are enriched in He (e.g. σ Ori E) and the ones among the later ones are He poor (e.g. 3 Cen A). Most of the examples in this category have been found to have magnetic fields.

- **Bp.** In addition to He, B stars can have anomalous abundances of other elements. Some of them are the hot versions of the classical magnetic Ap stars described below. Others are enriched in singly-ionized mercury and manganese and are accordingly called HgMn stars (Paunzen et al., 2021). They have spectral subtypes between B7 and B9 and luminosity classes between V and III.
- **Be and B shell.** Be stars are the most common type of peculiar B stars, to the point that already Secchi created a class for them (V, see above). They are characterized by having some (at least Hα) or all of the Balmer lines in emission but with an extreme variety in intensity (see Fig. 5) and in the lines affected, as objects with an intense Be phenomenon also have other lines (e.g. from He I and Fe II) in emission. Be stars are highly variable, both in the emission lines themselves (Dimitrov et al., 2018) and photometrically in general (Maíz Apellániz et al., 2023). Indeed, a Be star can go through a non-Be phase where its emission lines disappear but even then it is considered a Be star i.e. "once a Be, always a Be" (Porter and Rivinius, 2003). The Be phenomenon includes a diversity of objects, but the most common ones are classical Be stars, which are of luminosity classes V to III (and sometimes II) and for which the emission lines are produced in a disk around it that is tied up to pulsations in the star. Be stars with weak emission lines are easy to classify following the same criteria as normal B stars, but those with strong emission lines can be notoriously difficult. Some Be stars can experience a B shell phase, where narrow cores in the Balmer lines and absorption lines of singly ionized metals appear. See the A-star subsection for the Herbig Be stars.
- **B[e].** B[e] stars are objects that, in addition to strong Balmer emission, show emission in forbidden metal lines, mostly of [Fe II] and [O I]. The B[e] phenomenon has diverse origins (Lamers et al., 1998): supergiant stars in one of the LBV phases (Walborn and Fitzpatrick 2000, see below), PMS stars (see below for Herbig AeBe stars), symbiotic stars with a cool and a hot component, and even some for which the origin is currently unknown.
- **B Iape.** These objects are the early-B extension of the O Iafpe stars (Walborn and Fitzpatrick, 2000).
- **BN/BC.** BN and BC stars are the cooler equivalents of ON and OC stars, see above.

4.3 A stars

The A stars are the first spectral class where the population is divided into three distinct types according to their luminosity. Most dwarfs are low-mass stars[7] and are the majority of the population while supergiants are evolved massive stars in a brief stage of their evolution, making them rare in absolute numbers but easy to observe as they are some of the most luminous stars in the optical due to their small bolometric correction compared to earlier or later spectral types. In between, we find different types of objects, from low-mass stars around the end of their hydrogen core burning to intermediate-mass stars evolving to the right or the left of the HRD and low-metallicity horizontal branch (HB) stars burning helium in their cores.

4.3.1 Classification criteria for A stars

Spectral type. Originally, A0 stars were defined as those where He I lines were no longer visible, but with modern data that is no longer the case. There are three criteria used to determine the spectral type (Gray and Garrison, 1987, 1989b), which are showcased in Fig. 14:

- *H.* Balmer lines increase from A0 to A2 and decrease afterwards.
- *Ca.* Ca II λ3934 (or Ca K), already detectable for late-B stars, greatly increases with subtype for A stars. Two notes are made in this respect: for A stars Ca II λ3968 (or Ca H) is mixed with Hϵ (dominated by the latter at A0 but comparable for late subtypes) and both Ca K+H can be significantly contaminated by interstellar component(s).
- *Metallic lines.* The overall metallic contribution increases with subtype, with a nearly featureless spectrum for early subtypes (much as for late-B stars) to a large number of lines for late subtypes (mostly weak at this stage, as the transition from Secchi's class I to II takes place for F stars, see below). Among the useful lines we find Ca I λ4226, Fe I λ4271, and the Mn I λ4030 blend.

Luminosity class. The primary luminosity criterion for A stars is the profile (width and EW) of the Balmer lines. As it happens for the B stars, both have a negative luminosity effect, but they also depend on the spectral subtype. The effect is especially strong for the early subtypes (Fig. 14), where some authors divide the V class into Va (normal MS) and Vb (ZAMS) and even introduce Va$^-$ for the intermediate class between the two and Va$^+$ for the intermediate one between Va and IV-V. This can be done because of the significant separation in the HRD between the normal V sequence and the ZAMS for this spectral type, see Fig. 6. For the late subtypes the Balmer lines become less sensitive to luminosity and metallic lines with a positive luminosity effect have to be used instead, in particular different blends of Fe II and Ti II at 4172-4179 Å, 4395 Å, 4400 Å, and a forest of lines around 4500 Å (Fig. 14).

Two complications arise with the spectral classification of A stars. The first is the significant number of fast rotators, something that was also seen for O and B stars, which hampers the classification by making lines less prominent (Fig. 4). The second is the large fraction of A stars with chemical peculiarities, already present in B stars but more important for A stars. As there are three spectral classification criteria for A stars, it is possible to derive three different spectral subtypes, leading to a notation such as kA2hA9mF2. This corresponds to A2 for the Ca K-line subtype (k), A9 for the hydrogen-line type (h), and F2 for the metallic-line type (m). This notation is used for some of the peculiar A stars and for HB stars (population II objects).

4.3.2 Peculiar A stars

Here we briefly describe the peculiar categories for A stars.

- **Am.** Metallic-line or Am stars have different spectral classifications according to the K-line and the metallic-line criteria, with the first

[7] They only reach helium burning and ignite it with a flash.

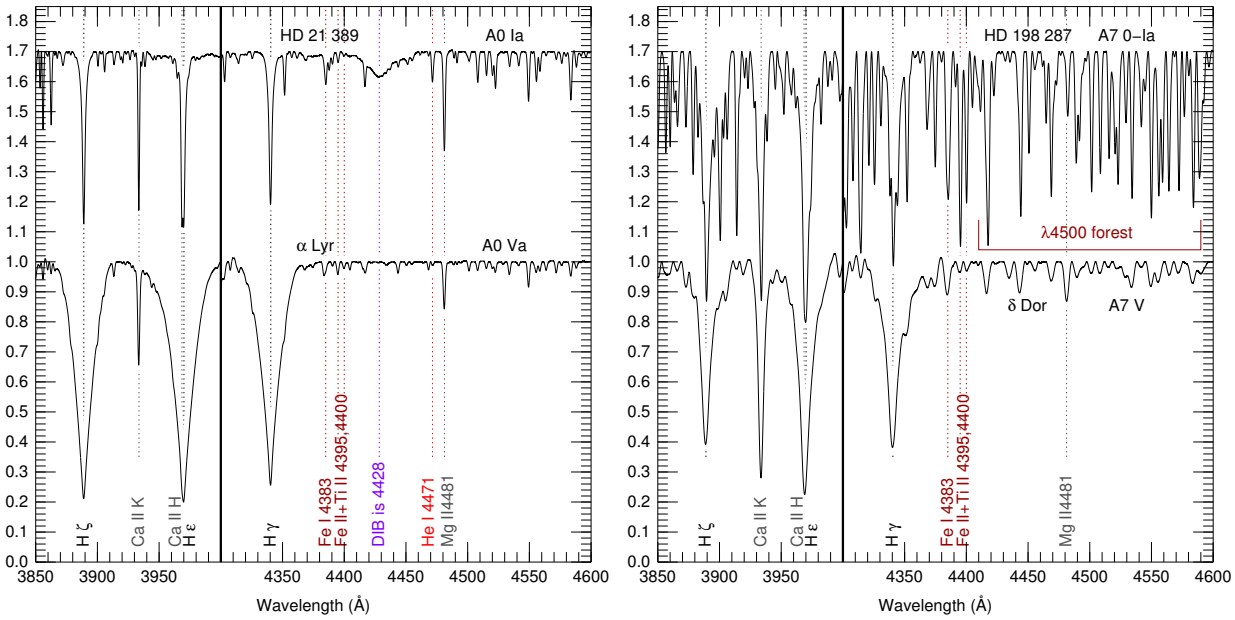

Fig. 14 Selected spectral regions (3850–4000 Å and 4300–4600 Å) of A0 (left) and A7 (right) dwarfs (bottom) and supergiants (top) at $\mathcal{R} \sim 2500$. Spectra are rectified, separated by 0.7 continuum units, and from LiLiMaRlin.

being earlier and the second later, possibly as much as F, as in the example given in the previous subsubsection. The origin of Am stars is the chemical separation in their interiors caused by their slow rotation.

- **Ap.** The Ap stars are the extension of the He strong, He weak, and Bp stars to the B-star regime, that is, objects in which only a few selected heavy elements are enhanced in the stellar atmosphere (as opposed to most heavy elements for Am stars). In terms of notation, the enhanced elements are listed behind the p suffix. As with their B-type counterparts, the chemical peculiarities are associated with magnetic fields (Hümmerich et al., 2020). Many Ap stars are spectroscopic variables.
- **λ Bootis stars.** They are metal-poor (population-II) A-type stars. The k-h-m notation described above is used followed by λ Boo.
- **Herbig Ae/Be stars.** These objects are PMS stars that are the hotter equivalent to T Tauri stars, discussed below. They are usually associated with interstellar clouds detected as a thermal IR excess, dark cloud, and/or reflection nebula, all of them produced by cool and/or hot dust. They are photometrically variable and their light is polarized.
- **A-type shell stars.** A-type shell stars have most spectral features of late-B to early-F stars of luminosity classes V to III but their Fe II and Ti II lines are enhanced, as it would happen in A supergiants.

4.4 Other hot stars

In this subsection we discuss early-type stars in advanced stages of stellar evolution and/or those whose spectra are radically different from the previous "normal" stars. Two differences between the stars here and the previous ones are a more diverse range of masses, with some objects having initial values lower than those of a mid-F star in the MS, and a more disorganized distribution in the HRD, as some of these stars occupy locations unexplored until now or can be found in the same locations as "normal" stars but with quite different initial masses.

4.4.1 Wolf-Rayet stars, Luminous Blue Variables, and iron stars

Massive stars, especially the most massive ones, can experience phases where their winds are so strong and/or their variability is so high as to defy the traditional assignment of fixed spectral classes through the analysis of absorption lines. There is a whole zoo of such stars (Walborn and Fitzpatrick, 2000), of which we have already seen some examples. In this subsubsection, we analyze the two most extreme cases, Wolf-Rayet stars and Luminous Blue Variables (LBVs).

As already mentioned, WR stars were one of the first types of peculiar stars to be identified (Wolf and Rayet, 1867). The spectra of WR stars are dominated by broad emission lines of H, He, C, N, and/or O, with few or no absorption lines (intrinsic or caused by companions). Depending on the dominant CNO species in the emission spectrum, they are divided into two classes with significant membership, WN and WC, and one with a few known examples, WO. Sequences for each of them based on the ratios of lines from different ionization states can be used to provide spectral subtypes, see Smith et al. (1996) for WN stars and Crowther et al. (1998) for WC and WO stars, and Table 1 for qualifiers.

The defining characteristic for WR stars is their strong wind responsible for the emission lines. This can happen in four ways:

- **Initial stage of very massive stars.** The most massive stars of all (~ 100 $M_\odot$ or more) have very strong winds from the start of their lives and are classified as WNh stars, with the h indicating a strong hydrogen component in the Balmer lines (instead of pure He II lines, see Table 1). Some examples are the central stars at the core of NGC 3603 (Drissen et al., 1995) and R136 (Crowther et al., 2010;

Bestenlehner et al., 2020). They are located at the hot extreme end of the sequence for normal O stars in the HRD (Fig. 6).

- **Final stage of massive stars.** The only stars of O type in the ZAMS that become red supergiants are those of the latest subtypes[8]. The rest lose enough mass after they leave the MS to change the direction of their evolution in the HRD diagram (Humphreys and Davidson 1979, see LBVs below) and become WR stars before their core collapses. This is called the Conti's scenario for WR production (Maeder, 1996) and is likely to be the primary one, at least at solar metallicities. These WR stars are hotter than O stars but are less luminous than the WRs that represent the initial stage of very massive stars (Fig. 6).
- **End product of binary evolution.** As an alternative to the Conti's scenario, a massive star may also lose enough mass through mass transfer to a binary companion to become a WR star (De Greve, 1996). It is still unclear whether the majority of WR stars are formed through this channel or through the previous one i.e. whether binary mass transfer or stellar winds are the dominant effect. The results of both channels are called classical Wolf-Rayet stars.
- **Planetary Nebula Nuclei (PNNi).** Some low-mass stars can have stellar winds at the end of their lives when at the planetary nebula stage (see below) strong enough to have a WR-like spectrum. They are designated as [WR] stars (Gorny and Stasińska, 1995).

Luminous Blue Variables (also known as S Dor stars and Hubble-Sandage Variables) are evolved very luminous blue stars (Fig. 6) that experience large photometric and spectroscopic variations (Conti, 1984). The instability is caused by their proximity to the Eddington limit. Their spectroscopic variations are large enough to make them move horizontally across the top left of the HRD diagram from a quiescent state with a hot $T_{\rm eff}$ to an active phase with a cool $T_{\rm eff}$ in time scales of years, with very different spectral types in each (see Walborn et al. 2017 for examples). They can also experience eruptions, the most famous of which took place in the mid-19th century, causing η Car to become the second brightest star in the sky (Smith and Frew, 2011; Smith, 2011). During some of its phases, the spectrum of an LBV is dominated by Fe II emission lines, in which case it is called an iron star (Walborn and Fitzpatrick, 2000).

4.4.2 Horizontal Branch stars and RR Lyrae

At the stage where population-I low-mass stars burn helium in their cores they form a structure in the HRD diagram called the Red Clump (RC) and they are classified as late-G or early-K giants. Their population II counterparts, however, form a structure at similar luminosities called the Horizontal Branch (HB) and most of its members are classified as B, A, and F stars, with its left end below the MS (see below for hot subdwarfs) and its right one above it.

The (low-metallicity) HB is divided into red and blue parts. In the gap in between we find the RR Lyrae, which are A and F giants with variable spectral types (Fig. 6). This is a class of variable stars presenting cyclical changes in their brightness. The length of these cycles is proportional to the intrinsic brightness of the star, as in classical cepheids (discussed below), and RR Lyrae are their low-luminosity equivalents on the same instability strip. Their location is marked by a photometric variability maximum in the top right panel of (Fig. 6) even with the blurring introduced by Galactic extinction. Their spectral types are variable through their cycles, but most of the time they appear as F-type giants with weak metallic lines (see below for metallicity effects on F and later-type stars).

4.4.3 Hot subdwarfs, stripped stars, white dwarfs, and cataclysmic variables

The term subdwarf originally described only (late-type) population-II MS stars which, due to their low metallicity, were located below[9]. the luminosity class V sequence in the HRD diagram. However, a population of hot subluminous stars (hot or OBA sudwarfs) also exists (Fig. 6). Most of them are extreme HB stars (core He burning, see above) that are the result of binary evolution but some may have been formed by other mechanisms such as two white dwarfs merging (Heber, 2016). Drilling et al. (2013) have developed a classification system to integrate hot subdwarfs into the MK system.

Hot subdwarfs are the low-mass equivalent of the massive Wolf-Rayet stars formed through the binary channel. But what about the masses in between the two ranges? Those objects are called stripped stars (Fig. 6); they have been only recently studied in detail, and they have spectral characteristics that are intermediate between those of sdOBA and WR stars (Götberg et al., 2018, 2023).

White Dwarfs (WDs) are the end point of stellar evolution for most[10] low- and intermediate-mass stars. Their spectral classification follows a different scheme from the MK system, with the symbols described in Table 2 and indicating the different types of lines detected in the spectrum. The symbols are followed by a numerical index from .1 to 13 i.e. DA.1…DA.9, DA1, DA1.5, DA2…DA13 that represents 50.4 kK/$T_{\rm eff}$, so the sequence above runs from a $T_{\rm eff}$ of 504 kK to one of 3.9 kK. They are located at the bottom of the HRD (Fig. 6).

Cataclysmic variables are binary systems composed of a white-dwarf primary and a mass-donor secondary, with an accretion disk usually involved in the process. They come in different varieties, are usually located in the region between the class V and WD sequences, and their membership includes some of the most variable stars known (top right panel of Fig. 6).

4.4.4 Post-Asymptotic Giant Branch stars, Planetary Nebula Nuclei, and PG 1159 stars

At the end of their lives, low-mass stars cross the HRD from the upper right (Asymptotic Giant Branch or AGB phase) to the lower left (WD phase). They do so by quickly moving first near-horizontally to the left until they reach extremely hot $T_{\rm eff}$ values, and then downwards.

The first phase corresponds to post-AGB (pAGB) stars. These objects can be classified as peculiar supergiants of K to O type (depending on the evolutionary moment at which they are caught). They have peculiar abundances due to their strong mass loss rates, infrared excesses from the recently ejected dust, and a mismatch between their spectroscopic luminosity classification as supergiants and their location in the

[8] The precise subtype may depend on metallicity.
[9] Actually, to the left, as those stars are mostly bluer, not fainter, than their high-metallicity counterparts (Fig. 6)
[10] We say "most" instead of "all' because, once binaries are included, other scenarios are possible.

Table 2 Spectral classification symbols for white dwarfs from Gray and Corbally (2009).

Symbol	Definition
Main symbols	
DA	Only Balmer lines, no He I or metallic lines present
DB	Only He I lines, no Balmer or metallic lines present
DC	Continuous spectrum, no lines deeper than 5% in the whole electromagnetic spectrum
DO	He II strong, He I or Balmer lines present
DZ	Metallic lines only, no Balmer or He I lines present
DQ	Carbon (atomic or molecular) features present somewhere in the electromagnetic spectrum
Additional symbols	
P	Magnetic WDs with detectable polarization
H	Magnetic WDs without detectable polarization
X	Peculiar or unclassifiable spectrum
E	Emission lines present
? or :	Uncertain spectral classification
V	Variable
d	Circumstellar dust present
C I, C II, O I, O II	Added within parentheses for hot DQ types to indicate presence of those species

HRD somewhat below (as their masses are lower than those of the usual denizens of the region, their gravity is lower than that expected at their luminosity).

Once the extremely hot ($T_{\rm eff}$ ~200 kK, Fig. 6) degenerate core is exposed, the ejected layers become a planetary nebula and the core, a planetary nebula nucleus (PNN), some of which have WR-like features (see [WR] stars above). This phase lasts only a few tens of ka, with the star moving downwards in the HRD on its way to become a WD. In between the two phases, the object is known as a PG 1159 star (after the prototype PG 1159−035), which resembles a hot DQ spectrum but is even hotter (Fig. 6).

5 Spectral classification of cool stars

As previously mentioned, we define cool (or late-type) stars as those with low values of $T_{\rm eff}$ and, more specifically, as those that would correspond to the original II, III, and IV Secchi's classes. We have divided this section in five parts:

- **F stars.** They are the transition type between hot and cool stars.
- **G+K stars.** We group them together because of their similarities.
- **Cool luminous stars.** They are the FGKM giants and supergiants, which we group together due to their significantly different nature or evolutionary state compared to cool dwarfs.
- **M dwarfs.** They constitute the most numerous of all the stellar categories in this paper and represent the lowest end of the stellar mass function.
- **Ultracool dwarfs.** They are the most recent addition to the spectral classes and are objects of substellar mass (but see below).

5.1 F stars

In many senses, F-type stars represent a transition. Early-F stars still have a radiative envelope, with only superficial convection zones, but later types have fully-developed convective envelopes. Beyond this transition, magnetic breaking is effective, and fast rotators are rare, except among very young stars, an effect that can be directly observed when comparing spectra (Kraft, 1967; Beyer and White, 2024). Chemical peculiarities are not observed in main-sequence stars with convective envelopes, except for some rare cases of contamination by a companion. It must be noted, however, that Am stars are observed with spectral types as late as F2.

In the earliest F subtypes, Balmer lines have an important negative luminosity effect, as seen in A-type stars. The Balmer lines, however, weaken significantly with increasing subtype, and by late F, they have become weak and not responsive to luminosity. Conversely, the overall metallic spectrum strengthens both with decreasing temperature and increasing luminosity. These combined effects mean that F-type stars may present very different appearances. An extreme case is shown in Fig. 15. The spectrum of a fast-rotating early-F star is still dominated by the Balmer lines, and its overall appearance is that of an early-type star. Conversely, a late-F star looks decidedly like a cool star.

5.1.1 Classification criteria for F stars

Spectral type. At solar metallicity, the main criterion to classify F subtypes is the increasing strength of metallic lines when compared to Balmer lines (Gray and Garrison, 1989a). The decreasing strength of the Balmer lines on its own gives a very good approximation to the subtype, thus providing a useful tool to classify low metallicity stars (more on this below). A number of metallic lines that are not sensitive to luminosity, such as Ca I λ4226 or Fe I λ4046,4383, can be used as comparators to the Balmer lines. An important feature for classification

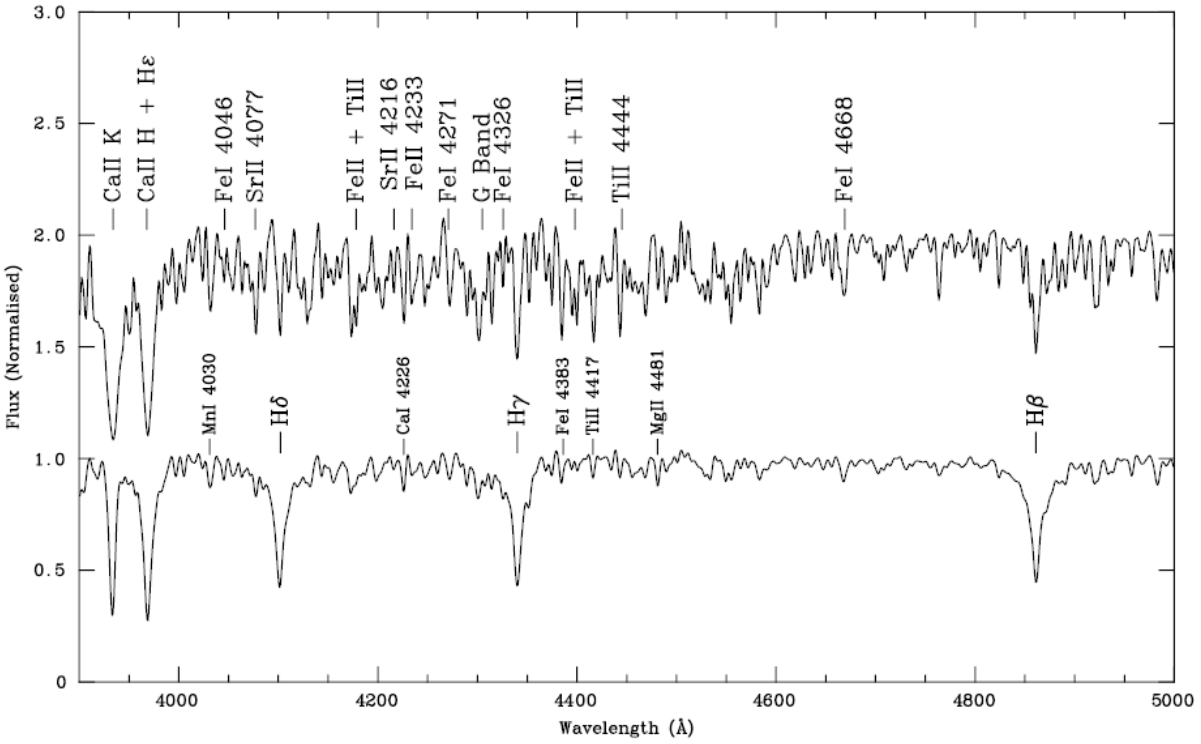

Fig. 15 These two extreme spectra illustrate the very different morphologies that can correspond to F-type stars. The bottom spectrum is that of the fast-rotating ($v \sin i \approx 160$ km s^{-1}; Royer et al. 2007) F0 V star 89 Tau (HD 29 375), which looks decidedly like a hot star. The top spectrum corresponds to the F8 Ia supergiant δ CMa (HD 54 605), which would have gone into Secchi's class II. The spectra have been adapted from the MILES spectral library (Falcón-Barroso et al., 2011). Lines useful for classification are indicated.

is Fraunhofer's G band. First seen before F5, this is a broad feature due to the diatomic molecule CH, which becomes prominent in late-F, G, and early-K stars (Fig. 2). Centred around λ4307, it can extend over about 20 Å and become strengthened by several Fe I and Ca I lines.

Luminosity class. The luminosity class of stars up to F5 is primarily determined by the strength of Fe II and Ti II lines compared to metallic lines insensitive to luminosity, such as those mentioned in the previous paragraph. The lines of ionized Fe and Ti appear mostly in blends, giving rise to strong features at $\lambda\lambda$4172–8, or $\lambda\lambda$4395–4400. These lines become weaker with decreasing temperature, and they are thus not very useful for classification of late-F stars, except for the supergiants. In late subtypes, the Sr II lines at λ4077 and λ4216 compared to Fe I lines provide the main criterion.

The issue of metallicity. Hot stars, with a few exceptions such as HB, pAGB, sdOBA stars, or WDs (see above), are relatively young objects, belonging to Population I. When we reach mid-F types, however, we start to find Population II stars. The oldest stars known to be still on the main sequence, such as those in globular clusters or the halo "turn-of", have temperatures corresponding to F types, but very weak metallic spectra, more typical of the A-type dwarf standards. Phillip Keenan tried to develop a classification system to take into account differing metallicities by adding a qualifier Fe followed by a numerical index (for example, Fe-3 for a star with very weak metallic lines). It is, however, very difficult to find relevant matches between stars with really low metallicities and MK standards, all of which have approximately solar metallicity.

Naturally, this issue extends to later spectral types. In recent years, stars with metallicities as low as [Fe/H] < -5 have been found. These objects present ratios between chemical elements that are extremely different from those of MK standards (for example, they are very rich in C in comparison to other elements; e.g. Aguado et al. 2018). Such objects cannot be accurately classified within the system without an extension to further dimensions.

5.1.2 Peculiar F stars

A peculiar type of F dwarfs (see below for peculiar luminous F stars) are barium dwarfs. These are late-F main-sequence stars that display enhanced lines of *s*-process elements. This is mainly evident in the very strong Sr II λ4077 and Sr II λ4216 lines. Since these two lines are used in primary luminosity classification criteria, the main-sequence nature of these star must be established from other ratios. They are called barium dwarfs in analogy with the barium giants (discussed below). The heavy-element contamination is believed to be due to a binary companion, which produced it during its AGB phase and is now a white dwarf.

5.2 G+K stars

There is a smooth transition between late-F and early-G stars (compare α Cen A to α CMi in Fig. 2), and FGK stars of low luminosity are sometimes grouped together as cool dwarfs. The most salient characteristic of G-type stars in the classification region is Fraunhofer's G band, which extends around λ4307 (Fig. 2). At longer wavelengths, the Mg I $\lambda\lambda\lambda$5167,72,84 triplet (Fraunhofer's b band) increases in strength with decreasing temperature, but also responds to luminosity. The Balmer lines have become weak, and lost all sensitivity to gravity. They gradually weaken with decreasing temperature, and their ratio to the G band or metallic lines can be used as a quick estimator of spectral type for G and K types.

The G band increases in strength until about K2 (it is very strong in the spectrum of α Cen B, K1 V, in Fig. 2), and then fades in later K stars, where two MgH bands become noticeable. The Ca I λ4226 line is very strong in dwarfs, especially in mid-K types, but it has a very important negative luminosity effect (which can be easily noticed in Fig. 17). The spectra of M-type stars are dominated by TiO bands, which grow in strength as temperature decreases, until most of the blue continuum has been eroded away (see the spectrum of α Cen C in Fig. 2). For this reason, it is preferable to use spectra extending into the green (or even the red) to classify M-type stars, as done in Figures 16 and 17.

5.2.1 Classification criteria for G and K stars

The same characteristics that we saw in late-F stars continue into later types. Balmer lines become progressively weaker, with Hγ being of about the same depth as the G band at G0, but becoming inconspicuous when compared to neighbouring metallic lines by late G. Similarly, Hβ is a salient feature in early G stars, but is lost in the metallic forest by early K. Ca I λ4226 increases in strength with decreasing temperature and becomes very prominent in mid-K dwarfs. The same ratios of neutral Fe I λ lines to Balmer lines used for F stars can be applied to classify G and K stars at solar metallicity. In stars with lower metal content, ratios between Cr I and Fe I λ lines are used, notably Cr I λ4254/Fe I λ4250 and Cr I λ4290/Fe I λ4326. These ratios can also be used at solar metallicity.

In the green region, the Mg I $\lambda\lambda\lambda$5167,72,84 triplet is a very salient feature that increases in strength with decreasing temperature, although it is also sensitive to luminosity. This feature increases in strength with decreasing temperature in G dwarfs.

The original system (e.g. Johnson and Morgan, 1953) did not contain subtypes K6, K8 or K9. In later years, Keenan introduced fractional subtypes for K stars (i.e. K0.5, K1.5, and so on) and occasionally used the K6 subtype (e.g. Gl 529 is K6 Va in Keenan and McNeil 1989). There is also an example of K8 (HD 142 574 is K8 IIIb) and Gl 638 is even given as K7.5 Ve in Keenan and McNeil (1989). Nevertheless, he never considered these fine classifications to represent full subtypes. The only true subtypes admitted in Keenan (1984) are G0, G2, G5, G8, K0, K1, K2, K3, K4, K5 and M0 (followed by all the integer M subtypes). The reasoning behind this choice is that stars must be evenly distributed into subtypes, while possible subdivisions are utilized only for interpolation whenever the quality of the data renders their use reasonable. In any event, as can be seen in Fig. 16, the differences between mid-K and early-M giants are marginal, and the use of these late-K types is therefore uncommon.

5.2.2 Luminosity criteria for G and K stars

In stars of higher luminosity, molecular bands strongly affect the shape of the continuum. The violet system of CN bands is hardly seen in dwarfs, but generates deep depressions in the spectra of giants (and more luminous stars) between G5 and early K. The λ4215 band creates a shallow depression between $\sim \lambda$4120 and λ4215 in the spectra of giants, which is deeper in supergiants. These features are also very strongly dependent on metallicity, and Phillip Keenan developed a qualifier CN to indicate their strength, in an analogous manner to the Fe qualifier.

At lower temperatures, TiO bands start to be visible. They are not noticeable in dwarfs before type M, but they can be clearly seen in mid-K giants (note, for example, the prominent bandhead at λ6158 and incipient bandheads at λ4954, 5446 in the spectrum of the K4.5 III star HD 99 167 in Fig. 16). Conversely, the MgH band around λ5200 produces a broad depression between λ5000 and λ5240 in mid-K dwarfs, but is hardly seen in high luminosity stars. A second MgH band, around λ4780, gives rise to a much narrower feature, which also shows a marked negative luminosity effect. The G band also shows a negative luminosity effect, although it is still moderately strong in supergiants.

For accurate luminosity classification, the ratios of Sr II λ4077 and Sr II λ4216 to neighbouring Fe I lines can be used. The best criterion in the blue part of the spectrum is the ratio of Y II λ4367 to Fe I λ4383.

5.2.3 Peculiar G+K stars

A peculiar type of low-luminosity G+K stars (see below for peculiar luminous G+K stars) with high astrophysical relevance are T Tauri stars. These young stars are divided into classical T Tauri stars (CTTSs) and weak-lined T Tauri stars (WTTSs). The former are very young stars that retain a remnant of their natal envelope, resulting in the presence of emission lines, frequently strong, most notably Hα and other Balmer lines, but also others from Ca II and Fe II. These emission lines originate from infalling channels of plasma and neutral gas from circumstellar protoplanetary disks, or from the disks themselves. CTTSs sometimes present P Cygni profiles or forbidden emission lines. Their underlying spectrum, which may be veiled, normally corresponds to luminosity classes III to V, with the latter being more frequent (see their typical location in the HRD in Fig. 6). The nature of T Tauri stars can be confirmed through other observational characteristics, such as photometric variability, infrared excess, or X-ray emission. Their spectra experience "veiling", a general loss of contrast, accompanied by blurring of atomic lines (Fang et al., 2020), as Mira variables also do (see below). CTTSs stars have G to M types, though some F-type T Tauri stars are known, but not so well studied. It has also been suggested that the T Tauri phase extends to brown dwarfs, as there are very young M-type objects with masses below the hydrogen-burning limit in star-forming regions exhibiting very similar characteristics

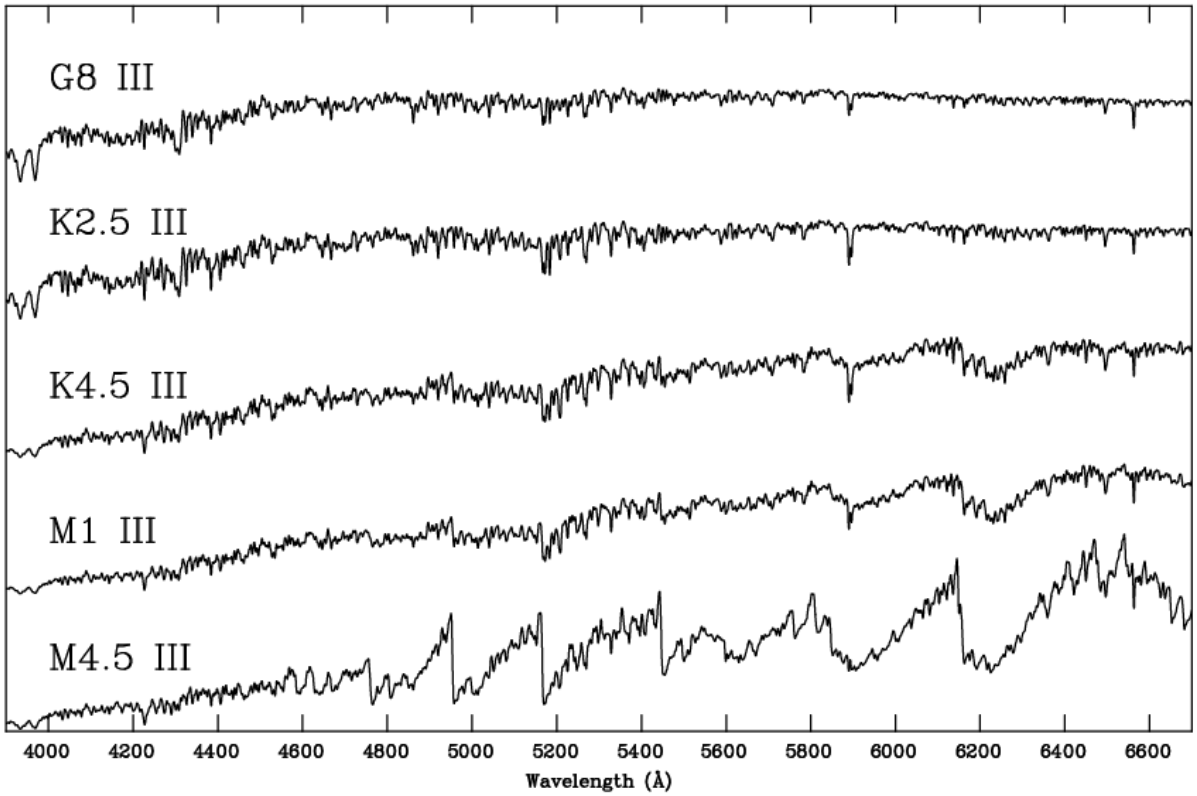

Fig. 16 Temperature sequence for late-type giants. The stars displayed are, from top to bottom, HD 10 761, HD 216 640, HD 99 167, HD 102 212, and HD 123 657. The spectra have been adapted from the Indo-US spectral library (Valdes et al., 2004), and spectral types are from Keenan and McNeil (1989). See Fig. 17 for the most relevant spectral features. Note the high similarity between the K4.5 III and M1 III stars, which explains the lack of definition for late-K types.

to CTTSs. While CTTSs are the low-mass counterpart of Herbig Ae/Be stars, WTTSs represent the low-activity counterparts of CTTSs, having lost most of their natal envelopes. The peculiar characteristics in their spectra are thus weak.

5.3 Cool luminous stars

Cool stars of high luminosity, i.e. FGKM giants and supergiants, despite the overall resemblance of their spectra, include a wide variety of stellar types. While a star classified as O9 III and a star classified as O9 Ia share most characteristics and are essentially the same sort of object, a K0 III star is likely a He-burning low-mass star in the RC, but a K0 Ia star is likely a massive star in a rare, transitional phase. Nevertheless, differences between their spectra are moderately subtle, when compared – for example – with a main sequence star of the same spectral type. It is important to remark once again that spectral classification is morphological; the fact that a star is classified as a supergiant does not necessarily imply that it is a massive star, as some have been found to be of intermediate mass. This is in contrast to OBA stars, where normal (non-pAGB) supergiants are always massive stars.

There are very few high-luminosity supergiants of G and K type at solar metallicity, to the point that the original list of MK standards by Johnson and Morgan (1953) only contains the K3 Iab standard o^1 CMa (later given as K2.5 Iab in Morgan and Keenan (1973) and K2 Iab in Keenan and McNeil 1989) and no Ia standards between G0 and M0. The few objects observed tend to be very luminous and highly variable, such as the hypergiant ρ Cas, which has been observed at spectral types between F and M. Contrarily, there are many supergiants of M type. These correspond mainly to the He-core burning phase of massive stars between $\sim$ 10 and 25 $M_\odot$, although some objects of luminosity class Ib can correspond to lower-mass giant branch or AGB stars. An example at hand is the MK standard α Her (Rasalgheti), M5 Ib–II, which is believed to be an AGB star of intermediate mass (2.3–3 $M_\odot$). True supergiants tend to be weakly variable in spectral type but more significantly so from a photometric point of view. Most are of early-M type, with mid-M types generally observed amongst those believed to be more massive. It must be noted, however, that the properties of He-core burning massive stars are very strongly dependent on metallicity. In the SMC, there are few M-type supergiants; luminous red supergiants have types G and K and tend to show moderate spectral type variability (Dorda et al., 2016).

Given the variety of masses and evolutionary phases found among cool luminous stars, there are significant differences in their photometric variability. For example, studies of open clusters show that low-mass RC stars typically have spectral types in the G6 III–K2 III range (e.g. Morgan and Hiltner, 1965; Mermilliod and Mayor, 1989) and recent *Gaia* analyses have shown those to be quite stable from the

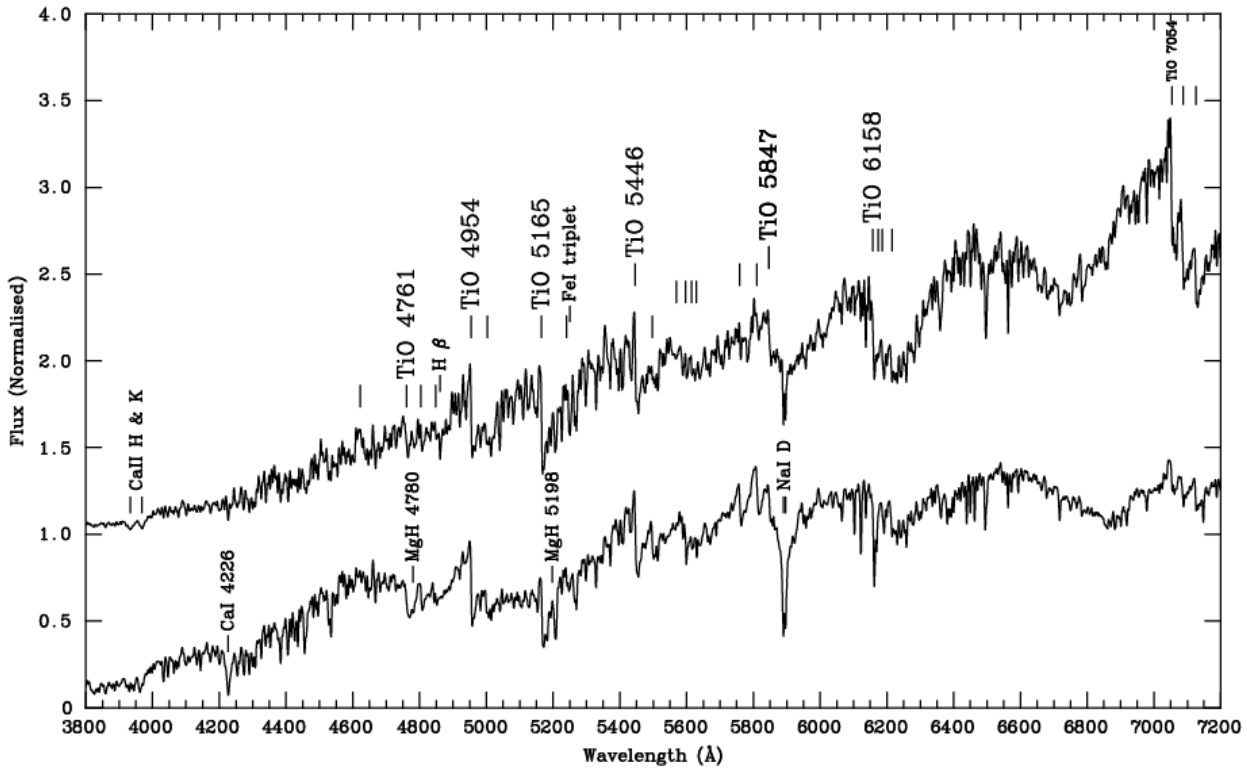

Fig. 17 Comparison of a red dwarf (HD 147 379; M1 V, bottom) to a red supergiant of very similar temperature (6 Gem; M1–M2 Ia-Iab). The spectra have been adapted from the Indo-US spectral library (Valdes et al., 2004), and spectral types are from Keenan and McNeil (1989). The spectral type of the planet-host star HD 147 379 has been revised with newer redder data to M0.0 V (Alonso-Floriano et al., 2015; Reiners et al., 2018).

photometric point of view (Maíz Apellániz et al., 2023), see top right panel of Fig. 6. On the other hand, stars with masses between 4 $M_\odot$ and 8 $M_\odot$ in the He-core burning phase appear as late-G or K-type stars of luminosity class II or Ib (e.g. Alonso-Santiago et al., 2019, 2020). He-core burning stars with masses higher than $\sim 5\ M_\odot$ can loop blueward, and then they will appear as yellow supergiants, with spectral type F and luminosity class Ib or II. Some of these objects are periodically variable in spectral type and luminosity, the classical cepheids. Many giants and supergiants of M type are photometrically variable (Maíz Apellániz et al., 2023). Variations can be irregular, semi-regular and (quasi-)periodic, many of which are classified as long period variables (LPVs). When a period can be defined, stars can be sorted into families according to their period/luminosity relation (e.g. Lebzelter et al., 2019). Most LPVs are AGB stars, the He shell burning for stars of intermediate and low-mass, with the two types forming two branches in the *Gaia* CAMD (Fig. 6) and the latter reaching a significantly redder location in $G_{BP} - G_{RP}$ than the former. M-type LPVs constitute a major subclass of Mira variables (or Miras, for short), which show very large photometric amplitudes and large changes in their spectra, attributed to thermal pulsations.

A modern guide to classification of cool luminous stars, which gathers information spread over many classical references, including the use of features in the green region of the spectrum, can be found in Dorda et al. (2018).

5.3.1 M giants and supergiants

The vast majority of type M stars are dwarfs. For example, about 70 % of the almost 500 stars in the immediate vicinity of the Sun at $d < 10$ pc are M dwarfs (Reylé et al., 2021), while there are only a dozen giants (luminosity class III) in the 8× larger volume of 20 pc (Kirkpatrick et al., 2024). Nevertheless, M-type giants have radii thousands of times larger than those of M dwarfs, and are thus many orders of magnitude brighter. As a result, while the brightest M dwarf, Lacaille 8760 (AX Mic), is at $V \sim 6.7$ mag slightly fainter than the naked-eye limit, there are six M-type giants and supergiants with apparent magnitudes $V < 2.5$ mag among the 100 brightest stars in both hemispheres: Betelgeuse, Antares, Gacrux, Mirach, β Gru, and β Peg. For this obvious reason, the first spectral classification studies of M stars focused on M giants and supergiants, starting with Secchi and his "class III" (orange to red stars with complex band spectra) and in subsequent pioneering work (e.g. Wildt 1936; Keenan 1942).

The spectral type of M-type giants and supergiants on photographic plates was determined by the progressive appearance of different TiO bandheads in the blue part of the spectrum (Keenan et al., 1974). These bands are much stronger than in dwarfs of the same type. On modern spectrograms, ratios of TiO bands are preferable for a number of reasons, among which the possibility of "veiling" in Mira variables (Crowe and Garrison, 1988). Strong bands reach saturation and stop growing, while weaker bands become visible at later types. Some of

the line ratios that are used for K-type stars can still be used in early-M giants, but the loss of the continuum makes them disappear at later types. A remarkable exception is the Ca I λ4226 line. This line, which is weak in luminous early-M stars because of a marked luminosity effect (see Fig. 17) becomes very strong in giants of types M5 and later (compare the M4.5 III star HD 123 657 with the earlier giants in Fig. 16).

Nevertheless, the spectral classification of luminous late-M stars is complex. Most of them are variable in spectral type, and thus not suitable as standards. Moreover, when we reach mid-M spectral types, the strength of the TiO band systems has increased so much that there is no continuum left anywhere in the classical classification region. As a consequence, the subsequent increase of the band strengths with decreasing temperature does not result in large changes in the spectrum. It becomes mandatory to resort to redder regions of the spectrum (Solf, 1978). Inclusion of the visual region allows the use of VO bands to help defining spectral types. Starting at M5, the VO bandheads can be seen as relatively weak, narrow features appearing within the dominant TiO bands.

Although the latest reference spectra given by Keenan and McNeil (1989) are M8, it is possible to extrapolate the even later subtypes M9 and M10, which are only observed in LPVs, such as Miras. The extreme object VX Sgr, which has luminosity class Ia, and could be either a very peculiar supergiant or an extremely luminous AGB star (Tabernero et al., 2021), was used by Solf (1978) to define M10, but many Miras reach M9 during their cycles. The use of M10 indicates that spectral type L is not considered for luminous stars (type M11 has been employed in some references).

Similarly, exact luminosity classification is tricky. Some criteria based on line ratios that are used for K-type stars can also be used in the M type, until they lose applicability because the lines involved disappear within growing TiO band strength (Dorda et al., 2018). The criterion reaching later types is the ratio of Y II λ4367 to Fe I λ4383, which can be used effectively up till ~M5. For later types, the general strength of the metallic line spectrum is a useful guide, but must be employed with caution, because of "veiling" in Mira variables.

Most M supergiants are mildly variable, with Keenan and McNeil (1989) giving ranges of spectral types for a significant number of them. For example, TV Gem (HD 42 475) is listed as M0–M1.5 Iab. The supergiant with the latest spectral type listed as a reference is EV Car (HD 89 845), at M4.5 Ia. There are a few supergiants of later type (e.g. MY Cep in NGC 7419; Marco and Negueruela 2013), but their exact luminosity class cannot be given. Late-M giants are very luminous, as bright as the fainter supergiants, but their luminosity class is difficult to determine. See Negueruela et al. (2012) for an attempt at finding criteria in the nearest infrared, where some strong metallic lines are visible at classification resolution, and references to classical sources.

5.3.2 Peculiar cool luminous stars

In a sense, all cool luminous stars are peculiar, with the possible exception of normal clump stars, as they are subject to photometric and, in many cases, spectroscopic variability. Here we list some of the most relevant cases.

- **Cepheids.** Classical cepheids are variable stars whose intrinsic magnitude undergoes cyclical variability. The recognition of a direct relation between the length of their period and their intrinsic brightness (Leavitt and Pickering, 1912) represents the first step in the distance scale and the foundation of modern cosmology. Classical cepheids are He-core burning stars of between ~ 5 $M_\odot$ and ~ 12 $M_\odot$ that are passing through the instability strip (clearly seen in the top right panel of Fig. 6) as part of their blue loop evolution (e.g. Anderson et al., 2014). Along their cycle, they also display spectral variability. All cepheids have a base spectral type at maximum light not far from F8 Ib (some can be as early as F5 and the less luminous examples will have luminosity class II). Throughout their photometric cycle, they will move to later spectral types, with the most luminous (and, hence, massive) cepheids reaching into the K type (e.g. Clark et al., 2015).
- **CN-strong stars.** Some giants have stronger CN (and C_2) bands than normal stars of the same spectral type. This anomaly is also marked with the CN qualifier, this time followed by a positive numerical index.
- **Barium stars.** Some G and K giants display enhanced lines of *s*-process elements, specifically Ba II λ4554 and the Sr II lines. The heavy-element contamination is caused by a binary companion, which produced it during its AGB phase and is now a white dwarf.
- **Mira variables.** Mira-type variables are intrinsically very red LPV stars with some reaching photometric amplitudes larger than ~ 2.5 mag in the optical bands (top right panel of Fig. 6) and $\gtrsim 1$ mag in the near infrared. Their photometric (quasi)periods are longer than ~ 150 d. Physically, they are stars that have completed He core burning and are now on the second phase of the AGB, characterized by alternating episodes of H-shell and He-shell burning. This irregular energy injection leads to very large pulsations of the whole envelope (the thermal pulses), which result in the observed variability.

  There are three main types of Miras: O-rich (which appear as M giants), S stars (characterized by strong bands of ZrO) and C-rich (carbon stars, Secchi's group IV). Lower-mass stars (up to a limit of 3–4 $M_\odot$, depending on metallicity) undergo evolution M $\rightarrow$ S $\rightarrow$ C (intermediate stages are known). This is understood as a sequence of progressive enrichment of the atmosphere with C generated during the He-shell burning flashes, due to the third dredge-up. More massive stars do not raise so much C to the atmosphere and remain O-rich (see Herwig 2005 for an overview of the AGB). In consequence, the Miras with the longest periods ($\gtrsim 1000$ d; and, hence, the highest luminosities) are expected to be very late-M giants (although some are S stars; e.g. Smith et al. 1995). However, many of these high-luminosity Miras are enshrouded in thick dust shells, due to their very heavy mass loss, which reprocess their emitted light into infrared wavelengths (e.g. García-Hernández et al., 2007).

  Miras show a very high degree of spectral variability. Their spectral type changes through the photometric cycle, normally by several subtypes. When close to maximum light, they generally display emission lines, with very strong Balmer emission, and weaker lines of Fe I (and sometimes Fe II) and other metals. In addition, they suffer from "veiling" (Crowe and Garrison, 1988). These changes are not consistent, in the sense that they do not always happen at a given phase of the photometric cycle.

  Carbon stars are generally classified in two (parallel) temperature sequences, which correspond to the old R and N spectral types of

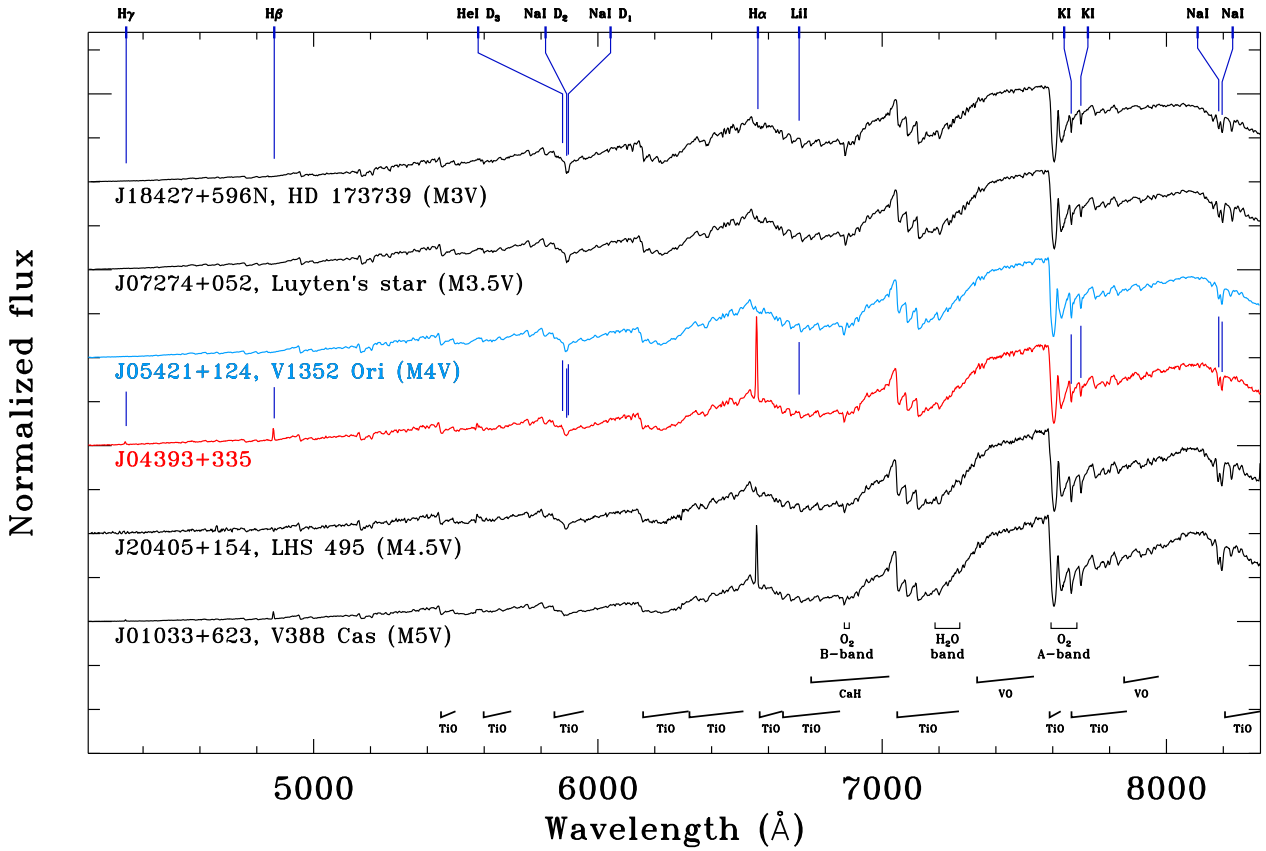

Fig. 18 Six representative spectra of mid-M dwarfs from Alonso-Floriano et al. (2015). From top to bottom, spectra of standard stars with spectral type 1.0 and 0.5 subtypes earlier than the target (black), standard star with the same spectral type as the target (cyan), the target star (red; in this case, V583 Aur B, M4.0 V), and standard stars with spectral type 0.5 and 1.0 subtypes later than the target (black). We mark activity-, gravity-, and youth-sensitive lines and doublets at the top of the figure (Hγ, Hβ, He I λ5876, Na I $\lambda\lambda$5890,6, Hα, Li I λ6708, K I $\lambda\lambda$7665,99, and Na I $\lambda\lambda$8183,95, from left to right) and molecular absorption bands at the bottom. Note the three first lines of the Balmer series in emission in the spectrum of the target star. All the spectra were collected with CAFOS/2.2 m Calar Alto and the same instrumental configuration.

Cannon, although much more complex classifications have been devised (Keenan, 1993, and references). The S stars have subtypes that intend to mirror those of M-type giants, together with a C/O index that runs from 1 to 10, where stars with index 7 to 10 are considered intermediate SC stars that merge into the C-N sequence.

- **Symbiotic stars.** A symbiotic binary (or symbiotic star) is a binary system whose spectrum shows very different components. In general, symbiotic stars show the spectrum of a cool giant superimposed with strong nebular emission, similar to a planetary nebula. The hot component is, in most cases, a white dwarf, which can be seen in UV spectra. The high excitation lines generate in an extended envelope or circumstellar disk created by material lost from the red giant, as it is illuminated by energetic photons coming from the white dwarf. See Munari (2019) for a review of related phenomena.

5.4 M dwarfs

M dwarfs are among the coolest and smallest stars, preceded only by old early L-type stars (see below for further details). The study of M dwarfs has been revived because of their importance in the last decade for low-mass exoplanet detection and characterization (e.g., Bonfils et al. 2013; Ribas et al. 2023). As introduced above, their spectra were first described in the 19th century by Secchi (1866), although he referred to M giants. Until the first parallax measurements of such faint objects, in the first two decades of the 20th century, the high proper motion of M dwarfs with respect to those of M giants and the subtle variations in their spectra, afterwards ascribed mainly to very different log g, were the only observable differences between M dwarfs and giants. With new parallaxes in hand, Adams and Joy (1922a) and Luyten (1922) were the first to prepare M-dwarf catalogs. Furthermore, Adams and Joy (1922a) assigned spectral type M (actually, Ma and Mb) to stars previously classified as K8, which inaugurated the curious "gap" in spectral type between K7 and M0.0 stars.

The main feature of the M spectral type is the prevalence of molecular bands at optical wavelengths, especially the ones produced by titanium oxide (TiO). These bands have been used to establish subtypes since Morgan (1938b) described the M0, M1 and M2 subtypes, followed by the studies of Kuiper (1942), Joy (1947), and Keenan and Schroeder (1952), who expanded the classification to mid- and late-M

dwarfs based on the strength of the TiO molecular bands. However, it was not until Joy and Abt (1974) and Boeshaar (1976) when the first standard classification of M subtypes from M0 to M6 was established over the optical wavelength region (4400–6800 Å), which was further extended to M7, M8 and M9 subtypes in later publications (Lee, 1984; Bidelman, 1985; Boeshaar and Tyson, 1985). This primordial classification was based on the strength of TiO bands for early M dwarfs, and on the ratio between the molecular bands of vanadium oxide (VO) at 5736 Å and TiO at 5759 Å, together with the appearance of the calcium hydroxide (CaOH) molecular band at 5530 Å, for later M subtypes. However, longer wavelengths become more important for the spectral classification according to the advance of the spectral type sequence towards cooler subtypes, showing other easily recognisable molecular bands, such as additional VO and CaOH molecular features. The strength of TiO bands are distinguishable from mid-K to M6, after which the VO bands and the sharper slope of the pseudocontinuum stand out (e.g., VO bandhead at 7300 Å). To the contrary of stars of earlier spectral types, the spectral continuum in M dwarfs cannot be defined because of the virtual omnipresence of molecular absorption bands; however, a pseudocontinuum can indeed be defined, at least locally.

It was Kirkpatrick et al. (1991) who reanalyzed the entire M-dwarf sequence using CCDs and longer wavelengths in the far red (from 6300 to 9000 Å) and provided a new, more complete, spectral-type classification in agreement with previous ones (except for an offset of up to one subtype in early M dwarfs with respect to MK). Kirkpatrick et al. (1991) identified a list of M-dwarf reference stars and of M giants for calibration purposes, and compiled a number of molecular bands (TiO, VO, and CaOH, but also CaH, CN) and neutral and ionized atomic lines (Na I, Mg I, K I, Ti I, Fe I, Ba II) in absorption used for spectral classification. Some atomic lines (e.g. Hα, Ca II) are also sensitive to $T_{\rm eff}$, although they are so much more to chromospheric activity and, therefore, to rotation and age. The Li I λ6708 Å line (actually a triplet) is a more reliable age indicator, since the original lithium is destroyed in a few tens of megayears in the interior of M dwarfs, which have extended convective envelopes (spectral type $\lesssim$ M4 V) or are even completely convective (spectral type $\gtrsim$ M4 V).

Following Kirkpatrick et al. (1991), there have been a number of remarkable studies on spectral classification of M dwarfs, such as those under the umbrella of the Palomar/Michigan State University nearby star spectroscopic survey (PMSU: Reid et al. 1995, 2002; Hawley et al. 1996; Gizis et al. 2002) or those by Riaz et al. (2006), Lépine and Gaidos (2011), and Lépine et al. (2013). To date, Alonso-Floriano et al. (2015) have provided the most exhaustive study of M-dwarf spectral classification, including an updated list of reference stars from M0.0 V to M8.0 V, a comparison with previous works, and a comprehensive summary of spectral indices previously used in the literature. They employed two independent methods for spectral typing: χ^2 minimization of the difference between target and standard spectra, and spectral indices. The spectral indices methodology for spectral typing is based on computing flux ratios at certain wavelength intervals in low-resolution spectra. Alonso-Floriano et al. (2015) compiled virtually all indices used in spectral classification of M dwarfs in the last decades (Kirkpatrick et al., 1991, 1995; Reid et al., 1995; Martin and Kun, 1996; Martín et al., 1996, 1999; Hawley et al., 2002; Lépine et al., 2003; Wilking et al., 2005; Shkolnik et al., 2009). Of the 31 tabulated indices, nine were related to TiO features, seven to VO, six to CaH, three to the pseudocontinuum (i.e., relative absence of features), and the rest to H and neutral metallic lines (Na I, Ti I). Some indices are sensitive not only to spectral type (i.e., $T_{\rm eff}$), but also to $\log g$, metallicity, or even activity. A few more spectral indices, mostly related to the TiO bands, may be defined in the blue region, but in most occasions the low observed flux of M dwarfs at these wavelengths would prevent their use. There are five spectral indices that have the widest range of application and least scatter in the dataset of Alonso-Floriano et al. (2015), who used CAFOS at the 2.2 m Calar Alto telescope with spectral resolution $\mathcal{R} \sim 1500$ and wavelength range 4200–8300 Å. The indices are TiO 2 and TiO 5 (Reid et al., 1995), PC1 (Martín et al., 1996), VO-7912 (Martín et al., 1999), and Color-M (Lépine et al., 2003).

In spite of the huge effort for over a century to determine the best spectral types in M dwarfs, recent papers on low-mass transiting planets around nearby stars tend to forget or ignore previous spectral-type determinations (and even classical star designations; e.g., Dai et al. 2024). Instead, some modern authors prefer to use quantitative spectroscopy only to (re-)determine their own model-dependent $T_{\rm eff}$, which are subject to a number of unsettled uncertainties that come from gravity and metallicity effects, the data themselves, and different methodologies, grids of models, and line libraries (Marfil et al., 2021). See the text in the introduction on the need for spectral classification as a prior step for quantitative spectroscopy, which is opposed to the modern suggestion that in most cases a combination of information on stellar luminosity (from the integration of multi-wavelength spectral energy distribution and precise *Gaia* parallaxes; Cifuentes et al. 2020) and on metallicity either from high-resolution spectroscopy (Passegger et al., 2022) or photometry (Duque-Arribas et al., 2023) can replace most of the information provided by spectral typing in M dwarfs. For those who still believe in the usefulness of simple, model-free spectral classification of M dwarfs, here we report a few final hints:

- **Subtype.** The uncertainty of the adopted spectral types can be down to 0.5 subtype. As a result, in M dwarfs the zero at the right of the dot should be written when the spectral type is derived with 0.5 subtype accuracy (e.g. "M3.0 V" instead of "M3 V"). More precise classifications should rather carefully consider gravity and metallicity effects and avoid using more than one digit after the decimal point.
- **K–M and M–L boundaries.** For continuity with the original HD scale, possible spectral types of late K and early M dwarfs in the MK, Kirkpatrick et al. (1991) and Alonso-Floriano et al. (2015) classification schemes are "K5, K7, M0.0, M0.5, M1.0, M1.5...". As a result, there are no K6, K8 or K9 dwarfs and the gap between K7 and M0.0 remains. On the other end, the latest M dwarf has spectral type M9.5, the next cooler spectral type being L0.0 (Kirkpatrick, 2005).
- **Configuration.** For internal consistency of derived spectral types, both standard and target stars in a homogeneous data set must be observed with the same instrumental configuration and reduced with the same pipeline (especially instrumental response correction). If spectra with different instrumental configurations are compared, precise spectral types cannot be determined either from χ^2 fitting or from spectral indices.
- **Emission.** Related to the suffixes/qualifiers used for spectral classification in Table 1, the qualifier "e" for emission lines was extensively used in the astronomical literature of M dwarfs in the 1980s and 1990s. Such emission lines are in general the Balmer series and the

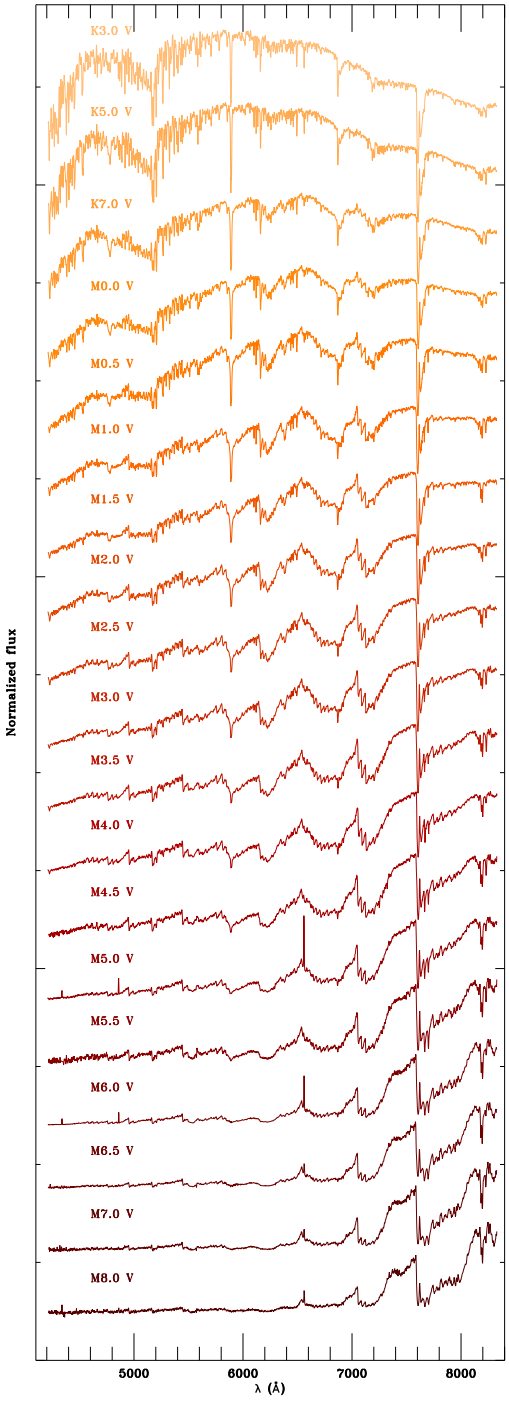

Fig. 19 CAFOS spectra of the prototype stars in Alonso-Floriano et al. (2015). From top to bottom, K3 V, K5 V, K7 V, M0.0–7.0 V in steps of 0.5 subtypes, and M8.0 V. Note the strengthening of molecular absorption bands, the weakening of the Na I D line, and the decrease of flux at the bluest wavelengths with the spectral sequence. Although standard M dwarfs were selected to be quiet, some of them have the Balmer series in emission (here Hα, Hβ, Hγ).

Ca II H & K doublet and infrared triplet. However, a large portion of mid- and late-M dwarfs, if not all during a significant part of their lives, have such chromospheric lines in emission (Jeffers et al. 2018 and references therein). This chromospheric emission must be differentiated from the much more intense emission from accretion from protoplanetary disks (White and Basri, 2003; Barrado y Navascués and Martín, 2003). As a result, the "e" qualifier should not be used for field M dwarfs, but for really active, very young, M-type T Tauri stars displaying emission lines from accretion. If not the case, virtually all M dwarfs except the oldest ones would also carry the "e" qualifier.

- **Subdwarfs.** In rare occasions, a qualifier "pec" is also used for peculiar M dwarfs (that is, identical to "p"). The usual suspect for this peculiarity, once the close M+WD binarity scenario is discarded, is very low metallicity. Actually, very low metallicity in M dwarfs can be detected in general only on high-S/N, high-resolution spectra and with specific software that simultaneously compares the EWs of a large number of faint Fe I, Fe II, and Ti I lines with those from a grid of synthetic spectra. Just in those rare occasions, the metallicity

is so low ([Fe/H] $\ll -1$) that its effect is visible in low-resolution spectra. When the peculiarity is confirmed to be ascribed to low metallicity (i.e., old age) based on the spectra themselves, kinematics compatible with the Galactic thick disk or the halo, and colours often much bluer than stars of the same $T_{\rm eff}$, the prefix "sd" for subdwarfs is used instead of the class (Jao et al., 2008). The qualitative nomenclature "esd" and "usd" has also been proposed for extreme and ultra subdwarfs, respectively, with far lower metallicity than "sd" (Gizis, 1997; Lépine et al., 2003, 2007; Burgasser et al., 2009). Low-metallicity subdwarfs are core-hydrogen burning stars (hence, in the main sequence from an evolutionary point of view) but not class V objects, as they are located below (or, more precisely, to the left of) the dwarf sequence in an H-R diagram.

- **Pre-main sequence stars (and brown dwarfs).** On the other side of the subdwarfs, there are other "M dwarfs" that have not arrived to the main sequence yet. Stars with masses less than about 0.6 $M_{\odot}$ and ages of a few tens of megayears are in the L vs. $T_{\rm eff}$ diagram in the vertical Hayashi tracks above the zero-age main sequence. These young M stars are overluminous with respect to M dwarfs of the same $T_{\rm eff}$ because of their larger radius. Spectroscopically, they are characterized by weaker gravity-sensitive alkali lines, as in the case of M giants. Besides, and perhaps more importantly, most young stars rotate fast and, therefore, develop strong magnetic fields and have intense chromospheric emission lines in their spectra; some M stars are so young that even have accretion from a disk (see above). Since they have not had time to fully contract and reach the typical $\log g$ of 4.5–5.5 of M dwarfs, this nomenclature or the class V should not be used for M stars in very young nearby kinematic groups, open clusters, and associations. Furthermore, some very late, very young M-type objects have masses below the hydrogen burning mass limit and, therefore, never become stars. They are instead brown dwarfs.

5.5 L, T and Y ultracool dwarfs

There have been numerous theoretical and observational studies dedicated to clarifying the existence of objects with masses intermediate between those of stars and planets. More than sixty years ago, Kumar (1963) and Hayashi and Nakano (1963) proposed that stable thermonuclear fusion of the lightest isotope of hydrogen (^{1}H) in a stellar core would not take place below a certain mass, beyond which electronic degeneration pressure would compensate for gravitational collapse to maintain hydrostatic balance. These types of objects were named with the term brown dwarfs by Tarter (1976). Brown dwarfs, along with giant exoplanets, whose mass is insufficient even for stable deuterium (^{2}H) combustion, are the two types of substellar objects.

Observational efforts to detect these bodies took more than a quarter of a century to bear fruit. In the same year that the first giant exoplanet around a solar-like star was discovered with the radial velocity method, 51 Pegasi b (Mayor and Queloz, 1995), the brown dwarfs were unveiled at the cosmic fauna zoo: Teide 1 in the Pleiades cluster (Rebolo et al., 1995) and GJ 229 B orbiting at about 45 au from an M2.0 V star (Nakajima et al., 1995). Despite its relatively recent discovery, the number of candidates for substellar objects already amounts to several thousands and grows month by month.

The effective temperatures that have been determined in substellar objects vary between about 3000 K for the most massive brown dwarfs in very young star-forming regions and less than 300 K (a typical room temperature!) for old Y dwarfs at less than 10 pc from the Sun, not counting planetary companions in wide orbit to stars. Due to their low surface temperature, substellar objects emit most of their energy in the near and medium infrared (1–10 μm), with hardly any emission in the optical. The classic spectral series O, B, A, F, G, K, M had to be extended to encompass such cool bodies with the new spectral types L and T, first (Martín et al., 1999; Kirkpatrick et al., 1999; Burgasser et al., 2002; Geballe et al., 2002), and Y afterwards (Delorme et al., 2008; Cushing et al., 2011; Kirkpatrick et al., 2012; Kirkpatrick et al., 2021), as illustrated by Fig. 20. As in earlier spectral types, spectral classification is carried out based on the intensity of some easily identifiable features in the photospheric spectra (absorption lines of alkaline elements, bands of metal oxides, water vapor, methane, or ammonia, slope of the pseudocontinuum). There is a mix of spectral classifications and standard ultracool dwarfs in the far red (only for L dwarfs) and in the near infrared (for L, T, and Y) that do not agree completely, yet. In any case, all of those classifications are in general performed with very low spectral resolutions, down to $\mathcal{R} \sim 100$ or even less, as their spectra are very faint and dominated by broad bands with a poorly defined continuum, as for M dwarfs.

One must not mix up the terms substellar object, brown dwarf, ultracool dwarf, and the different late spectral types. Substellar objects can be split into brown dwarfs ($M \sim 0.072$–0.013 M$_{\odot}$; they do not burn ^{1}H but burn ^{2}H) and "planetary-mass objects" ($M \lesssim 0.013$ M$_{\odot}$; they burn neither ^{1}H nor ^{2}H). In isolation, the later seem to originate from the star and brown-dwarf formation process extrapolated to very low masses (Caballero, 2018), while in orbit to stars they seem to originate in protoplanetary disks, as the planets of our Solar System. There are extremely young objects with late M spectral types that are brown dwarfs (e.g. in the star-forming regions of Orion, Taurus, or Upper Scorpius), while there are very old objects with early L spectral types that are stars (e.g. in the solar neighbourhood). As a result, one cannot assign a stellar or substellar mass to a late-M- or an early-L-type object unless its age is determined. Moreover, there can be extremely young T- and moderately-young Y-type objects that are not brown dwarfs, but planetary-mass objects beyond the deuterium-burning limit. For convention, in the field the term "ultracool" is used to denominate any object with spectral type M7.0 or later, regardless of its mass and age. The wide use of the term "dwarf" for such ultracool mixture of stars at the bottom of the main sequence, brown dwarfs, and giant exoplanets is only historical: while one cannot certify whether some of them have fusion reactions in their interiors, at least one can be sure of their extreme faintness, which prevented their discovery for decades. Such faintness of ultracool dwarfs has also led to difficulties in their spectral characterization.

5.5.1 L dwarfs

The first discovered L dwarf was GD 165 B, which orbits a white dwarf (Becklin and Zuckerman, 1988). Its spectrum was nevertheless so different from what was known at that time that a decade had to elapse for it to be recognised as an L dwarf (Kirkpatrick et al., 1999),

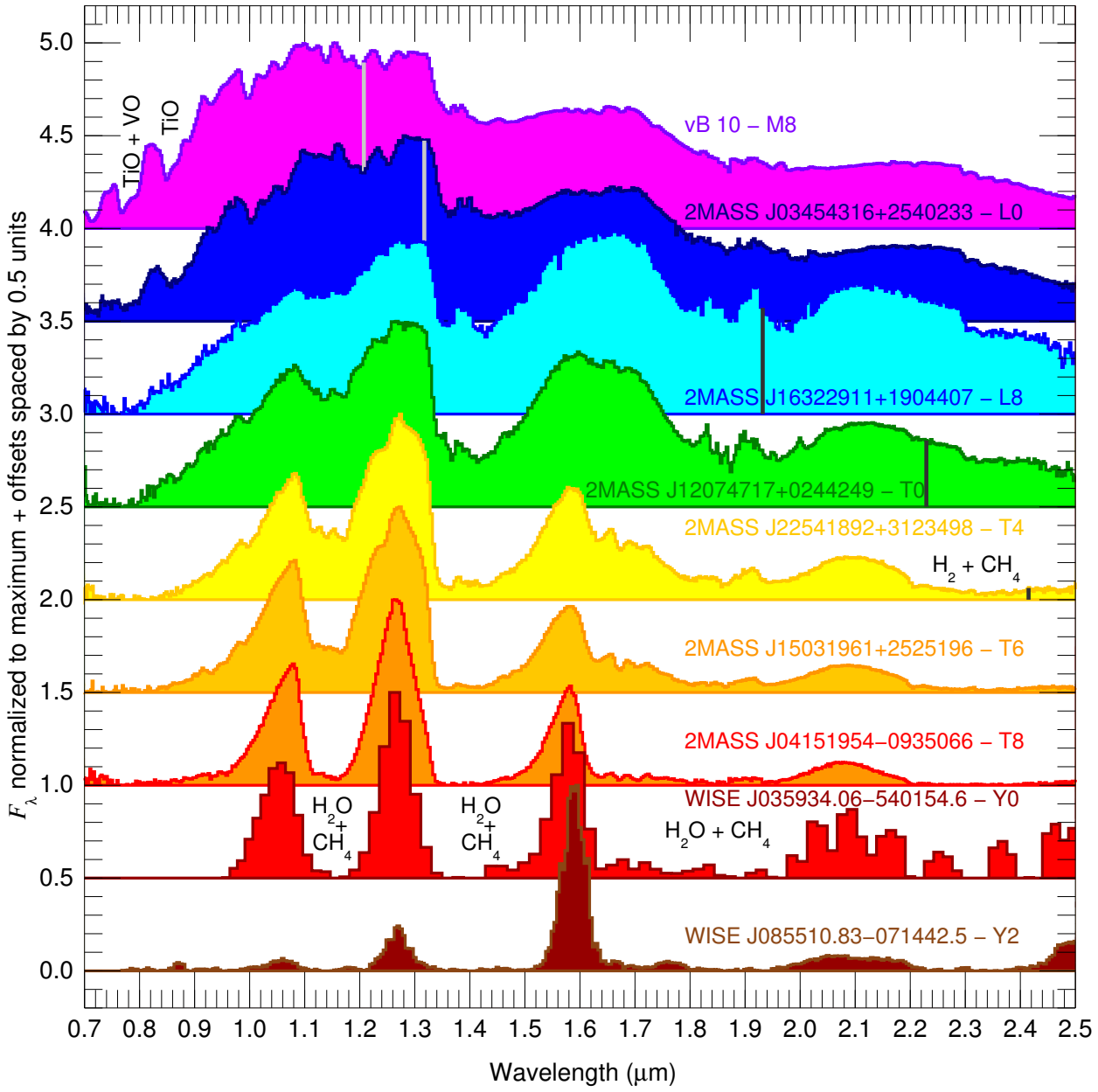

Fig. 20 NIR spectral sequence in normalized F_λ for the M8-Y2 spectral range. For the top five stars, the wavelength at which the peak of a black body of the same $T_{\rm eff}$ would be located is marked with a vertical line (for the bottom four, it would be outside the frame to the right). Some relevant absorption bands are marked. Note that for T and Y stars the flux is concentrated in four windows similar to the $YJHK$ terrestrial ones, mostly due to the effect of H_2O and CH_4 bands. All spectra were taken from the SpeX Prism Spectral Libraries, maintained by Adam Burgasser at `http://www.browndwarfs.org/spexprism`, except for the Y dwarfs, which were taken from Beiler et al. (2023) and Luhman et al. (2024).

especially after the first DENIS and Kelu-1 discoveries (Delfosse et al., 1997; Martín et al., 1997; Ruiz et al., 1997). The atmospheres of L dwarfs, as the spectral sequence progresses, are characterized by the increasing weakening and disappearance of the absorption bands of metal oxides (TiO and VO, especially), due to their condensation in solid grains of dust of refractory species (such as perovskite —$CaTiO_3$— and corundum —Al_2O_3—). The intensity of the molecular bands of metal hydrides (CrH, FeH, CaH), which replace the oxides, and water vapor (H_2O), grows along the L sequence. In turn, the absorption of alkali metal neutrals (Li I, Na I, K I, Rb I, Cs I) in the optical also increases considerably as the effective temperature decreases. On the other hand, as there are fewer donor electrons, the opacities due to H^- and H_2^- ions decrease. However, these opacities are still decisive when it comes to depressing the continuum, as is the collision-induced absorption (often named CIA) between H_2 and He molecules. Atmospheric dust masks some of the weakest spectral features and carbon is

mainly found in the form of monoxide, CO (Burrows and Sharp, 1999; Kirkpatrick et al., 1999; Martín et al., 1999; Allard et al., 2001). Li I is also sensitive to $T_{\rm eff}$ because the alkali atom bonds to hydrogen to form lithium hydride (LiH).

The Greek letters α, β, and γ are used as a proxy of the gravity instead of the luminosity class, which must not be used in brown dwarfs (and, by extension, LTY ultracool dwarfs). As an example, an L3β has the same $T_{\rm eff}$ but lower $\log g$ than an L3α, and the same $T_{\rm eff}$ but greater $\log g$ than an L3γ. The α letter is often dropped. Low-gravity L dwarfs have weaker alkali lines and fainter VO bands than their regular counterparts. Their spectra may also display a triangular shape of the pseudocontinuum in the H band. A Greek letter δ has been proposed for extremely low-gravity L dwarfs, too, but is not as extensively used. Other used qualifiers are in common to M dwarfs, such as "sd" and "pec", although "red" and "blue" (related to metallicity and unresolved multiplicity) are also found.

5.5.2 T dwarfs

Decreasing even further in temperature, the sequence of spectral type T dwarfs begins with the appearance of the methane (CH_4) bands, and continues with the strengthening of the H_2O and methane bands in the infrared, especially in the H and K bands, and the condensation of alkaline species in the form of chlorides, which makes the resonance doublet of Li I λ6707.8 disappear in the coldest T dwarfs (Burrows and Sharp, 1999; Burgasser et al., 2002; Geballe et al., 2002). The rich chemical diversity presented above is subject to significant changes in the physical conditions of the atmosphere, which cause temporal and spatial variations in the concentration of molecular species, gravitational sedimentation, formation of dust cloud layers (above or below the photosphere) or opening of holes in the cloud cover (which would allow additional flow to emerge from warmer inner layers). These phenomena are especially important in the transition between L and T dwarfs and explain the overluminosity of early T dwarfs in the J band (Ackerman and Marley, 2001; Burgasser et al., 2002) and enhanced photometric variability at the L–T boundary (Artigau et al., 2009). The first T dwarf, GJ 229 B, was discovered in 1995, and it took over a further decade to discover the first Y dwarfs.

5.5.3 Y dwarfs

While the M–L and L–T boundaries are at about 2200 K and 1300 K, respectively, the letter "Y" was already identified by Kirkpatrick et al. (1999) as a potential spectral type cooler than the coolest T dwarfs at about 700 K. With the advent of the Wide-field Infrared Survey Explorer (WISE, Wright et al. 2010), which operated in the bands centred at 3.4, 4.6, 12, and 22 μm, the first Y dwarfs were discovered. They no longer have photospheric CH_4 clouds, but mainly H_2O vapour and ammonia (NH_3). The carbon is instead bonded to oxygen in CO and CO_2 molecules, although traces of CH_4 remain in early Ys. At the moment of writing this lines (September 2024), there are only about 50 Y dwarfs known (Kirkpatrick et al., 2024; Luhman et al., 2024). All of them are within 20 pc, have masses near the deuterium burning limit (i.e. brown dwarf-planet boundary), and display spectral types Y0–2. There are, however, a few Y dwarfs that may be later, such as WISE J053516.80–750024.9, WISE J182831.08+265037.7, or, especially, WISE J085510.83–071442.5, with about 285 K (Luhman et al., 2024; Martín et al., 2024). Phosphine (PH_3) and H_2O ice clouds are now being looked for, and the metallicity, fast rotation, impact on its atmosphere of such clouds are being investigated. The future of Y-dwarf classification will have to be supported by mid-infrared observations, with e.g. *James Webb* Space Telescope. In ten years, this paragraph on Y-dwarf spectral classification will be wildly outdated. In a futuristic (or, rather, sci-fi) future, it may happen that Jupiter, with an equilibrium temperature of 88 K, is given the spectral type H0, just slightly cooler than the Y9 given to *Nemesis*, a hypothetical ultracool dwarf at a distance closer than Proxima Centauri.

Acknowledgments

This article would not have been possible without the knowledge of spectral classification that Nolan R. Walborn passed on to us. We thank Paul Crowther, Danny Lennon, and Brian Skiff for helpful suggestions. We acknowledge support from the Spanish Government Ministerio de Ciencia e Innovación and Agencia Estatal de Investigación (10.130 39/501 100 011 033) through grants PID2022-136 640 NB-C22 (J.M.A.), PID2022-137 241NB-C42 (J.A.C.) and PID2021-122 397 NB-C22 (I.N.).

References

Ackerman AS and Marley MS (2001). Precipitating condensation clouds in substellar atmospheres. *ApJ* 556 (2): 872–884.

Adams WS and Joy AH (1922a). A list of dwarf M-type stars. *PASP* 34 (199): 174.

Adams WS and Joy AH (1922b). A spectroscopic method of determining the absolute magnitudes of A-type stars and the parallaxes of 544 stars. *ApJ* 56: 242.

Aguado DS, Allende Prieto C, González Hernández JI and Rebolo R (2018). J0023+0307: A mega metal-poor dwarf star from SDSS/BOSS. *ApJL* 854 (2), L34.

Allard F, Hauschildt PH, Alexander DR, Tamanai A and Schweitzer A (2001). The limiting effects of dust in brown dwarf model atmospheres. *ApJ* 556 (1): 357–372.

Alonso-Floriano FJ, Morales JC, Caballero JA, Montes D, Klutsch A, Mundt R, Cortés-Contreras M, Ribas I, Reiners A, Amado PJ, Quirrenbach A and Jeffers SV (2015). CARMENES input catalogue of M dwarfs. I. Low-resolution spectroscopy with CAFOS. *A&A* 577, A128.

Alonso-Santiago J, Negueruela I, Marco A, Tabernero HM, González-Fernández C and Castro N (2019). A comprehensive study of NGC 2345, a young open cluster with a low metallicity. *A&A* 631, A124.

Alonso-Santiago J, Negueruela I, Marco A, Tabernero HM and Castro N (2020). Three open clusters containing cepheids: NGC 6649, NGC 6664, and Berkeley 55. *A&A* 644, A136.

Anderson RI, Ekström S, Georgy C, Meynet G, Mowlavi N and Eyer L (2014). On the effect of rotation on populations of classical cepheids. I. Predictions at solar metallicity. *A&A* 564, A100.

Arias JI, Walborn NR, Simón Díaz S, Barbá RH, Maíz Apellániz J, Sabín-Sanjulián C, Gamen RC, Morrell NI, Sota A, Marco A, Negueruela I, Leão JRS, Herrero A and Alfaro EJ (2016). Spectral classification and properties of the OVz stars in the Galactic O-Star Spectroscopic Survey (GOSSS). *AJ* 152, 31.

Artigau É, Bouchard S, Doyon R and Lafrenière D (2009). Photometric variability of the T2.5 brown dwarf simp J013656.5+093347: Evidence for evolving weather patterns. *ApJ* 701 (2): 1534–1539.

Balona L and Crampton D (1974). The Hγ-absolute magnitude calibration. *MNRAS* 166: 203–217.

Barrado y Navascués D and Martín EL (2003). An empirical criterion to classify T Tauri stars and substellar analogs using low-resolution optical spectroscopy. *AJ* 126 (6): 2997–3006.

Becklin EE and Zuckerman B (1988). A low-temperature companion to a white dwarf star. *Nature* 336 (6200): 656–658.

Beiler SA, Cushing MC, Kirkpatrick JD, Schneider AC, Mukherjee S and Marley MS (2023). The first JWST spectral energy distribution of a Y dwarf. *ApJL* 951 (2), L48.

Bestenlehner JM, Crowther PA, Caballero-Nieves SM, Schneider FRN, Simón-Díaz S, Brands SA, de Koter A, Gräfener G, Herrero A, Langer N, Lennon DJ, Maíz Apellániz J, Puls J and Vink JS (2020). The R136 star cluster dissected with Hubble Space Telescope/STIS - II. Physical properties of the most massive stars in R136. *MNRAS* 499 (2): 1918–1936.

Beyer AC and White RJ (2024). The Kraft break sharply divides low mass and intermediate mass stars `arXiv:2408.02638`.

Bidelman WP (1985). G.P. Kuiper's spectral classifications of proper-motion stars. *ApJS* 59: 197–227.

Boeshaar PC (1976). The Spectral Classification of M-Dwarf Stars. Ph.D. thesis, The Ohio State University.

Boeshaar PC and Tyson JA (1985). New limits on the surface density of M dwarfs. I. Photographic survey and preliminary CCD data. *AJ* 90: 817–822.

Bonfils X, Lo Curto G, Correia ACM, Laskar J, Udry S, Delfosse X, Forveille T, Astudillo-Defru N, Benz W, Bouchy F, Gillon M, Hébrard G, Lovis C, Mayor M, Moutou C, Naef D, Neves V, Pepe F, Perrier C, Queloz D, Santos NC and Ségransan D (2013). The HARPS search for southern extra-solar planets. XXXIV. A planetary system around the nearby M dwarf GJ 163, with a super-Earth possibly in the habitable zone. *A&A* 556, A110.

Burgasser AJ, Kirkpatrick JD, Brown ME, Reid IN, Burrows A, Liebert J, Matthews K, Gizis JE, Dahn CC, Monet DG, Cutri RM and Skrutskie MF (2002). The spectra of T dwarfs. I. Near-infrared data and spectral classification. *ApJ* 564 (1): 421–451.

Burgasser AJ, Witte S, Helling C, Sanderson RE, Bochanski JJ and Hauschildt PH (2009). Optical and near-infrared spectroscopy of the L subdwarf SDSS J125637.13-022452.4. *ApJ* 697 (1): 148–159.

Burrows A and Sharp CM (1999). Chemical equilibrium abundances in brown dwarf and extrasolar giant planet atmospheres. *ApJ* 512 (2): 843–863.

Caballero JA (2018). A review on substellar objects below the deuterium burning mass limit: Planets, brown dwarfs or what? *Geosciences* 8 (10): 362.

Cannon AJ and Mayall MW (1949). The Henry Draper extension. II. *AnHar* 112: 1–295.

Cannon AJ and Pickering EC (1901). Spectra of bright southern stars photographed with the 13-inch Boyden telescope as part of the Henry Draper Memorial. *Annals of Harvard College Observatory* 28: 129–P.6.

Cifuentes C, Caballero JA, Cortés-Contreras M, Montes D, Abellán FJ, Dorda R, Holgado G, Zapatero Osorio MR, Morales JC, Amado PJ, Passegger VM, Quirrenbach A, Reiners A, Ribas I, Sanz-Forcada J, Schweitzer A, Seifert W and Solano E (2020). CARMENES input catalogue of M dwarfs. V. Luminosities, colours, and spectral energy distributions. *A&A* 642, A115.

Clark JS, Negueruela I, Lohr ME, Dorda R, González-Fernández C, Lewis F and Roche P (2015). A long-period cepheid variable in the starburst cluster VdBH 222. *A&A* 584, L12.

Conti PS (1984), Basic observational constraints on the evolution of massive stars, Maeder A and Renzini A, (Eds.), Observational Tests of the Stellar Evolution Theory, IAU Symposium, 105, pp. 233.

Conti PS and Alschuler WR (1971). Spectroscopic studies of O-type stars. I. Classification and absolute magnitudes. *ApJ* 170: 325.

Cropper et al. (2018). Gaia Data Release 2. Gaia Radial Velocity Spectrometer. *A&A* 616, A5.

Crowe RA and Garrison RF (1988). The visible spectra of southern hemisphere Mira variable stars. *ApJS* 66: 69.

Crowther PA and Bohannan B (1997). The distinction between Oiafpe and WNLha stars. A spectral analysis of HD 151 804, HD 152 408 and HDE 313 846. *A&A* 317: 532–547.

Crowther PA and Smith LJ (1997). Fundamental parameters of Wolf-Rayet stars. VI. Large Magellanic Cloud WNL stars. *A&A* 320: 500–524.

Crowther PA and Walborn NR (2011). Spectral classification of O2-3.5 If*/WN5-7 stars. *MNRAS* 416: 1311–1323.

Crowther PA, De Marco O and Barlow MJ (1998). Quantitative classification of WC and WO stars. *MNRAS* 296 (2): 367–378.

Crowther PA, Schnurr O, Hirschi R, Yusof N, Parker RJ, Goodwin SP and Kassim HA (2010). The R136 star cluster hosts several stars whose individual masses greatly exceed the accepted 150 $M_\odot$ stellar mass limit. *MNRAS* 408: 731–751.

Curtiss RH (1932). Classification and description of stellar spectra. *Handbuch der Astrophysik* 5: 1.

Cushing MC, Kirkpatrick JD, Gelino CR, Griffith RL, Skrutskie MF, Mainzer A, Marsh KA, Beichman CA, Burgasser AJ, Prato LA, Simcoe RA, Marley MS, Saumon D, Freedman RS, Eisenhardt PR and Wright EL (2011). The discovery of Y dwarfs using data from the Wide-field Infrared Survey Explorer (WISE). *ApJ* 743 (1), 50.

Dai et al. (2024). An earth-sized planet on the verge of tidal disruption. *AJ* 168 (3), 101.

De Angeli et al. (2023). Gaia Data Release 3. Processing and validation of BP/RP low-resolution spectral data. *A&A* 674, A2.

de Burgos A, Simón-Díaz S, Urbaneja MA and Puls J (2024). The IACOB project. X. Large-scale quantitative spectroscopic analysis of Galactic luminous blue stars. *A&A* 687, A228.

De Greve JP (1996), Binary WR: an alternative channel for Conti's scenario, WR stars in the Framework of Stellar Evolution, pp. 55.

Delfosse X, Tinney CG, Forveille T, Epchtein N, Bertin E, Borsenberger J, Copet E, de Batz B, Fouque P, Kimeswenger S, Le Bertre T, Lacombe F, Rouan D and Tiphene D (1997). Field brown dwarfs found by DENIS. *A&A* 327: L25–L28.

Delorme P, Delfosse X, Albert L, Artigau E, Forveille T, Reylé C, Allard F, Homeier D, Robin AC, Willott CJ, Liu MC and Dupuy TJ (2008). CFBDS J005910.90-011401.3: Reaching the T-Y brown dwarf transition? *A&A* 482 (3): 961–971.

Dimitrov DP, Kjurkchieva DP and Ivanov EI (2018). A study of the Hα variability of Be stars. *AJ* 156, 61.

Dorda R, Negueruela I, González-Fernández C and Tabernero HM (2016). Spectral type, temperature, and evolutionary stage in cool supergiants. *A&A* 592, A16.

Dorda R, Negueruela I, González-Fernández C and Marco A (2018). An atlas of cool supergiants from the Magellanic Clouds and typical interlopers. A guide for the classification of luminous red stars. *A&A* 618, A137.

Drilling JS, Jeffery CS, Heber U, Moehler S and Napiwotzki R (2013). An MK-like system of spectral classification for hot subdwarfs. *A&A* 551, A31.

Drissen L, Moffat AFJ, Walborn NR and Shara MM (1995). The dense galactic starburst NGC 3603. I. HST/FOS spectroscopy of individual stars in the core and the source of ionization and kinetic energy. *AJ* 110: 2235–2241.
Duque-Arribas C, Montes D, Tabernero HM, Caballero JA, Gorgas J and Marfil E (2023). Photometric calibrations of M-dwarf metallicity with Markov chain Monte Carlo and Bayesian inference. *ApJ* 944 (1), 106.
Evans CJ and Howarth ID (2003). Characteristics and classification of A-type supergiants in the Small Magellanic Cloud. *MNRAS* 345 (4): 1223–1235.
Falcón-Barroso J, Sánchez-Blázquez P, Vazdekis A, Ricciardelli E, Cardiel N, Cenarro AJ, Gorgas J and Peletier RF (2011). An updated MILES stellar library and stellar population models. *A&A* 532, A95.
Fang M, Hillenbrand LA, Kim JS, Findeisen K, Herczeg GJ, Carpenter JM, Rebull LM and Wang H (2020). The first extensive spectroscopic study of young stars in the North America and Pelican nebulae. *ApJ* 904 (2), 146.
Feast MW, Thackeray AD and Wesselink AJ (1960). The brightest stars in the Magellanic Clouds. *MNRAS* 121: 337.
García-Hernández DA, García-Lario P, Plez B, Manchado A, D'Antona F, Lub J and Habing H (2007). Lithium and zirconium abundances in massive Galactic O-rich AGB stars. *A&A* 462 (2): 711–730.
Garrison RF (1994), A hierarchy of standards for the MK process, Corbally CJ, Gray RO and Garrison RF, (Eds.), The MK Process at 50 Years: A Powerful Tool for Astrophysical Insight, Astronomical Society of the Pacific Conference Series, 60, pp. 3.
Garrison RF and Gray RO (1994). The late B-type stars: Refined MK classification, confrontation with Strömgren photometry, and the effects of rotation. *AJ* 107: 1556–1564.
Geballe et al. (2002). Toward spectral classification of L and T dwarfs: Infrared and optical spectroscopy and analysis. *ApJ* 564 (1): 466–481.
Gilmore et al. (2012). The Gaia-ESO public spectroscopic survey. *The Messenger* 147: 25–31.
Gizis JE (1997). M-subdwarfs: Spectroscopic classification and the metallicity scale. *AJ* 113: 806–822.
Gizis JE, Reid IN and Hawley SL (2002). The Palomar/MSU nearby-star spectroscopic survey. III. Chromospheric activity, M dwarf ages, and the local star formation history. *AJ* 123 (6): 3356–3369.
Gorny SK and Stasińska G (1995). On the status of planetary nebulae with WR-type nuclei. *A&A* 303: 893.
Götberg Y, de Mink SE, Groh JH, Kupfer T, Crowther PA, Zapartas E and Renzo M (2018). Spectral models for binary products: Unifying subdwarfs and Wolf-Rayet stars as a sequence of stripped-envelope stars. *A&A* 615, A78.
Götberg Y, Drout MR, Ji AP, Groh JH, Ludwig BA, Crowther PA, Smith N, de Koter A and de Mink SE (2023). Stellar properties of observed stars stripped in binaries in the Magellanic Clouds. *ApJ* 959 (2), 125.
Gray RO and Corbally J. C (2009). Stellar Spectral Classification, ISBN: 978-0-691-12511-4.
Gray RO and Garrison RF (1987). The early A-type stars: Refined MK classification, confrontation with Strömgren photometry, and the effects of rotation. *ApJS* 65: 581.
Gray RO and Garrison RF (1989a). The early F-type stars: Refined classification, confrontation with Strömgren photometry, and the effects of rotation. *ApJS* 69: 301.
Gray RO and Garrison RF (1989b). The late A-type stars: Refined MK classification, confrontation with Strömgren photometry, and the effects of rotation. *ApJS* 70: 623.
Gray RO, Corbally CJ, Garrison RF, McFadden MT and Robinson PE (2003). Contributions to the Nearby Stars (NStars) project: Spectroscopy of stars earlier than M0 within 40 parsecs: The northern sample. I. *AJ* 126: 2048–2059.
Hawley SL, Gizis JE and Reid IN (1996). The Palomar/MSU nearby-star spectroscopic survey. II. The southern M dwarfs and investigation of magnetic activity. *AJ* 112: 2799.
Hawley et al. (2002). Characterization of M, L, and T dwarfs in the Sloan Digital Sky Survey. *AJ* 123 (6): 3409–3427.
Hayashi C and Nakano T (1963). Evolution of stars of small masses in the Pre-Main-Sequence stages. *Progress of Theoretical Physics* 30 (4): 460–474.
Hearnshaw JB (1990). The Analysis of Starlight, ISBN: 0-521-39916-5.
Heber U (2016). Hot subluminous stars. *PASP* 128 (8): 082001.
Herwig F (2005). Evolution of Asymptotic Giant Branch stars. *ARA&A* 43 (1): 435–479.
Holgado G, Simón-Díaz S, Barbá RH, Puls J, Herrero A, Castro N, Garcia M, Maíz Apellániz J, Negueruela I and Sabín-Sanjulián C (2018). The IACOB project. V. Spectroscopic parameters of the O-type stars in the modern grid of standards for spectral classification. *A&A* 613, A65.
Holgado G, Simón-Díaz S, Herrero A and Barbá RH (2022). The IACOB project. VII. The rotational properties of Galactic massive O-type stars revisited. *A&A* 665, A150.
Hubrig S, Schöller M, Järvinen SP, Cikota A, Abdul-Masih M, Escorza A and Jayaraman R (2024). Detection of extragalactic magnetic massive stars. *A&A* 686, L4.
Hümmerich S, Paunzen E and Bernhard K (2020). A plethora of new, magnetic chemically peculiar stars from LAMOST DR4. *A&A* 640, A40.
Humphreys RM and Davidson K (1979). Studies of luminous stars in nearby galaxies. III. Comments on the evolution of the most massive stars in the Milky Way and the Large Magellanic Cloud. *ApJ* 232: 409–420.
Jao WC, Henry TJ, Beaulieu TD and Subasavage JP (2008). Cool subdwarf investigations. I. New thoughts on the spectral types of K and M subdwarfs. *AJ* 136 (2): 840–880.
Jeffers SV, Schöfer P, Lamert A, Reiners A, Montes D, Caballero JA, Cortés-Contreras M, Marvin CJ, Passegger VM, Zechmeister M, Quirrenbach A, Alonso-Floriano FJ, Amado PJ, Bauer FF, Casal E, Diez Alonso E, Herrero E, Morales JC, Mundt R, Ribas I and Sarmiento LF (2018). CARMENES input catalogue of M dwarfs. III. Rotation and activity from high-resolution spectroscopic observations. *A&A* 614, A76.
Johnson HL and Morgan WW (1953). Fundamental stellar photometry for standards of spectral type on the revised system of the Yerkes spectral atlas. *ApJ* 117: 313–352.
Joy AH (1947). Radial velocities and spectral types of 181 dwarf stars. *ApJ* 105: 96.
Joy AH and Abt HA (1974). Spectral types of M dwarf stars. *ApJS* 28: 1.
Keenan PC (1942). Luminosities of the M-type variables of small range. *ApJ* 95: 461.
Keenan PC (1984), What is wrong with the MK system?, Garrison RF, (Ed.), The MK Process and Stellar Classification, pp. 29.
Keenan PC (1993). Revised MK spectral classification of the red carbon stars. *PASP* 105: 905.
Keenan PC and McNeil RC (1989). The Perkins catalog of revised MK types for the cooler stars. *ApJS* 71: 245.
Keenan PC and Schroeder LW (1952). An infrared system of bands of VO in M-type stars. *ApJ* 115: 82.
Keenan PC, Garrison RF and Deutsch AJ (1974). Revised catalog of spectra of Mira variables of types ME and Se. *ApJS* 28: 271.
Kirkpatrick JD (2005). New spectral types L and T. *ARA&A* 43 (1): 195–245.
Kirkpatrick JD, Henry TJ and McCarthy Donald W. J (1991). A standard stellar spectral sequence in the red/near-infrared: Classes K5 to M9. *ApJS* 77: 417.
Kirkpatrick JD, Henry TJ and Simons DA (1995). The solar neighborhood. II. The first list of dwarfs with spectral types of M7 and cooler. *AJ* 109: 797.

Kirkpatrick JD, Reid IN, Liebert J, Cutri RM, Nelson B, Beichman CA, Dahn CC, Monet DG, Gizis JE and Skrutskie MF (1999). Dwarfs cooler than "M": The definition of spectral type "L" using discoveries from the 2 Micron All-Sky Survey (2MASS). *ApJ* 519 (2): 802–833.
Kirkpatrick JD, Gelino CR, Cushing MC, Mace GN, Griffith RL, Skrutskie MF, Marsh KA, Wright EL, Eisenhardt PR, McLean IS, Mainzer AK, Burgasser AJ, Tinney CG, Parker S and Salter G (2012). Further defining spectral type "Y" and exploring the low-mass end of the field brown dwarf mass function. *ApJ* 753 (2), 156.
Kirkpatrick et al. (2021). The field substellar mass function based on the full-sky 20 pc census of 525 L, T, AND Y dwarfs. *ApJS* 253 (1), 7.
Kirkpatrick et al. (2024). The initial mass function based on the full-sky 20 pc census of ∼3600 stars and brown dwarfs. *ApJS* 271 (2), 55.
Kraft RP (1967). Studies of stellar rotation. V. The dependence of rotation on age among solar-type stars. *ApJ* 150: 551.
Kuiper GP (1942). The nearest stars. *ApJ* 95: 201.
Kumar SS (1963). The structure of stars of very low mass. *ApJ* 137: 1121.
Lamers HJGLM, Zickgraf FJ, de Winter D, Houziaux L and Zorec J (1998). An improved classification of B[e]-type stars. *A&A* 340: 117–128.
Leavitt HS and Pickering EC (1912). Periods of 25 variable stars in the Small Magellanic Cloud. *Harvard College Observatory Circular* 173: 1–3.
Lebzelter T, Trabucchi M, Mowlavi N, Wood PR, Marigo P, Pastorelli G and Lecoeur-Taïbi I (2019). Period-luminosity diagram of long period variables in the Magellanic Clouds. New aspects revealed from Gaia Data Release 2. *A&A* 631, A24.
Lee SG (1984). Spectral classification of high-proper-motion stars. *AJ* 89: 702–719.
Lennon DJ (1997). Revised spectral types for 64 B-supergiants in the Small Magellanic Cloud: metallicity effects. *A&A* 317: 871–882.
Lennon DJ (1999), Spectral morphology and classification of massive stars in the Small Magellanic Cloud: effects of metallicity., Morrell NI, Niemela VS and Barbá RH, (Eds.), Rev. Mex. Astron. Astrofís. (conference series), 8, 21–28.
Lépine S and Gaidos E (2011). An all-sky catalog of bright M dwarfs. *AJ* 142 (4), 138.
Lépine S, Rich RM and Shara MM (2003). Spectroscopy of new high proper motion stars in the northern sky. I. New nearby stars, new high-velocity stars, and an enhanced classification scheme for M dwarfs. *AJ* 125 (3): 1598–1622.
Lépine S, Rich RM and Shara MM (2007). Revised metallicity classes for low-mass stars: Dwarfs (dM), subdwarfs (sdM), extreme subdwarfs (esdM), and ultrasubdwarfs (usdM). *ApJ* 669 (2): 1235–1247.
Lépine S, Hilton EJ, Mann AW, Wilde M, Rojas-Ayala B, Cruz KL and Gaidos E (2013). A spectroscopic catalog of the brightest (J < 9) M dwarfs in the northern sky. *AJ* 145 (4), 102.
Lesh JR (1968). The kinematics of the Gould Belt: an expanding group? *ApJS* 17: 371–444.
Luhman KL, Tremblin P, Alves de Oliveira C, Birkmann SM, Baraffe I, Chabrier G, Manjavacas E, Parker RJ and Valenti J (2024). JWST/NIRSpec observations of the coldest known brown dwarf. *AJ* 167 (1), 5.
Luyten WJ (1922). A list of new and suspected dwarfs of class M. *PASP* 34 (202): 342.
Maeder A (1996), The Conti scenario for forming WR stars: past, present and future, WR stars in the Framework of Stellar Evolution, pp. 39.
Maíz Apellániz J (2024). Extinction, the elephant in the room that hinders optical Galactic observations : arXiv:2401.01116.
Maíz Apellániz J and Weiler M (2018). Reanalysis of the Gaia Data Release 2 photometric sensitivity curves using HST/STIS spectrophotometry. *A&A* 619, A180.
Maíz Apellániz J, Sota A, Walborn NR, Alfaro EJ, Barbá RH, Morrell NI, Gamen RC and Arias JI (2011), The Galactic O-Star Spectroscopic survey (GOSSS), Highlights of Spanish Astrophysics VI, 467–472, arXiv:1010.5680.
Maíz Apellániz J, Pellerin A, Barbá RH, Simón-Díaz S, Alfaro EJ, Morrell NI, Sota A, Penadés Ordaz M and Gallego Calvente AT (2012), The Galactic O-Star Spectroscopic (GOSSS) and Northern Massive Dim Stars (NoMaDS) surveys, the Galactic O-Star Catalog (GOSC), and Marxist Ghost Buster (MGB), Drissen L, Robert C, St-Louis N and Moffat AFJ, (Eds.), Astronomical Society of the Pacific Conference Series, 465, pp. 484.
Maíz Apellániz J, Sota A, Barbá RH, Morrell NI, Pellerin A, Alfaro EJ and Simón-Díaz S (2014), First results from a study of DIBs with thousands of high-quality massive-star spectra, IAUS, 297, 117–120.
Maíz Apellániz J, Sota A, Arias JI, Barbá RH, Walborn NR, Simón-Díaz S, Negueruela I, Marco A, Leão JRS, Herrero A, Gamen RC and Alfaro EJ (2016), May. The Galactic O-Star Spectroscopic Survey (GOSSS). III. 142 additional O-type systems. *ApJS* 224, 4.
Maíz Apellániz J, Trigueros Páez E, Jiménez Martínez I, Barbá RH, Simón-Díaz S, Pellerin A, Negueruela I and Souza Leão JR (2019a), LiLiMaRlin, a **Li**brary of **Li**braries of **Ma**ssive-Star High-**R**esol**u**t**i**o**n** Spectra with applications to OWN, MONOS, and CollDIBs, Highlights of Spanish Astrophysics X, pp. 420, arXiv:1810.10943.
Maíz Apellániz J, Trigueros Páez E, Negueruela I, Barbá RH, Simón-Díaz S, Lorenzo J, Sota A, Gamen RC, Fariña C, Salas J, Caballero JA, Morrell NI, Pellerin A, Alfaro EJ, Herrero A, Arias JI and Marco A (2019b). MONOS: Multiplicity of northern O-type spectroscopic systems. I. Project description and spectral classifications and visual multiplicity of previously known objects. *A&A* 626, A20.
Maíz Apellániz J, Holgado G, Pantaleoni González M and Caballero JA (2023). Stellar variability in Gaia DR3. I. Three-band photometric dispersions for 145 million sources. *A&A* 677, A137.
Marco A and Negueruela I (2013). NGC 7419 as a template for red supergiant clusters. *A&A* 552, A92.
Marfil et al. (2021). The CARMENES search for exoplanets around M dwarfs. stellar atmospheric parameters of target stars with SteParSyn. *A&A* 656, A162.
Martin EL and Kun M (1996). Spectroscopy of possible Hα emission stars in regions of high Galactic latitude molecular clouds. *A&AS* 116: 467–471.
Martín EL, Rebolo R and Zapatero-Osorio MR (1996). Spectroscopy of new substellar candidates in the Pleiades: Toward a spectral sequence for young brown dwarfs. *ApJ* 469: 706.
Martín EL, Basri G, Delfosse X and Forveille T (1997). Keck HIRES spectra of the brown dwarf DENIS-P J1228.2-1547. *A&A* 327: L29–L32.
Martín EL, Delfosse X, Basri G, Goldman B, Forveille T and Zapatero Osorio MR (1999). Spectroscopic classification of late-M and L field dwarfs. *AJ* 118 (5): 2466–2482.
Martín EL, Zhang JY, Lanchas H, Lodieu N, Shahbaz T and Pavlenko YV (2024). Optical properties of Y dwarfs observed with the Gran Telescopio Canarias. *A&A* 686, A73.
Martins F and Palacios A (2017). Spectroscopic evolution of massive stars on the main sequence. *A&A* 598, A56.
Maury AC and Pickering EC (1897). Spectra of bright stars photographed with the 11-inch Draper telescope as part of the Henry Draper memorial. *Annals of Harvard College Observatory* 28: 1–128.
Mayor M and Queloz D (1995). A Jupiter-mass companion to a solar-type star. *Nature* 378 (6555): 355–359.
Mermilliod JC and Mayor M (1989). Red giants in open clusters. I. Binarity and stellar evolution in five Hyades-generation clusters: NGC 2447, 2539, 2632, 6633 and 6940. *A&A* 219: 125–141.
Morgan WW (1937). On the spectral classification of the stars of types A to K. *ApJ* 85: 380.
Morgan WW (1938a). On the determination of color indices of stars from a classification of their spectra. *ApJ* 87: 460.
Morgan WW (1938b). On the spectral types and luminosities of the M dwarfs. *ApJ* 87: 589.
Morgan WW (1951). Application of the principle of natural groups to the classification of stellar spectra. *Publications of Michigan Observatory*

10: 33.
Morgan WW and Hiltner WA (1965). Studies in spectral classification. I. The HR Diagram of the Hyades. *ApJ* 141: 177.
Morgan WW and Keenan PC (1973). Spectral classification. *ARA&A* 11: 29.
Morgan WW, Keenan PC and Kellman E (1943). An atlas of stellar spectra, with an outline of spectral classification.
Morgan WW, Abt HA and Tapscott JW (1978). Revised MK Spectral Atlas for stars earlier than the Sun.
Munari U (2019). The symbiotic stars : arXiv:1909.01389.
Muñoz MS, Wade GA, Faes D and Carciofi A (2020), The photometric and polarimetric variability of magnetic O-type stars, Wade G, Alecian E, Bohlender D and Sigut A, (Eds.), Stellar Magnetism: A Workshop in Honour of the Career and Contributions of John D. Landstreet, 11, 148–155, arXiv:2004.13594.
Nakajima T, Oppenheimer BR, Kulkarni SR, Golimowski DA, Matthews K and Durrance ST (1995). Discovery of a cool brown dwarf. *Nature* 378 (6556): 463–465.
Nazé Y, Barbá R, Bagnulo S, Morrell N, Gamen R, Petit V and Neiner C (2016). The puzzling properties of the magnetic O star Tr16-22. *A&A* 596, A44.
Nazé Y, Neiner C, Grunhut J, Bagnulo S, Alecian E, Rauw G, Wade GA and BinaMIcS Collaboration (2017). How unique is Plaskett's star? A search for organized magnetic fields in short period, interacting or post-interaction massive binary systems. *MNRAS* 467: 501–511.
Negueruela I, Steele IA and Bernabeu G (2004). On the class of Oe stars. *AN* 325: 749–760.
Negueruela I, Marco A, González-Fernández C, Jiménez-Esteban F, Clark JS, Garcia M and Solano E (2012). Red supergiants around the obscured open cluster Stephenson 2. *A&A* 547, A15.
Negueruela I, Simón-Díaz S, de Burgos A, Casasbuenas A and Beck PG (2024). The IACOB project XII. A new grid of northern standards for the spectral classification of B-type stars. arXiv:2407.04163.
Passegger VM, Bello-García A, Ordieres-Meré J, Antoniadis-Karnavas A, Marfil E, Duque-Arribas C, Amado PJ, Delgado-Mena E, Montes D, Rojas-Ayala B, Schweitzer A, Tabernero HM, Béjar VJS, Caballero JA, Hatzes AP, Henning T, Pedraz S, Quirrenbach A, Reiners A and Ribas I (2022). Metallicities in M dwarfs: Investigating different determination techniques. *A&A* 658, A194.
Paunzen E, Hümmerich S and Bernhard K (2021). New mercury-manganese stars and candidates from LAMOST DR4. *A&A* 645, A34.
Payne CH (1925). Stellar Atmospheres; a Contribution to the Observational Study of High Temperature in the Reversing Layers of Stars. Ph.D. thesis, Radcliffe College.
Pickering EC (1890). The Draper Catalogue of stellar spectra photographed with the 8-inch Bache telescope as a part of the Henry Draper memorial. *Annals of Harvard College Observatory* 27: 1–388.
Pickering EC (1897). The spectrum of ζ Puppis. *Harvard College Observatory Circular* 16: 1–2.
Pickering EC and Fleming M (1897). Miscellaneous investigations of the Henry Draper memorial. *Annals of Harvard College Observatory* 26: 193–P.XI.2.
Porter JM and Rivinius T (2003). Classical Be stars. *PASP* 115: 1153–1170.
Prusti et al. (2016). The Gaia mission. *A&A* 595, A1.
Randich et al. (2022). The Gaia-ESO public spectroscopic survey: Implementation, data products, open cluster survey, science, and legacy. *A&A* 666, A121.
Rebolo R, Zapatero Osorio MR and Martín EL (1995). Discovery of a brown dwarf in the Pleiades star cluster. *Nature* 377 (6545): 129–131.
Recio-Blanco et al. (2023). Gaia Data Release 3. Analysis of RVS spectra using the general stellar parametriser from spectroscopy. *A&A* 674, A29.
Reid IN, Hawley SL and Gizis JE (1995). The Palomar/MSU nearby-star spectroscopic survey. I. The northern M dwarfs - bandstrengths and kinematics. *AJ* 110: 1838.
Reid IN, Gizis JE and Hawley SL (2002). The Palomar/MSU nearby-star spectroscopic survey. IV. The luminosity function in the solar neighborhood and M dwarf kinematics. *AJ* 124 (5): 2721–2738.
Reiners et al. (2018). The CARMENES search for exoplanets around M dwarfs. HD 147 379 b: A nearby Neptune in the temperate zone of an early-M dwarf. *A&A* 609, L5.
Reylé C, Jardine K, Fouqué P, Caballero JA, Smart RL and Sozzetti A (2021). The 10 parsec sample in the Gaia era. *A&A* 650, A201.
Riaz B, Gizis JE and Harvin J (2006). Identification of new M dwarfs in the solar neighborhood. *AJ* 132 (2): 866–872.
Ribas et al. (2023). The CARMENES search for exoplanets around M dwarfs. Guaranteed time observations data release 1 (2016-2020). *A&A* 670, A139.
Roman NG (1950). A correlation between the spectroscopic and dynamical characteristics of the late F - and early G - type stars. *ApJ* 112: 554.
Rountree J and Sonneborn G (1991). Criteria for the spectral classification of B stars in the ultraviolet. *ApJ* 369: 515.
Royer F, Zorec J and Gómez AE (2007). Rotational velocities of A-type stars. III. Velocity distributions. *A&A* 463 (2): 671–682.
Ruiz MT, Leggett SK and Allard F (1997). Kelu-1: A free-floating brown dwarf in the solar neighborhood. *ApJL* 491 (2): L107–L110.
Saha MN (1921). On a physical theory of stellar spectra. *Proceedings of the Royal Society of London Series A* 99 (697): 135–153.
Secchi A (1866). Spectrum of α Orionis. *MNRAS* 26: 214.
Shkolnik E, Liu MC and Reid IN (2009). Identifying the young low-mass stars within 25 pc. I. Spectroscopic observations. *ApJ* 699 (1): 649–666.
Simon KP and Sturm E (1994). Disentangling of composite spectra. *A&A* 281: 286–291.
Simón-Díaz S, Caballero JA, Lorenzo J, Maíz Apellániz J, Schneider FRN, Negueruela I, Barbá RH, Dorda R, Marco A, Montes D, Pellerin A, Sanchez-Bermudez J, Sódor Á and Sota A (2015). Orbital and physical properties of the σ Ori Aa, Ab, B triple system. *ApJ* 799, 169.
Smith N (2011). Explosions triggered by violent binary-star collisions: application to η Carinae and other eruptive transients. *MNRAS* 415: 2020–2024.
Smith N and Frew DJ (2011). A revised historical light curve of η Carinae and the timing of close periastron encounters. *MNRAS* 415: 2009–2019.
Smith VV, Plez B, Lambert DL and Lubowich DA (1995). A survey of lithium in the red giants of the Magellanic Clouds. *ApJ* 441: 735.
Smith LF, Shara MM and Moffat AFJ (1996). A three-dimensional classification for WN stars. *MNRAS* 281 (1): 163–191.
Smith Neubig MM and Bruhweiler FC (1997). UV spectral classification of O and B stars in the Small Magellanic Cloud. *AJ* 114: 1951.
Smith Neubig MM and Bruhweiler FC (1999). Ultraviolet spectral classification of O and B stars in the Large Magellanic Cloud. *AJ* 117: 2856.
Solf J (1978). Spectral type and luminosity classification of late-type M stars from near-infrared image tube coudé spectrograms. *A&AS* 34: 409–416.
Sota A, Maíz Apellániz J, Walborn NR, Alfaro EJ, Barbá RH, Morrell NI, Gamen RC and Arias JI (2011). The Galactic O-Star Spectroscopic Survey. I. Classification system and bright northern stars in the blue-violet at R~2500. *ApJS* 193: 24.
Sota A, Maíz Apellániz J, Morrell NI, Barbá RH, Walborn NR, Gamen RC, Arias JI and Alfaro EJ (2014). The Galactic O-Star Spectroscopic Survey (GOSSS). II. Bright southern stars. *ApJS* 211, 10.
Struve O (1929). The Stark effect as a means of determining comparative absolute magnitudes. *ApJ* 70: 237–242.
Tabernero HM, Dorda R, Negueruela I and Marfil E (2021). The nature of VX Sagitarii. is it a TŻO, a RSG, or a high-mass AGB star? *A&A* 646,

A98.
Tarter JC (1976), Brown dwarfs, lilliputian stars, giant planets and missing mass problems., Bulletin of the American Astronomical Society, 8, pp. 517.
Valdes F, Gupta R, Rose JA, Singh HP and Bell DJ (2004). The Indo-US library of Coudé feed stellar spectra. *ApJS* 152: 251–259.
Vink et al. (2023). X-Shooting ULLYSES: Massive stars at low metallicity. I. Project description. *A&A* 675, A154.
Wade GA, Bagnulo S, Keszthelyi Z, Folsom CP, Alecian E, Castro N, David-Uraz A, Fossati L, Petit V, Shultz ME and Sikora J (2020). No evidence of a sudden change of spectral appearance or magnetic field strength of the O9.7 v star HD 54 879. *MNRAS* 492 (1): L1–L5.
Walborn NR (1971a). On the existence of OB stars with anomalous nitrogen and carbon spectra. *ApJL* 164: L67–L69.
Walborn NR (1971b). Some extremely early O stars near η Carinae. *ApJL* 167: L31–L33.
Walborn NR (1971c). Some spectroscopic characteristics of the OB stars: an investigation of the space distribution of certain OB stars and the reference frame of the classification. *ApJS* 23: 257–282.
Walborn NR (1972). Spectral classification of OB stars in both hemispheres and the absolute magnitude calibration. *AJ* 77: 312–318.
Walborn NR (1974). Some morphological properties of WN spectra. *ApJ* 189: 269–271.
Walborn NR (1976). The OBN and OBC stars. *ApJ* 205: 419–425.
Walborn NR (1982a). The O3 stars. *ApJL* 254: L15–L17.
Walborn NR (1982b). Ofpe/WN9 circumstellar shells in the Large Magellanic Cloud. *ApJ* 256: 452–459.
Walborn NR (2011), Morphological characteristics of OB spectra and environments, Highlights of Spanish Astrophysics VI, 25–35.
Walborn NR and Fitzpatrick EL (1990). Contemporary optical spectral classification of the OB stars - A digital atlas. *PASP* 102: 379–411.
Walborn NR and Fitzpatrick EL (2000). The OB zoo: A digital atlas of peculiar spectra. *PASP* 112: 50–64.
Walborn NR, Nichols-Bohlin J and Panek RJ (1985). IUE Atlas of O-Type Spectra from 1200 to 1900 Angstroms, NASA RP-1155.
Walborn NR, Parker JW and Nichols-Bohlin J (1995). IUE Atlas of B-Type Spectra from 1200 to 1900 Angstroms, NASA RP-1363.
Walborn NR, Howarth ID, Lennon DJ, Massey P, Oey MS, Moffat AFJ, Skalkowski G, Morrell NI, Drissen L and Parker JW (2002). A new spectral classification system for the earliest O stars: Definition of type O2. *AJ* 123: 2754–2771.
Walborn NR, Sota A, Maíz Apellániz J, Alfaro EJ, Morrell NI, Barbá RH, Arias JI and Gamen RC (2010). Early results from the Galactic O-Star Spectroscopic Survey: C III emission lines in Of spectra. *ApJL* 711: L143–L147.
Walborn NR, Maíz Apellániz J, Sota A, Alfaro EJ, Morrell NI, Barbá RH, Arias JI and Gamen RC (2011). Further results from the Galactic O-Star Spectroscopic Survey: Rapidly rotating late ON giants. *AJ* 142, 150.
Walborn NR, Sana H, Simón-Díaz S, Maíz Apellániz J, Taylor WD, Evans CJ, Markova N, Lennon DJ and de Koter A (2014). The VLT-FLAMES Tarantula Survey. XIV. the O-type stellar content of 30 Doradus. *A&A* 564, A40.
Walborn NR, Morrell NI, Nazé Y, Wade GA, Bagnulo S, Barbá RH, Maíz Apellániz J, Howarth ID, Evans CJ and Sota A (2015a). Spectral variations of Of?p oblique magnetic rotator candidates in the Magellanic Clouds. *AJ* 150, 99.
Walborn NR, Sana H, Evans CJ, Taylor WD, Sabbi E, Barbá RH, Morrell NI, Maíz Apellániz J, Sota A, Dufton PL, McEvoy CM, Clark JS, Markova N and Ulaczyk K (2015b). Broad Balmer wings in BA hyper/supergiants distorted by Diffuse Interstellar Bands: Five examples in the 30 Doradus region from the VLT-FLAMES Tarantula Survey. *ApJ* 809, 109.
Walborn NR, Gamen RC, Morrell NI, Barbá RH, Fernández Lajús E and Angeloni R (2017). Active Luminous Blue Variables in the Large Magellanic Cloud. *AJ* 154, 15.
Weiler M, Carrasco JM, Fabricius C and Jordi C (2023). Analysing spectral lines in Gaia low-resolution spectra. *A&A* 671, A52.
White RJ and Basri G (2003). Very low mass stars and brown dwarfs in Taurus-Auriga. *ApJ* 582 (2): 1109–1122.
Wildt R (1936). Low-dispersion spectra of red stars. *ApJ* 84: 303.
Wilking BA, Meyer MR, Robinson JG and Greene TP (2005). Optical spectroscopy of the surface population of the ρ Ophiuchi molecular cloud: The first wave of star formation. *AJ* 130 (4): 1733–1751.
Wolf C and Rayet G (1867). Spectroscopie stellaire. *Academie des Sciences Paris Comptes Rendus* 65: 292–296.
Wright et al. (2010). The Wide-field Infrared Survey Explorer (WISE): Mission description and initial on-orbit performance. *AJ* 140, 1868.